Alma Mater Studiorum – Università di Bologna

DOTTORATO DI RICERCA IN

SCIENZE BIOCHIMICHE E BIOTECNOLOGICHE

Ciclo XXVIII

Settore Concorsuale di afferenza: 05/E1

Settore Scientifico disciplinare: BIO/10

Crucial role of miR-9 and miR-155 in cartilage homeostasis and osteoarthritis pathology

Presentata da: Dott.ssa Stefania D'Adamo

Coordinatore Dottorato
Prof. Santi Maria Spampinato

Relatore
Prof. Flavio Flamigni

Corelatore
Dott.ssa Silvia Cetrullo

Esame finale anno 2016

INDEX

ABSTRACT

Lack of efficacy in current pharmacotherapy, applied in osteoarthritis (OA) treatment, is spurring community to spend a lot of work and resources so as to unveil new molecular targets implicated in the pathogenesis of OA.

Several studies have reported beneficial effects of autophagy in preventing chondrocyte death, OA-like changes in gene expression and cartilage degeneration and many miRs have been identified as key modulators of autophagy pathway. So far, to our knowledge no relationship has been revealed between nutraceutical compounds and miR network in OA models.

First aim of this thesis is to evaluate molecular mechanisms of action of hydroxytyrosol (HT) a promising compound already tested for protective efficacy in OA chondrocytes in our recent published work.

HT increases markers of autophagy and protects chondrocytes from DNA damage and cell death induced by oxidative stress. The protective effect requires the deacetylase SIRT-1, which accumulated in the nucleus following HT treatment. In fact silencing of this enzyme prevented HT from promoting the autophagic process and cell survival. Furthermore HT supports autophagy even in a SIRT-1-independent manner, by increasing p62 transcription, required for autophagic degradation of polyubiquitin containing bodies.

Second aim consists in identifying a microRNA (miR) implicated in HT-mediated protective response to oxidative stress and examining the effects after modulation of miR levels by approach of transient transfection.

HT induces an increased expression of SIRT-1 protein, but without mRNA changes. After *in silico* analysis we identify miR-9 as a speculative candidate able to target SIRT-1 and confirm this hypothesis by means of luciferase gene-reporter assay. Moreover miR-9 mediates cell death induced by H_2O_2 and the protective effect of HT, as observed in human primary chondrocytes and

C/28-I2 cell line transfected with antimiR-9 and premiR-9 by trypan blue exclusion and caspase activity assays.

Third aim is to investigate the potential role of miR-155, found to be one of the most highly upregulated miRs in human OA knee cartilage, in autophagic pathway.

Autophagy flux induced by rapamycin and 2-DG was significantly increased by miR-155 LNA, and significantly decreased after miR-155 mimic transfection in T/C28a2 cells and in human primary chondrocytes. These effects of miR-155 on autophagy were related to suppression of gene and protein expression of key autophagy regulators including ULK1, FOXO3, ATG14, ATG5, ATG3, GABARAPL1, and MAP1LC3.

MiRs are promising targets as a single miR is able to regulate multiple genes in dysregulated pathways in a disease. Thus, the identification of a single miR, involved simultaneously in several disease-related pathways, discloses a potent therapeutic target. Indeed the unveiling of bioactive compounds, exerting a beneficial effect through induction of epigenetic changes, may open a new topic of research with huge potential and not yet well explored.

1. INTRODUCTION

1.1 Articular cartilage

Articular cartilage is a specialized connective tissue that covers the bone surfaces of diarthrodial joints. Cartilage in human body is classified into elastic, fibro-cartilage, fibro-elastic and hyaline cartilage; the latter is most known as articular cartilage and lies on the bones of synovial joints, giving them the lubricating feature and resistance to compression. Free movement and fractioning reduction is allowed thanks to the synovial fluid secreted by synovial membrane-resident cells.

Articular cartilage is devoid of blood vessels, lymphatics and nerve endings and is subject to a variable load and strong biomechanical stress during everyday life. Most important, this tissue has a limited capacity for intrinsic self-repair. Therefore, the preservation and health of articular cartilage are crucial to joint health.

The only cell population of hyaline cartilage is represented by chondrocytes that are responsible for synthesizing and maintaining the matrix infrastructure and homeostasis. Cellular component forms only 1-5% volume of cartilage tissue and the dense extracellular matrix (ECM) occupies the rest part.

Composition and structure of chondrocytes and ECM depend on the distance from the surface of cartilage and four different morphologically zones are distinguished (Fig.1.1).

The **superficial (tangential) zone** (STZ), the thinnest of the four, provides the articulating surface and is composed of flattened cells lying parallel to the joint surface. Chondrocytes in this region synthesize high amount of collagen (primary type II and IX), being packed tightly and in parallel to the articular surface, and very low amount of proteoglycan, so as to have the highest content of water. This zone is responsible of tensile and shears strength and its disruption contributes to the development of osteoarthritis.

The **middle** or **transitional zone** represents 40-60% of articular cartilage volume and provides a functional and anatomical bridge between the superficial and deep zones. It holds a low density of cells with spheroid shape surrounded by abundant matrix. Large diameter collagen fibrils are organized obliquely to the articular surface and higher amounts of proteoglycans compose the extracellular matrix of this region.

The **deep or radial zone** includes 30-40% of the total tissue volume and has the highest concentration of proteoglycans, the largest diameter of fibrils, the lowest cell density and the lowest water concentration. The chondrocytes are oriented in columns, parallel to the collagen fibers and perpendicular to the joint line.

In the **calcified cartilage zone**, chondrocytes show a very low metabolic activity with hypertrophic phenotype (*1*). This zone is embedded below the so-called "tide mark" that has a specific affinity for basic dyes, such as toluidine blue and the main function of this layer is to ensure the anchoring between cartilage and bone, by collagen fibrils that penetrate from the radial zone to the subchondral bone.

Each zone is distinguished in 3 different regions, named the pericellular region, the territorial region and the interterritorial region based on ECM composition. As the name suggests, the pericellular region lies around the chondrocyte. This thin layer is composed mainly in proteoglycans, as well as glycoproteins and non-collagenous proteins and exerts an actual role in signal transduction mechanisms.

The territorial region, that contains largely thin collagen fibers, is responsible of load bearing and protects the chondrocyte from mechanical stresses.

The interterritorial region is characterized by bundles of large collagen fibrils, organized parallel to the surface of the superficial zone, obliquely in the middle zone, and perpendicular to the joint surface in the deep zone. Proteoglycans are abundant in the interterritorial zone (*2*).

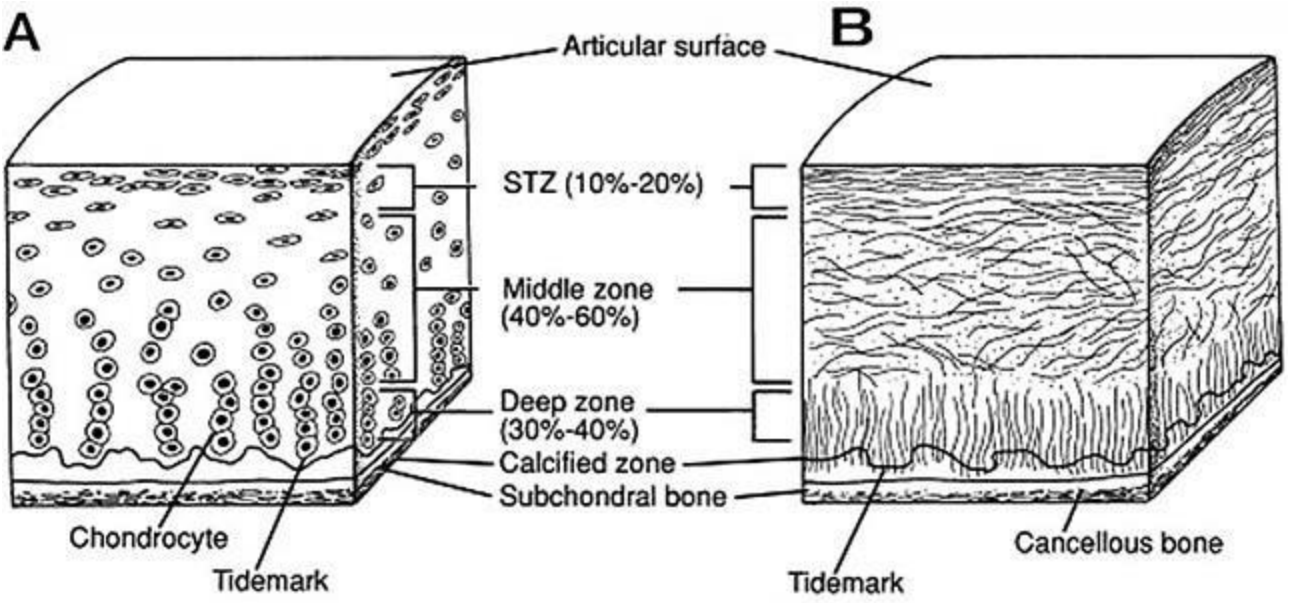

Figure 1.1: Schematic, cross-sectional diagram of healthy articular cartilage: **A**, cellular organization in the zones of articular cartilage; **B**, collagen fiber architecture. *Image modified from Sophia Fox et al. 2009* (*2*)

1.2 Extracellular matrix composition

Normal articular cartilage consists of 70% water and 30% of solid compound. The latter percentage is mainly represented by collagens and proteoglycans and a smaller amount by noncollagenous proteins, glycoproteins, lipids, phospholipids and inorganic compounds (*1*).

Proteoglycans consist in a core protein attached covalently to one or more glycosaminoglycan chains. The most abundant of this class of conjugated proteins is aggrecan, characterized by more than 100 of chondroitin sulphate and keratin sulphate chains. Aggrecan has a strong affinity to link hyaluronan forming large aggregates (*1, 3*). The chondroitin sulphate chain shows a structural function because of its negative charge, while the keratin sulphate domain does not exhibit any known function. The interaction between collagen and aggrecan confers to ECM a high degree of hydrophily, allowing strong capability of resistance to mechanical loads (*1*).

Collagen is the most abundant molecule in the ECM and collagen type II constitutes 90-95% of the total. The minor components, collagen types I, IV, V, VI, IX, and XI, assist to form the network of collagen type II fibrils. All members of the collagen family contain a region consisting of 3

polypeptide chains (α-chains) organized into a triple helix, namely procollagen, that are covalently bound at the level of C-terminal extension through disulphide bridges. When procollagens are secreted into the ECM, the N-terminal and C-terminal ends are removed by aggrecanases, e.g. A Disintegrin And Metalloproteinases with ThromboSpondin (ADAMTS)-2, -3, -14 and Bone Morphogenetic Protein (BMP)-1. The mature form of collagen spontaneously self-assembles in fibrils by covalent cross-linking (*4-6*).

Many other proteins support the fibre network, including thrombospondins, leucine-rich proteins (biglycan, decorin, fibromodulin, lumican), matrillins and fibronectin (*3*).

1.3 Biology of chondrocyte

As mentioned above, chondrocytes are the only resident cell type of articular cartilage and constitute about 5% of the wet weight of articular cartilage. Chondrocytes vary in shape, number, and size, depending on the zones of the articular cartilage. In the superficial zone they are flatter and smaller and generally have a greater density than the cells located deeper in the matrix. Being cartilage a non-vascularized tissue, chondrocytes receive nutrients and metabolites by diffusion from articular surface through synovial fluid. Therefore, the articular cartilage has a low oxygen level that varies depending on zone depth, 10% in the surface to less than 1% in the deep zone. Schipani et al. reports a survival role of hypoxia inducible factor -1 alpha (HIF-1α) in the hypoxia status by stimulating genes responsible of cartilage anabolism and differentiation, that is SOX9 and TGFβ (*7*).

Chondrocytes originate from mesenchymal stem cells (MSCs) and articular cartilage development partly reproduce a finely ordered process called endochondral ossification, which is structured in four steps: chondrogenesis, chondrocyte differentiation and hypertrophy, mineralization and invasion of bone cells, and finally formation of bone (*8, 9*). The MSCs undertake this fine process by migrating to the future area that will become bone. Then, they begin a phenomenon of

condensation, that is an increase of cellular volume without cellular proliferation. The ECM that surrounds undifferentiated MSCs is composed of collagen type I, III, V, hyaluronan, tenascin and fibronectin. During the differentiation of MSCs a switch in ECM composition happens and chondrocytes produce collagen type II, IX and XI, aggrecan, large chondroitin sulphate rich proteoglycan and link protein and no more collagen type I. Following further differentiation and hypertrophy, the chondrocyte decreases the production of collagen type II while begins to express collagen type X. After chondrogenesis, the chondrocytes hold a resting phenotype in the articular cartilage or enter a cascade of proliferation, terminal differentiation, hypertrophy and apoptosis. At the same time, cartilage undergoes an invasion by blood vessels that are responsible for carrying osteoblasts, whereby calcified hypertrophic cartilage will be resorbed and replaced by mineralized bone (*8, 10, 11*). During these events, matrix metalloproteinase (MMP) 9, 13, and 14, vascular endothelial growth factor (VEGF) and VEGF receptors are employed to convert a non-vascularized and hypoxic tissue to bone (*11*).

Unfortunately, chondrocytes have poor replicative strength thus conferring to cartilage a limited intrinsic capability of self-repair after mechanical injury. Therefore, cell integrity and health are critical for tissue biochemical properties and joint function. Moreover, in adult humans, chondrocytes has also a low activity of matrix turnover. Indeed, the half-life of collagen and aggrecan core protein is 100 years and 3-24 years, respectively, with a higher turnover rate in the pericellular region (*9*).

1.4 Osteoarthritis

Osteoarthritis (OA) is a multifactorial degenerative disease of the cartilage with the highest prevalence and socio-economic impact if we consider the loss of working time and early retirement of middle-aged individuals. OA is the most common form of arthritis, whose millions of people worldwide suffer, affecting 60% of men and 70% of women above 65 (*12*). Clinical symptoms are pain, stiffness and disability of joint motility that may lead to joint replacement (*13*). OA can

clinically be classified into two categories. Primary OA is featured by late onset and without a causative event, on the contrary secondary OA occurs after an identifiable event, such as trauma or pre-existing condition. The most common joint affecting by OA are the knee, hip, foot and hand (Fig. 1.3) that undergo severe changes, as loss of joint space, subchondral bone sclerosis, presence of osteophytes located at joint margins, degeneration of ligaments and hypertrophy of the joint capsule (Fig. 1.4).

Figure 1.3: Main districts affected by OA: knee (A), hip (B), foot (C) and hand (D).

These features are usually accompanied by chronic pain. Nevertheless, only half of people with radiographic OA complain significant symptoms and, on the other hand, not all elderly with chronic joint pain have radiographic OA features (*14*).

OA is a multifactorial disease whose aetiology appears to result from a complex system of biochemical and biomechanical causes. Many studies underlined the role of systemic factors (such as genetics, aging, dietary intake, estrogen use and bone density) and of local biomechanical factors (such as muscle weakness, obesity, joint laxity and injury) (*15*). However, the final common effect on cartilage destruction is due to the defective homeostatic balance between synthesis and degradation of ECM by chondrocyte population.

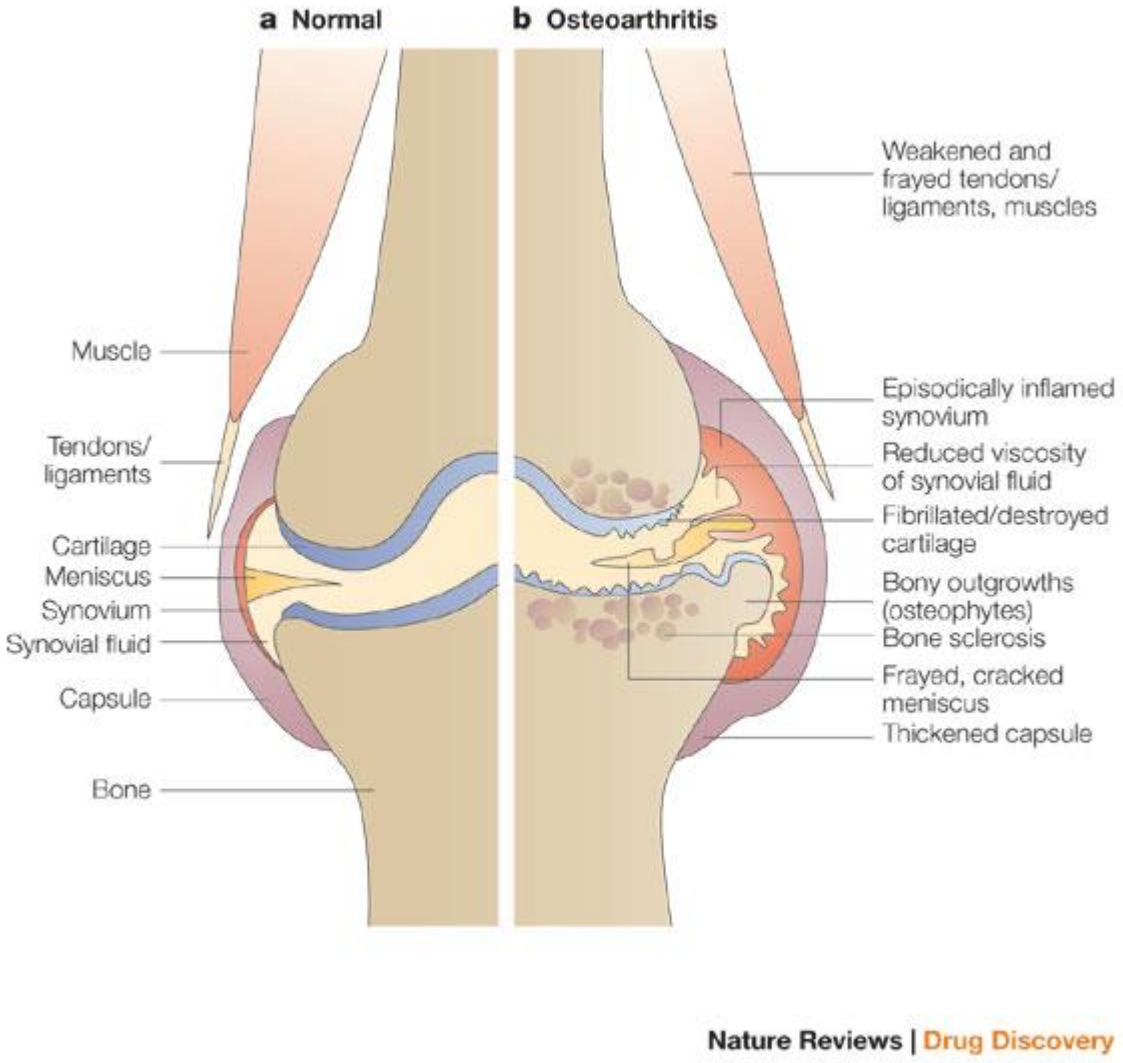

Figure 1.4: a Healthy tissue is shown: normal cartilage without any fissures, no signs of synovial inflammation. B Early focal degenerate lesion and 'fibrillated' cartilage, as well as remodelling of bone, is observed in osteoarthritis. This can lead to bony outgrowth and subchondral sclerosis. *Image modified from Wieland et al. 2005*(*16*)

Articular cartilage degeneration is a biphasic process including an initial biosynthesis step, aimed to damage repair, and a subsequent degenerative step, characterized by increase of matrix degrading proteinases, such as matrix metalloproteinases (MMPs), aggrecanases and other proteinases, and decrease of matrix components, mainly aggrecan. Moreover other phenotypic changes and abnormal phenomena in cell proliferation and death occur in OA chondrocytes (*17*). Cytokines, growth factors and matrix components trigger intracellular signals able to regulate chondrocyte metabolic activity and to switch on a pro-inflammatory and catabolic scenario. Indeed, the presence

of many inflammatory mediators, such as interleukin (IL)-1, IL-6, IL-7, IL-8 and tumour necrosis factor (TNF)-α, identifies OA as an inflammatory pathology much more than initially thought (*18*). These cytokines lead to cartilage destruction through activation of nuclear factor κB (NF-κB), phosphatidylinositol 3-kinase (PI3K)/Akt and transcription pathways, inducing the up-regulation of different metalloproteinases (MMPs) including MMP-13, the major type collagen II (Col2) degrading MMP. MMP-13-specific type II collagen cleavage products have been identified in OA cartilage together with cytokines (*19, 20*) and constitutive expression of MMP-13 in cartilage in mice produces OA-like changes in knee join (*21*). Furthermore other factors, such as fibrinogen, heat shock proteins or derivatives from hyaluronic acid, that are in surroundings during OA inflammation, can activate toll-like receptors (TLR) that, in turn, participate in the action of pro-inflammatory cytokines in the joint (*22, 23*).

Besides a stimulation of matrix-degrading proteinases, IL-1β and TNFα reduce *COL2A1* expression (*24*). Indeed, IL-1β is able to address inhibitory Smads (small mother against decapentaplegic), transcriptional regulators of TGF-β and BMP pathways, by up-regulating Smad7 and down-regulating Smad6 (*25*). TGFβ is responsible to maintain the anabolic activity in chondrocytes by eliciting an increase in aggrecan and collagen gene expression and triggers the signalling by binding transmembrane serine/threonine kinases, consisting of TGFβ receptor type I (TGFβ RI) and TGFβ RII. Then, TGFβ RI phosphorylates receptor-associated Smad 2(R-Smad2) and R-Smad3, in this way, turning on the intracellular signal. Smad2 and Smad3, forming a complex with Smad4, migrate to the nucleus and contribute to the transcriptional activation of target genes. Smad7 interacts with TGFβ RI, prevents Smad2 and Smad3 phosphorylation and their participation in the activation of downstream target transcription (*26*).

Surprisingly, an increased anabolic activity in OA cartilage has been reported and likely correlated to cytokine-induced production of prostaglandin E_2 (PGE_2) by promoting COX-2 activity and *COL2A1* expression (*27*), or to BMP-2 by activating *COL2A1* transcription (*28*). This opposite

effect may be due to the chondrocyte effort in counteracting the matrix degradation, like in a compensatory condition. Other studies support the hypothesis that *COL2A1* expression levels may vary in different zones of cartilage analysed and in different stages of OA samples (*29-31*). COL2A1 results predominantly up-regulated in cell samples deriving from middle and deep zones, rather than from the samples of degraded superficial region (*32*).

The best characterized anabolic factors in this tissue context are insulin-like growth factor (IGF)-I, the bone morphogenetic proteins (BMPs), including osteogenic protein-I (OP-I or BMP-7) and cartilage-derived morphogenetic proteins (CDMPs), TGF-β and fibroblast growth factors (FGFs). IGF-I and other anabolic factors, able to maintain cartilage matrix synthesis, reveal a gradual decreased expression or declined activity during aging progression. IGF-I can stimulate proteoglycan synthesis, promote chondrocyte survival and counteract catabolic cytokines. OA patients are hypo-sensitive to IGF-I, but they show normal or increased IGF-I receptor levels (*33*).

Increased levels of IGF binding proteins (IGFBPs) have been found to be responsible of this hypo-responsivity by interfering with IGF-I signalling (*34*). TGF-β 1, 2 and 3 stimulate proteoglycan and type II collagen synthesis in primary chondrocytes and cartilage explants in vitro. However, it has been reported that administration of TGF-β leads to side effects, such as osteophyte formation, swelling and synovial hyperplasia. These factors could be involved in physiological turnover of proteoglycans, since TGF-β is able to promote ADAMTS-4 expression and thus aggrecan degradation (*35*). BMPs, another class of the TGF-β family, are involved in chondrogenesis. BMP-2, -4, -6, -7, -9 and -13 enhance COL2 and aggrecan synthesis. BMP-7 can counteract IL-1β-induced catabolic actions, such as stimulation of MMP-1 and -13, inhibition of tissue inhibitors of metalloproteinases (TIMPs) expression and down-regulation of proteoglycan synthesis in adult chondrocytes (*36*).

1.5 The role of oxidative stress in aging and OA

Although aging is not the only responsible condition for the onset of OA, it is accepted that aging can promote the development of OA and has been proposed as the main risk factor of this pathology, followed by obesity (*37*). The real connection between aging changes in cells and the inclination to OA seems to be found in the role of cell senescence and in its morphological expression, the senescence-associate secretory phenotype (SASP) (*38*). This phenotype can be associated to an over production of reactive oxygen species (ROS) due to defective mitochondrial function and up-regulation of inflammatory pathways that participate in the "aging stress response" (*39*). Because of unpaired electrons, free radicals are very reactive and can affect cell components, thus causing damages.

An imbalance between ROS production in mitochondria and cell scavenging systems (superoxide dismutase-SOD, catalase, glutathione peroxidase, glutathione reductase and reduced glutathione levels) to detoxify these species, determines the oxidative stress condition and is strongly associated to aging and age-related diseases, including OA. The main ROS detected in chondrocytes are peroxynitrite ($ONOO^-$) and hydrogen peroxide (H_2O_2), derived from activation of inducible NO synthase (iNOS) and mitochondrial NADPH-dehydrogenase, respectively (*40, 41*). In chondrocytes iron Fe^{2+} and H_2O_2 release hydroxyl radicals ($OH^{\cdot}$) that react with unsaturated fatty acids of membrane lipids thus forming lipidic radicals ($RO^{\cdot}$, $ROO^{\cdot}$). Several studies in humans and experimental animal models reported a limited anti-oxidant capacity of the glutathione systems and some enzymes, such as SOD and catalase, in OA (*42, 43*).

In a pathological scenario, whether cellular antioxidant systems are altered and/or insufficient to detoxify the ROS excess, oxidative stress leads to membranes and nucleic acids damage and, also, breakdown of extracellular components, including proteoglycans and collagens, as well as down-regulation of glycosaminoglycan and collagen synthesis, and up-regulation of MMPs and aggrecanases. All these alterations contribute to promote cartilage derangement and destruction. It

should be noted that in physiological conditions, ROS are essential for the control of cellular function, e.g. signal transduction, by acting as messengers. However when in excess, ROS produce deregulated post-translational modifications of signalling proteins by oxidation and nitrosylation of amino acid residues, leading to altered activity of several cellular processes, e.g. apoptosis and cell proliferation (*44*). ROS can interact with other cellular components, such as advanced glycation end products (AGEs) that are noteworthy to be accumulated in aged tissues and OA cartilage (*45*). Furthermore, these events establish a positive feed-back loop: the cartilage degradation-derived products can promote further inflammation and oxidative stress in chondrocytes, leading to OA progression.

However, our organism has several adaptive molecular devices fighting stress-related alterations, thus promoting survival. One of these longevity factors is SIRT-1, a class III protein deacetylase. This story began at least 30 years ago when its homologous Sir2 (silent information regulator 2) was identified in yeast and found to be a silencer of specific genome regions, such as telomeric ends and homothallic mating (HM) loci. In this way it influences the replicative aging process of yeast. When the exact activity of Sir2 was discovered and characterized as NAD^+-dependent histone deacetylase, a mechanistic explanation became available for the actual role of this protein as a metabolic link between the energetic state and life span (*46*). Despite being principally a nuclear protein, SIRT-1 is provided with two nuclear localization signals and two nuclear exportation signals, via which it shuttles between nucleus and cytosol.

As described above, ROS at physiological levels are important cellular signalling molecules performing fundamental cell survival functions, whereas at higher doses can directly damage proteins, lipids and DNA. The free radical theory of aging refined by Hekimi and collaborators proposes a gradual ROS response hypothesis (*47*). As shown in Fig 1.5 an optimal level of ROS is required for the best healthspan and for extending the lifespan. This threshold matches with a specific and sustained activity of SIRT-1. Moreover SIRT-1 interacts with NF-κB signalling,

controlling the ROS production. It has been reported that SIRT-1 is able to deacetylate Lys310 of Rel/p65 component of NF-κB complex and, in this way, inhibit its transcriptional activity (*48*). However, until 2008 the actual potential of SIRT-1 as modulator of cellular processes was unclear. The missing piece in this complicated puzzle was the discovery that SIRT-1 may be involved in autophagy by deacetylating ATG5, ATG7, and ATG8. Actually, this finding did not come as a surprise, because both autophagy and SIRT1 are stimulated during starvation and fasting. It has been shown how SIRT1 deacetylates these autophagy-related proteins in a NAD^+-dependent fashion. Moreover, it has been found that FoxO3 deacetylation may control the transcription of autophagy-related genes such as LC3 and BCL-2/E1B 19 kDa interacting protein (BNIP3) in skeletal muscle, and that SIRT1 promotes starvation-induced autophagy by deacetylating FoxO in cardiac myocytes (*46*).

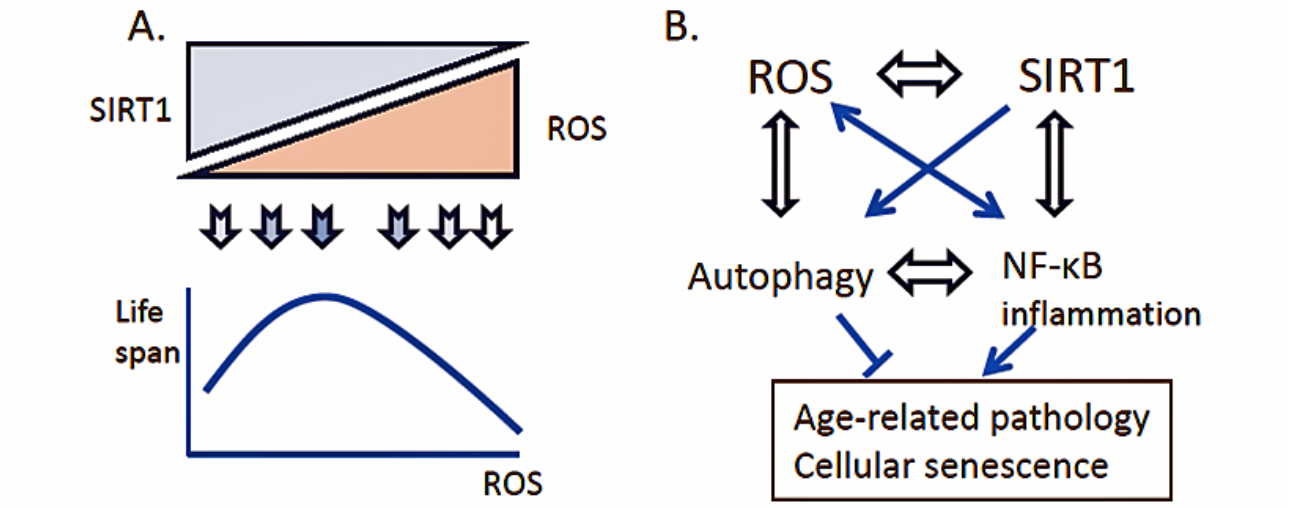

Figure 1.5: A schematic drawing representing the crosstalk between ROS and SIRT-1 activity. ROS concentration is inversely correlated to SIRT-1 level and the optimal level of ROS production is identified through interpolation of lifespan on y-axis (A). The interplay between ROS and SIRT-1 controls autophagy and NF-κB pathway and, in this way, promotes age-related changes and senescence (B). *Image modified from Salminen et al. 2013* (*49*).

It has been shown that SIRT-1 regulates gene transcription in human chondrocytes by increasing the expression of ECM components and inhibits apoptosis in human OA chondrocytes (*50*, *51*). An interesting *in vivo* study showed that SIRT-1-null mice also have defective cartilage, with facial

abnormalities and their long bones mineralized slower than normal. These mutants were predisposed to develop OA, especially with age, due to a higher level of cartilage breakdown and apoptosis (*52*).

1.6 Hydroxytyrosol and nutraceuticals as alternative therapies for OA

So far, pharmacotherapies for arthritic diseases are only based on palliative treatments that focus on symptoms, e.g. pain and inflammation, and mainly consist of analgesics and nonsteroidal anti-inflammatory drugs (NSAIDs) (*53*). This is the reason why they lack efficacy in slowing disease progression and, also, result in several side effects, mostly gastrointestinal and cardiovascular injuries. Therefore, an increasing need for alternative therapies, to improve the life quality or reverse the pathology of OA sufferers, is spurring the scientific community towards the basic and applied research on the potential of nutraceuticals. The term "nutraceutical" derives from a combination between "nutrition" and "pharmaceutical" and identifies a food or only a component of this with a scientifically proven beneficial effect for our organism. At present, nutraceuticals include dietary supplements at high concentration of a bioactive compound provided from food, like pills of food (Fig. 1.6). Many reports suggest that nutraceuticals exert a protective role for several pathologies, including cardiovascular disease, cancer, and OA (*54*, *55*)

Figure 1.6: A representative drawing of concept on nutraceuticals: pills of specific components originally derived from food. *Image modified from website http://www.marsing-sa.com/nutraceuticals/*

Nutraceuticals have shown to exhibit a role not merely as anti-oxidant or ROS scavengers, but also as efficient modulators of gene expression of key factors underlying the OA onset. A simplified scheme of the best studied pathways that mediate nutraceuticals action, is shown in Fig. 1.7. Many researchers have identified specific nutraceuticals able to inhibit NF-κB transcription factors, which are stimulated following toll-like receptors (TLRs) and IL-R activation by extracellular matrix fragments and IL1-β, respectively. Moreover, some polyphenols (e.g. sesamin and morin) have been found to suppress the up-regulation of pro-inflammatory cytokines and catabolic enzymes by inhibiting the mitogen-activated protein kinases (MAPKs) (*56, 57*). The mammalian target of rapamycin (mTOR) signalling has been reported to be regulated by poly-unsaturated fatty acids (PUFAs), lipids well known for their anti-inflammatory properties, leading to a protective stimulation of autophagy in chondrocytes (*58*). It is noteworthy that SIRT-1 downregulation results to address OA progression in induced and aged models (*59*). Indeed, SIRT-1 activation in the presence of resveratrol interferes with NF-kB signaling, resulting in anti-inflammatory effects during OA (*60*).

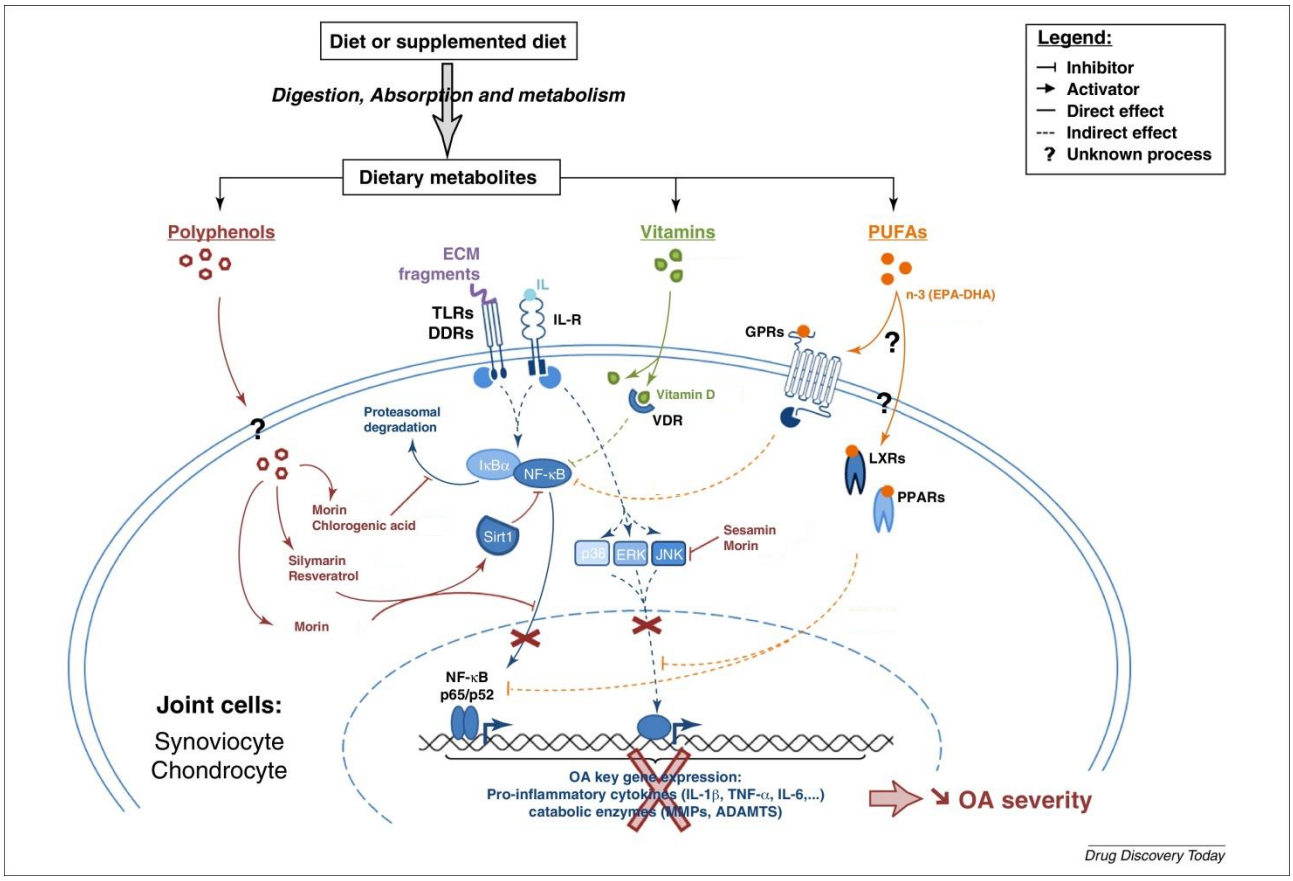

Figure 1.7: Mechanism of action of nutraceuticals in synoviocytes and chondrocytes. Nutraceuticals alleviate inflammation and cartilage degradation by modulating NF-κB and MAPKs (ERK1/2, p38 and JNK). These critical pathways are activated by IL-1β or extracellular matrix (ECM) fragments that are recognized as damage-associated molecular patterns (DAMPs), leading to the expression of MMPs and ADAMTS and, again, inflammatory cytokines, which participate in cartilage degradation. The supplementation of nutraceuticals can block many steps of these signaling pathways to decrease osteoarthritis (OA) severity. *Image modified from Mével et al. 2014* (*61*)

Even though several dietary factors and nutraceuticals are promising, extensive investigation in preclinical and clinical settings is required to prove their usefulness. On this purpose, we and others have showed the ability of sulforaphane, a natural isothiocyanate derived from edible cruciferous vegetables, to protect chondrocytes in vitro (*62, 63*), and, quite recently, a sulforaphane-rich diet was found effective in a murine OA model (*63*).

Another interesting candidate molecule is hydroxytyrosol (HT), a phenolic compound endowed of a powerful anti-oxidant action, mainly found in the fruits of olive tree (Olea europaea L.) and their derivatives, such as olive oil (*64*). From the point of view of chemical composition, olive oil can be

divided into major and minor fractions. The first one includes the saponificable fraction, that are mostly triacylglycerides, and represents 98-99% of the total weight. The main components of this fraction is oleic acid (18:1 n-9) and the others are palmitic, stearic, linoleic and α-linoleic acid. The minor fraction comprises the unsaponificable components and the soluble part, that are the phenolic compounds. Stress conditions, such as high temperature and ultraviolet radiation being usual in the Mediterranean area, promote a further metabolic process in vegetables, including olives and grapes. This pushes an increased synthesis of phenolic compounds with known antioxidant features. This group is classified in two sub-groups: lipophilic phenols (tocopherols and tocotrienols) and hydrophilic phenols. The latter sub-group can be divided into different classes: phenolic acids, phenolic alcohols, lignans and flavonoids. HT [(3,4-dihydroxyphenyl)ethanol] belongs to the second class together with tyrosol [(*p*-hydroxyphenyl)ethanol] and HT glucoside (*64*). The concentrations of HT and tyrosol in olive oil have been reported as 14.4 and 27.5 mg/kg, respectively (*65*).

As shown in figure 1.8, HT is a product obtained from the hydrolytic reaction of oleuropein occurring during the maturation of olives. Given that phenolic compounds are polar species, a great amount of HT is found in the residues of oil processing, including pomace olive oil, olive-mill waste water or, the rinse waters. On the other hand, HT shows amphipathic behaviour and, in this way, is also found in olive oil and in the olive leaf.

Mediterranean countries, e.g. Italy, Greece and Spain are the main providers and consumers, thanks to their long tradition of olive cultivation. Indeed, it has been estimated that these populations consume around 25-50 mL/die of olive oil, with thus 9 mg/die of polyphenols and, at least, 1 mg/die of HT and tyrosol (*64*).

The absorption of HT occurs in a dose-dependent manner in the small intestine and colon (*66*) and it is very rapid, with a maximum peak of HT concentration in plasma 5-10 minutes after ingestion. Tuck et al. reported that rats were able to absorbe 75% of HT in aqueous solution and 90% in oily

vehicle (*67*). HT is able to cross the blood-brain barrier, even if it should be considered that HT may result endogenously from dihydroxyphenylacetic acid in the brain. HT can also be generated from dopamine leading to consider both the dietary intake and the endogenous levels (*68, 69*).

Several studies, mostly performed in cell and animal models, have revealed a range of biological properties of HT, suggesting beneficial effects in the prevention or treatment of chronic and degenerative diseases, especially cardiovascular disease and cancer. In particular HT has been shown to display cytoprotective and anti-inflammatory actions in a variety of cell types (*70-74*)

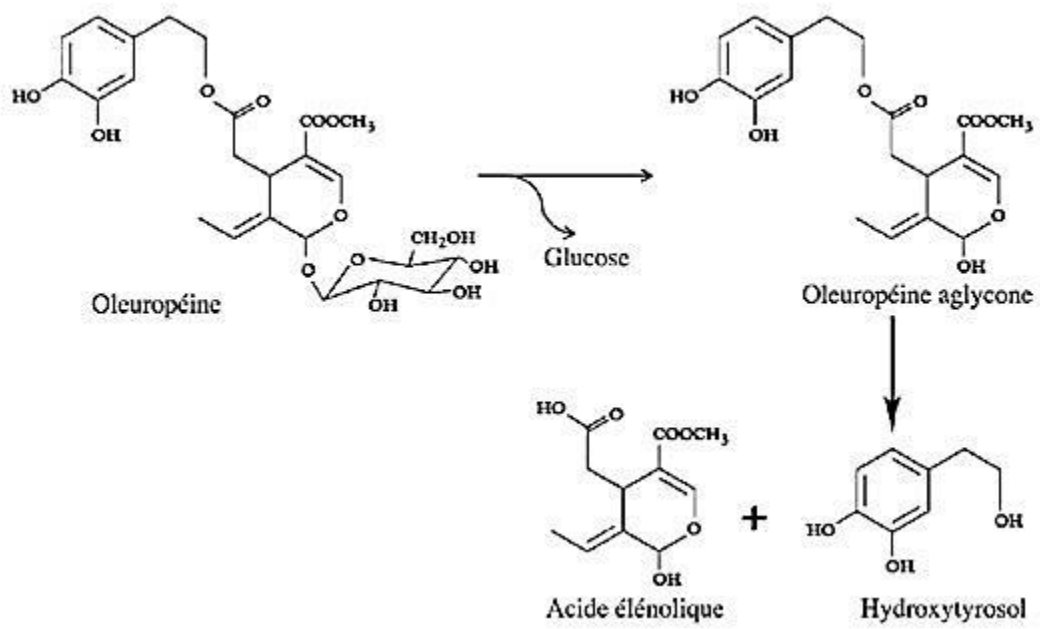

Figure 1.8: Origin of hydroxytyrosol from oleuropein. After the hydrolysis of oleuropein (resulting in oleuropein aglycone), which originates during the maturation of the olives, storage of the oil, and preparation of table olives, hydroxyrosol is given rise together with elenolic acid. These are responsible, in part, for the complex and varied flavour of the oil and the olives. *Image modified from Granados-Principal et al. 2010* (*64*).

1.7 Autophagy in OA

The word "autophagy" (from the Greek *auto* and *phagein*, meaning self-eating) was coined by Christian de Duve in 1963 following the discovery of cytosolic components and lysosomal hydrolases engulfed in membrane-bound vesicles. Autophagy is a catabolic process via lysosomes that plays crucial roles in several cellular aspects, including intracellular homeostasis, immunity,

internal quality checking, cell survival (*75-77*). Based on the type of cargo delivery, three different forms of autophagy have been described in mammals: macro-autophagy, micro-autophagy and chaperone-mediated autophagy, all of them characterized by proteolytic degradation of cytosolic components at the lysosome. Macro-autophagy is a bulk-degradation of cytosolic portions via the intermediary of a double membrane-bound vesicle, named autophagosome, fusing with the lysosome so as to form the autolysosome. Instead, micro-autophagy bypasses this step and cytosolic components are caught directly by mean of lysosomal membrane invagination. These types of autophagy are able to deliver large structures through selective and non-selective processes. In the last type, chaperone-mediated autophagy, chaperones, such as Hsc-70, binds targeted proteins to form a complex on the lysosomal membrane. Then, this complex is recognized by lysosomal-associated membrane protein-2A (LAMP-2A) leading to cargo (*78*).

This thesis focuses on a better understanding of molecular aspects of macro-autophagy, hereafter termed simply "autophagy", and on its involvement in pathological conditions of osteoarthritis. The remarkable molecular complexity of the basic autophagic machinery and its modulators is being unravelled and is emerging as described below.

The origin of autophagy is attributed to isolation of membranes, named phagophores, from the endoplasmic reticulum (ER) and/or the trans-Golgi and endosomes, even if the beginning is still unclear in mammals. This phagophore engulfs the cargo by "stretching" the ends around and thereby incorporating it in a double-membrane autophagosome. Then, the "stuffed" autophagosome is ready to fuse with the lysosome that is responsible to digest the content by means of proteases. Hence, some membrane carriers allow amino acids and other digestion products to get out to the cytoplasm where they can participate to recycling processes (*79*).

Although autophagy is active at basal conditions in most cell types by exerting a housekeeping role of cellular homeostasis, starvation is a clear inducer of autophagy. One of the main sensors of nutrient and energy status is the mammalian target of rapamycin (mTOR) kinase being a readout

key of response to growth factors, nutrients-derived signals, hypoxia and adenosine triphosphate (ATP) levels. MTOR is activated by AKT-PI3K pathway when nutrients and growth factors, such as insulin, are available so as to stimulate cell growth by increasing protein translation (*80*). Low ATP levels and thus high adenosine 5′-monophosphate (AMP)/ATP ratio lead to activation of AMP-activated protein kinase (AMPK) promoting the inhibition of the tumour suppressor proteins Tuberous sclerosis complex TSC1/TSC2 on RHEB, a small GTPase that is upstream of mTOR. Moreover, a reduced activity of AKT also inhibits mTOR (Fig. 1.9). The role of mTOR unveils the mode of action of its artificial inhibitor, rapamycin (RAPA) (*80*). It has been reported that RAPA, tested for cancer therapy in clinical trials, is able to block tumour growth by inhibiting protein translation and by stimulating autophagy (*81*). However, mTOR form two different complexes, named TORC1 and TORC2, but RAPA only shows an inhibitory activity on the first complex. mTOR interacts with two alternative subunits, RAPTOR to form mTORC1 and RICTOR to form mTORC2 (*82, 83*). The latter one is able to inhibit mTORC1 and may exert a positive influence on autophagy. This finding provides an interesting point of view to be discussed in the light of the results in this thesis.

Though a low level of basal autophagy is required to maintain the cellular homeostasis, a persistent self-digestion might impair the correct cellular equilibrium. By the way, this is the reason why every activated pathway needs to be inhibited through a negative feed-back loop. One of the main suppressor is the complex TORC1 and the mechanism by which it regulates negatively autophagy has first been reported in *Saccharomyces cerevisiae*. As shown in Fig. 1.9, once activated, TORC1 inhibits autophagy by suppressing the most upstream protein complex that comprises the serine/threonine kinase Atg1 as well as two accessory proteins Atg13 and Atg17. TORC1 phosphorylates several Atg13 at several serine residues so as to prevent Atg13 binding to Atg1 and, hence, Atg1-Atg13-Atg17 complex formation. Under nutrient deprivation or RAPA treatment, TORC1 inactivation leads to a prompt dephosphorylation of ATG13, to form the complex and

promote ATG1 kinase activity (*84, 85*). Actually, the involvement of ATG1 has been reported in several species, including *Caenorhabditis elegans* and *Drosophila melanogaster*, which express only one ATG1 homologue (*86, 87*). Although vertebrates have five different kinases related to ATG1, two of these, i.e. unc-51-like kinase-1 (ULK-1) and ULK-2, show the highest homology to ATG1 in *C. elegans*. Several studies showed the essential role of both proteins for a successful autophagy, whereas many others reported that they have partially redundant functions (*84*). These opposite results may be artificial and simply mirror the necessity of clearer and better defined guide lines of experimental settings for autophagy assays. Furthermore, the focal adhesion kinase (FAK) family-interacting protein of 200 kDa (FIP200), also called retinoblastoma 1-inducible coiled-coil 1 (RB1CC1), has been proposed as the functional counterpart of Atg17. FIP200 interacts with ULK-1/ULK-2 so as to promote ULK1 kinase activity and the translocation of the entire complex to the pre-autophagosomal membrane after starvation. Under nutrient-rich conditions, mTORC1 interacts with ULK1/2-ATG13-FIP200 complex via direct binding between RAPTOR and ULK1/2 and phosphorylates ATG13 and ULK1/2 thereby inhibiting its activity. Under starvation conditions or pharmacological inhibition of mTORC1, these sites are immediately dephosphorylated by unknown phosphatases. As shown in the panel A of fig. 1.10, ULK1/2 phosphorylates itself, FIP200 and ATG13 and triggers the autophagy process (*88*).

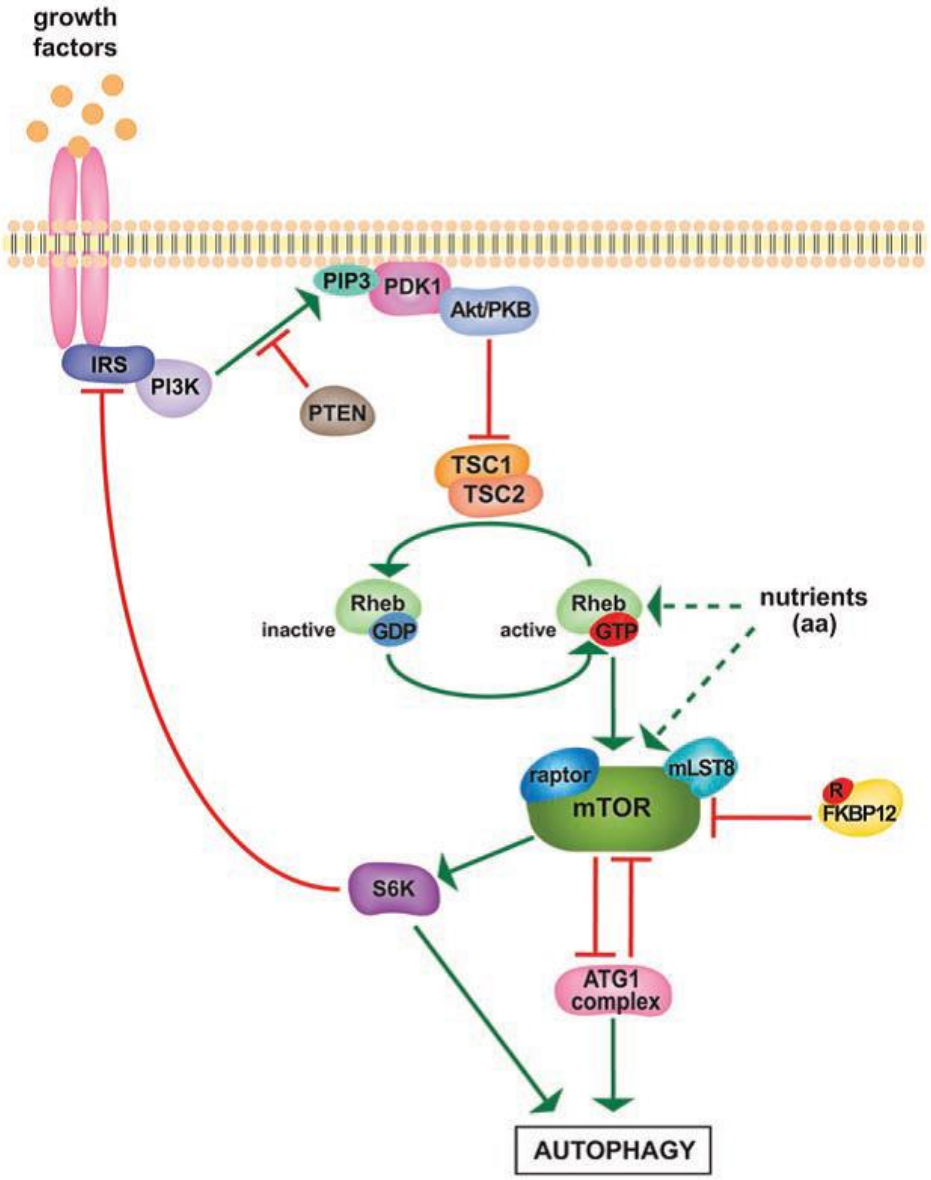

Figure 1.9: Control of autophagy by the mTOR signaling network in metazoans. mTORC1 responds to intracellular and extracellular stimuli, including amino acids (aa) and growth factors (insulin). Amino acids can activate the GTPase Rheb, which, in turn, activates mTORC1, while the growth factor signal is transduced to TSC1/TSC2. TSC1/TSC2 switch off mTORC1 by inactivating Rheb. When activated, mTORC1 suppresses autophagy by inhibiting the ATG1 complex. Green arrows represent activation, whereas red bars represent inhibition. Dashed lines refer to potential interactions. *Image modified from Diaz-Troya et al 2008* (*85*)

The next step involves Beclin-1, the mammalian homologue of yeast Atg6 and the core component of the class III phosphatidylinositol 3-kinase (PI(3)KC3) complex. This complex is characterized of six subunits, including VPS34 (the mammalian homologue of yeast Vps34), p150 (in yeast Vps15), BECLIN-1 (Atg6 in yeast), ATG14L (also known as Barkor; Atg14 in yeast), UVRAG (Vps38 in

yeast) and Rubicon (which has no yeast counterpart) (*89*). Russell et al demonstrated that ULK phosphorylates Beclin-1 in amino acids deprivation, and that this phosphorylation step is crucial for the function of Beclin-1 in autophagy (*90*). The complex is well-represented in the panel B of fig.1.10. VPS34 is widely involved in different membrane-sorting systems and, when associated with BECLIN-1, it exerts its role in nucleation step of phagophores during autophagy cascade. VPS34 is able to use phosphatidylinositol (PI) as substrate to make phosphatidylinositol trisphosphate (PIP3). This latter one is crucial for phagophore nucleation and elongation, and for recruitment of ATG proteins. VPS34 function is critical for this phase, however its association with BECLIN-1 results fundamental. BECLIN-1 activity is finely regulated by several factors, including BCL-2. Their interaction at ER leads to an inhibitory effect of BECLIN-1 activity, which instead may be restored by JNK-mediated phosphorylation of BCL-2 after starvation stimuli so as to promote autophagy. Cell fate seems to be dependent on BLC-2 localization: autophagy blocking when it lies at ER, vs apoptosis inhibition when located at outer mitochondrial membrane by stopping cytochrome c release (*91*).

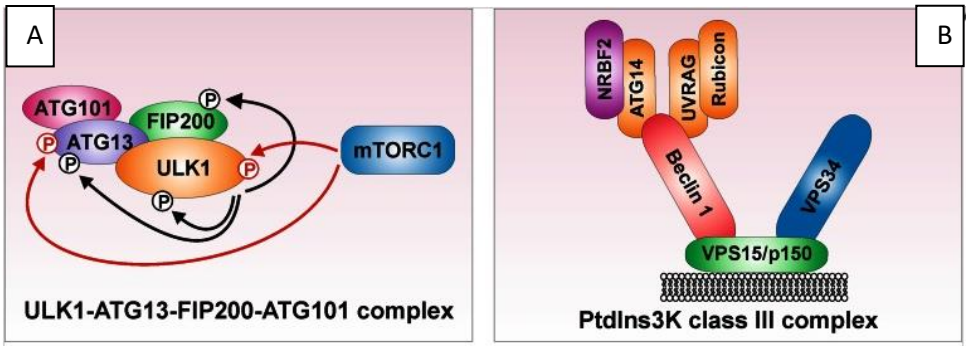

Figure 1.10: Two clusters of autophagy signaling. A The ULK1–ATG13–FIP200–ATG101 protein kinase complex, B the PtdIns3K class III complex containing the core proteins VPS34, VPS15 and Beclin 1. *Image modified from Wesselborg et al 2015* (*91*).

Two ubiquitin-like conjugation systems are responsible for autophagosome elongation and maturation steps. In the first one ATG7 acts as E1 ubiquitin activating enzyme by catching ATG12 through its carboxyterminal glycine residue. Hence, ATG12 is relocated to an E2-like ubiquitin carrier protein that promotes covalent binding to ATG5. These heterodimer complexes with a

homodimer ATG16 so as to associate to the phagophore and likely induce the correct curvature. When autophagosomes are completed this complex may be released. Indeed, many researchers consider ATG12-ATG5 conjugated as untrusted marker of the autophagy efficiency. The processing of microtubule-associated protein light chain 3 (LC3B), the mammalian homologue of ATG8 in yeast, is performed by another ubiquitin-like system. This protein is expressed as a cytosolic form and, following autophagy stimuli, it undergoes a ATG4- mediated proteolytic cleavage resulting in LC3B-I formation and priming for the next steps. Indeed, LC3B-I exposes its carboxyterminal glycine to binding by ATG7 and then is transferred by ATG3 (E2-like ubiquitin carrier) to phosphatydilethanolamine (PE) so as to generate LC3B-II. This latter processed form is engaged to phagophore membrane by means of ATG12-ATG5 system and becomes responsible for the fusion between membrane ends and for cargo selection. In fact LC3B-II acts as a phagophore receptor that recognizes P62/SQSTM1, an adaptor protein that links targets, such as poly-ubiquitinated protein aggregates and mitochondria, addressing them to autophagic degradation.

Actually Atg8 orthologs are identified in two subfamilies: the MAP1LC3, named LC3 above described, and the GABARAP (GABA[A] receptor-associated protein) family including GABARAP, GABARAP-like 1 (GABARAPL1), and GABARAPL2. At the beginning it was speculated that these subfamilies would exert redundant activity in autophagy. However in 2010, Weidberg et al. discovered that LC3 family is responsible of elongation phase and GABARAP group is involved in late maturation of autophagosomes (*92*). Moreover, another explanation about the abundance of members in this ATG8 homologue family is that each of these is involved in different types of selective autophagy (e.g., aggrephagy, mitophagy, pexophagy, ribophagy, or xenophagy) (*93*).

After the complete fusion of autophagosome ends, in the maturation step autophagosomes fuse with lysosomes to form the so-called “autolysosomes” where cargo is degraded and released in cytosol in order to be recycled (*94*). Furthermore, P62 is digested together with the content of autolysosome

and this event has been employed by many researchers as an important and very useful tool for autophagy assay. Indeed, late autophagy blocking is detected through the accumulation of P62 content. It is very common to monitor both LC3B-II and P62 variations as reliable readout key of successful autophagy. As a matter of fact, although partly stimuli-dependent, increased levels of LC3B-II are often accompanied to decreased levels of P62 (*95*).

Autophagy promotes cellular and organism health and exerts a fundamental role in cellular homeostasis by digesting long-lived protein aggregates and damaged organelles. For example the degradation of dysfunctional mitochondria via mitophagy is a cytoprotective process that limits both the production of reactive oxygen species (ROS) and the release of toxic intramitochondrial proteins. Autophagy dysregulation has been identified in several disorders, including metabolic diseases, neurodegenerative pathology and cancer, where its inhibition or activation addresses towards pathogenesis. On the other hand, inducers able to sustain autophagy cascade have been classified as longevity promoters, confirming the idea that ageing and longevity may exploit autophagy as a therapeutic target (*96*).

In certain physiological and pathological conditions, autophagy has been identified as type II programmed cell death. Roach et al in 2004 reported for the first time a specific variant of apoptosis in chondrocyte, called chondroptosis, characterized by presence of autophagic vacuoles and increasing amount of ER membrane (*97*). Changes in autophagy that have been reported in aging and OA-affected cartilage include reduced numbers and size of autophagosomes and this is, in part, related to a reduced expression of the autophagy proteins ULK1, BECLIN1 and LC3 (*98*) and mTOR overexpression (*99*). In healthy cartilage autophagy results sustained in order to modulate changes of gene expression in OA by regulating apoptosis and production of ROS. Actually during the initial degenerative phase at the beginning of OA pathologic process, autophagy may act as a protective response to environmental stress, but during OA progression, autophagy efficiency decreases leading to cell death. Several studies reported beneficial effects of autophagy in

preventing chondrocyte death, OA-like changes in gene expression and cartilage degeneration (*100-104*). Rapamycin, which is a direct suppressor of the mTOR pathway, induces expression of autophagy regulators and prevents chondrocyte death. Sasaki and colleagues investigated the role of autophagy in human chondrocytes and OA pathophysiology and observed that the inhibition of autophagy caused OA-like gene expression changes, and conversely the induction of autophagy prevented them. Furthermore, ROS activity was decreased by induction of autophagy (*103*). However, despite the remarkable number of scientists striving in this field, the mechanisms underlying the autophagy failure in OA are still unclear, specifically those related to the reduced expression of autophagy proteins.

1.8 MicroRNAs: molecular mechanisms and implications in OA

MicroRNAs (miRs) are an abundant, evolutionary conserved subfamily of short non-coding RNAs (22-25 nt) that are identified as potent post-transcriptional regulators. In 1993 Ambros and Ruvkun discovered the first miR, lin-4, as the main modulator of some phases in development of *C. elegans* by suppressing lin-14 levels. They detected several multiple sites of imperfect complementarity of lin-4 harbored in lin-14 mRNA 3'untranslated region (UTR) and indicated this antisense binding as able to block lin-14 translation (*105, 106*). Rheinart et al. in 2000 discovered a second miR in *C. elegans*, named let-7 (*107*). Since this miR was known to have well-described homologues in human and fly, the entire scientific community was spurred to identify this class of RNAs in higher species and a new topic was inaugurated, becoming object of intensive research. To date, 1881 sequences of miRs have been identified in human cells and uploaded in the main web databases miRBase based on the new human genome assembly (GRCh38) released. Computational predictions, tools also available in many others web databases (TargetScan, miRWalk2.0, miRanda), unveil that more than 50% of all human proteins are under potential regulation by miRs. Hence, finding miR targets became a necessity.

The genomic distribution of miRs is shown in figure 1.11. As initially found for *C. elegans* lin-4 and let-7, most of currently annotated miR genes lie in introns of protein coding genes or non-coding genes; these miRs can occur alone or in a cluster of several miRs and are thought to be regulated by the same promoter of host genes and likely generated from the host intron. Other miRs, called intergenic, lie in genomic regions distant from known genes and can be monocistronic or polycistronic, transcribed by their own promoter or in a primary transcript by a shared promoter. Another class of miRs, named mirtrons, are inserted in introns with splice sites on both sides; these miRs are processed during splicing of primary transcript by means of spliceosome. The last class consists of exonic miRs whose gene overlaps an exon and an intron of the host gene (*108*).

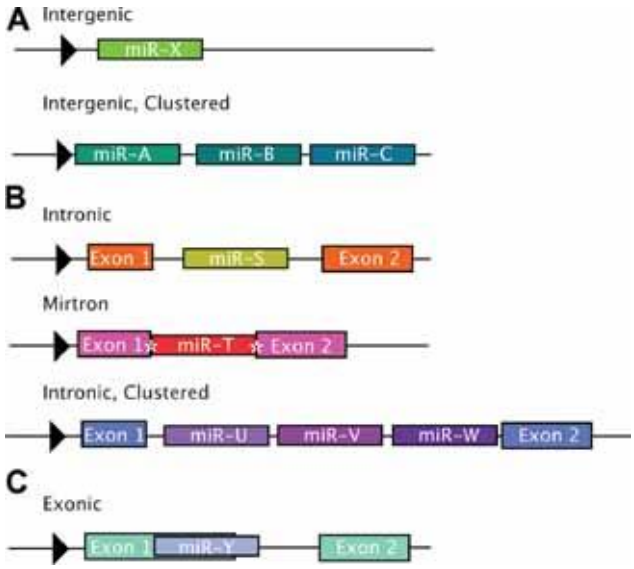

Figure 1.11: Genomic locations of miRs: A Intergenic miRs are found in genomic regions distinct from known transcription units. B: Intronic miRs are found in the introns of annotated genes, both protein coding and noncoding. In the special case of mirtrons (middle part), the intron is the exact sequence of the pre-miR with splice sites on either side (denoted by white asterisks). C: Exonic miRs are far more rare than either of the types above and often overlap an exon and an intron of a noncoding gene. (*109*).

The current model of mature miR biogenesis is shown in figure 1.12. Several observations provided indirect evidence that most of miRs are transcribed by RNA polymerase (pol) II, even though most of metazoan miRs are not polyadenylated as classical RNA pol II transcripts: miR transcript are longer than RNA pol III transcripts and have internal runs of uridine residues that would lead to

termination of maturation mediated by RNA pol III; many miRs are time-dependently expressed during development, just as pol II transcripts; observations on the expression of a chimera gene, derived from fusion between 5'end of miR gene and the open reading frame portion of a reporter gene, show a sustained strong expression like a capped pol II transcript. However it has been reported that some miRs are transcribed by RNA pol III (*110*).

The long RNA precursor with a single or several stem loops is called primary (pri)-miR. It looks like a hairpin with imperfect complementarity at the stem portion, where the mature miR lies. Then, pri-miR undergoes a cleavage by a miR processor composed of Drosha (a highly conserved RNase type III) and DGCR8 (DiGeorge syndrome critical region 8) in the nucleus. This complex generates a shorter hairpin structure, called pre-miR, of 70-100 nt that is transferred through exportin-5 to the cytoplasm, where undresses of the loop by another RNase III, Dicer, to form the double-stranded (ds) miR duplex. This ds-RNA is 22 nt in length and is composed of the mature miR and the so-called passenger miR. Generally, but not always, the latter (3' end) is degraded and the mature miR (5' end-termodinamically less stable) forms the RNA-induced silencing complex (RISC) alongside with the main components, Argonaute proteins (Agos). Hence, a specific miR addresses RISC complex towards specific mRNA targets by matching between them. Gene silencing mechanism depends on the degree of base-pairing complementarity of sequences. MiRs induce mRNA cleavage or deadenylation and then degradation in perfect complementarity condition, whereas translation repression occurs in imperfect complementarity condition. Perfect base-pairing and subsequent target degradation also takes place when exogenous short RNAs, such as siRNAs or virus RNAs, enter in the cytoplasm so as to suppress the complete target expression through the same RISC complex. Finally, the repressed target mRNAs and miRs aggregate in cytoplasmic foci, called polycomb bodies (P-bodies) where mRNA is decayed (*110, 111*). This process, well-known as RNA interference, has been discovered by Jorgensen and colleagues in 1990 (*112*) and characterized by Fire and Mello in 1998 with a first study in *C. elegans* showing

that dsRNA is much more potent at inhibiting gene expression than antisense RNA (*113*). This major breakthrough set the stage for understanding the role of miRs in development and gene regulation and conferred the Nobel Prize in Physiology and Medicine to Fire and Mello in 2006.

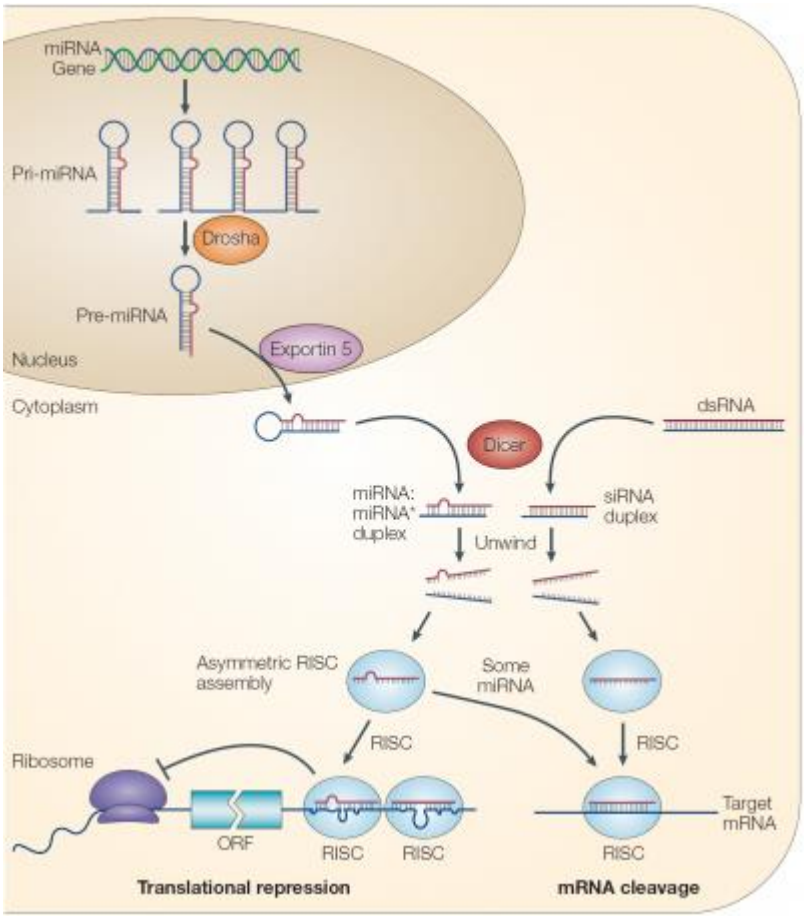

Figure 1.12: Molecular pathway of miR biogenesis and gene silencing mediated by RISC complex. *Image modified by Hannon et al. 2004* (*114*)

The base-pairing sequence, called seed sequence, is 2-8 nt long and lies at the 5′end of the mature miR. As mentioned above, the mechanism of action is mainly exerted by the matching of the miR to the mRNA 3′UTR but alternative bindings to the coding portion or to the 5′UTR have been confirmed (*115*)

Although the function of miRs needs further and deeper investigations, their involvement in cartilage and chondrocyte physiology has been established. Kobayashi et al. showed skeletal growth defects and premature death in Dicer-deficient chondrocytes derived from Dicer-null mice. Since Dicer composes the miR processor, this finding indirectly unveils the fundamental role of miRs in

chondrogenesis and bone development (*116*). Moreover, Iliopoulos and colleagues investigated the expression of 365 miRs by comparing articular cartilage derived from OA patients and normal patients without a history of joint disease. As shown in fig 1.13, they reported that 16 miRs were deregulated in OA versus normal cartilage. In particular, 9 miRs were up-regulated and 7 downregulated. These microarray-derived results were confirmed by means of Real Time PCR and Northern blot assay. Furthermore, a very interesting discovery was that some of these miRs showed a significant correlation with patient body mass index (BMI), opening a new window on the not-too-surprising involvement of miRs in obesity and inflammation.

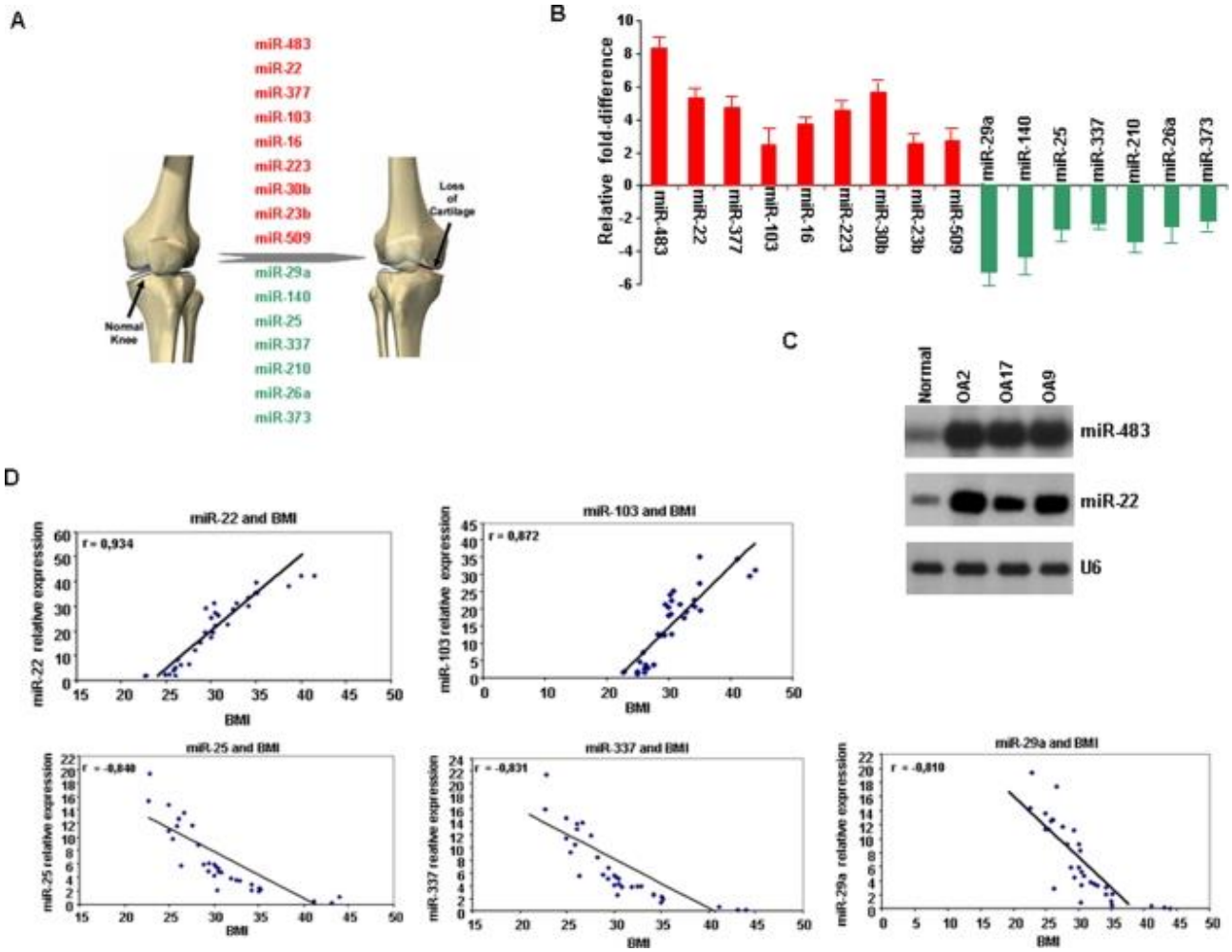

Figure 1.13: MiR gene signature in osteoarthritis (A) Up-regulated (red colour) and down-regulated (green colour) microRNAs by means of microarray platform. (B) Validation with Real-time RT-PCR. (C) Northern blot validation. MiR-483 and miR-22 expression in normal and osteoarthritic cartilage tissues (D) MiRs correlated with BMI (Body Mass Index). *Image modified by Iliopoulos et al. 2008* (*117*).

The best characterized microRNA is miR-140, whose gene is harboured between exons 16 and 17 of the E3 ubiquitin protein gene Wwp2 on chromosome 8 in mouse and chromosome 16 in human genome. Tuddenham et al. reported a study on miR-140 regarding its expression in cartilage in murine embryos and its direct target, the histone deacetylase 4 (*118*). Later, Miyaki et al. performed a gene-expression profiling through microarray technology and validation phase using quantitative polymerase chain reaction (qPCR) in human articular chondrocytes (hAC) and human mesenchymal stem cells (hMSCs). They demonstrated that miR-140 expression in MSC cultures increased in parallel with the expression of SOX9 and COL2A1 during chondrogenesis, and this expression was significantly reduced in OA tissue compared to normal cartilage. Moreover, they also showed how IL-1β is able to inhibit miR-140 expression in chondrocytes (*119*). Although, initially many researchers focused on miR-140 role in cartilage tissue and OA, then other miRs were identified as important post-transcriptional regulators of key pathways involved in OA pathogenesis. Table I shows a short summary of some miRs correlated to OA (*120*). Jones et al. showed that the over-expression of miR-9, miR-98 or miR-146 in isolated human chondrocytes suppressed IL-1β-induced TNF-α production and the modulation of miR-9 was able to modulate MMP13 secretion (*121*). Then, some scientists reported that IL-1β suppressed miR-27b expression that, in turn, resulted inversely correlated to MMP-13 production, so as to identify the linear IL-1β—miR-27b—MMP13 axis (*122*).

miR	Target	Species	Effect	Validation	Function
140	*Hdac4*	*M. musculus*	↓	+ on 3′UTR luciferase and WB	Protein deacetylation
	Cxcl12	*M. musculus*	↓	+ and − on 3′UTR luciferase and mRNA	Signalling
	IGFBP5	*H. sapiens*	↓	+ and − on mRNA	Signalling
	Smad3	*M. musculus*	↓	+ and − on 3′UTR luciferase and WB	Signalling
	ADAMTS5	*H. sapiens*	↓	+ on mRNA	Matrix-degrading enzyme
		M. musculus	↓	Gain and loss of function on mRNA, IHC and 3′UTR luciferase	
	Dnpep	*M. musculus*	↓	anti-Ago RNA immunoprecipitation, + on 3′UTR luciferase and WB	Signalling
22	*BMP7*	*H. sapiens*	↓	+ and − inhibition on WB	
	PPARα		↓	+ and − on WB	Signalling
27b	*MMP13*	*H. sapiens*	↓	+ and − on 3′UTR luciferase and ELISA	Matrix-degrading enzyme
675	*COL2A1 (indirect)*	*H. sapiens*	↑	+ and − on mRNA and WB	ECM component
34	*COL2A1 (IL1-induced)*	*H. sapiens*	↓	− on mRNA and IHC	ECM component
	iNOS (IL1-induced)				Signalling
18a	*CCN2*	*H. sapiens*	↓	+ on partial 3′UTR luciferase and ELISA	Signalling
145	*SOX9*	*H. sapiens*	↓	+ on 3′UTR luciferase and WB	Transcription
		M. musculus	↓	+ and − on 3′UTR luciferase and WB	
365	*HDAC4*	*G. gallus*	↓	+ on 3′UTR luciferase, + and − on WB	Protein deacetylation
455-3p	*ACVR2B*	*H. sapiens*	↓	+ on 3′UTR luciferase	Signalling
	SMAD2			+ on 3′UTR luciferase	Signalling
	CHRDL1			+ on 3′UTR luciferase	Signalling

Table I: miRs targeting OA and specific cartilage processes. +: overexpression; -: inhibition; WB: western blot. *Image modified from Barter and Young 2012* (*120*)

Recently the great potential of miRs as important regulators of a specific target and/or entire cellular processes has received much attention and also in the field of OA research many investigators are striving to identify the fine crosstalk between autophagy and miRs thereby discovering new intriguing molecular therapeutical targets. As shown in figure 1.15, several miRs have been reported as modulators of multiple steps along autophagy cascade. The final effect depends on miR targets. For example, ULK2, with a redundant function in case of ULK1 deficiency, is a direct target of miR-855-3p in response to chemotherapeutic drugs. Moreover, miR-855-3p shows seed-complementary sequence to other apoptosis and autophagy-related genes, such as MDM4, BCL-2, CASP-2, CASP-3, leading to the understanding that these small modulators are finely inserted in the complex regulation network of cellular processes (*123*). BECLIN-1 is targeted by several miRs, including miR-30a, miR-30d, miR-17, miR-216a, miR-365-2, miR-376a. The latter is also able to suppress ATG-4 expression thereby modulating different phases of autophagy pathway (see review (*124*)). Other findings showed that miR-375 suppresses autophagy by targeting ATG7, while its negative regulation of mTORC1 pathway is not sufficient to restore the autophagic process (*125*).

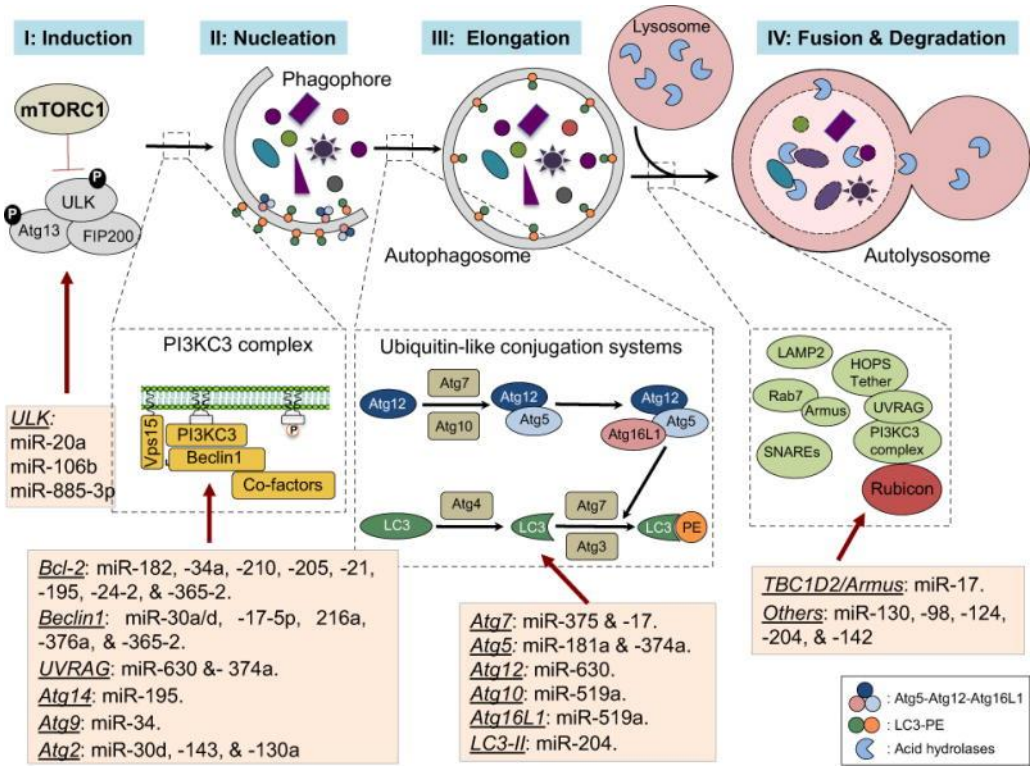

Figure 1.15: Schematic drawing of miRs-mediated regulation of the autophagic core. *Image modified from Yang and Liang, 2015* (*124*)

2. AIM OF THE STUDY

OA is the most frequent degenerative pathology of joints leading to pain and loss of function for many patients, in particular the elders. Lack of efficacy in current pharmacotherapy is spurring scientific community to spend a lot of work and resources so as to unveil new molecular targets implicated in the pathogenesis of OA. Indeed, the first step to discover new clinical treatments for preventing, slowing and possibly regressing the course of disease, consists in identifying new deregulated, pathogenic factors of OA scenario, and a valid strategy able to restore their correct pattern of expression.

Several studies have reported beneficial effects of autophagy in preventing chondrocyte death, OA-like changes in gene expression and cartilage degeneration (*100-104*) and many miRs have been identified as key modulators of autophagy pathway (*123-126*). So far, to our knowledge no relationship has been revealed between nutraceutical compounds and miR network in OA models. Thus, we have undertaken a task in order to deep our understanding on these molecular aspects implicated in the pathogenesis and the prevention of OA. Specific aims in this study were reached by evaluation of:

- ✓ the ability of HT to stimulate autophagic cascade in C-28/I2 cell line and human primary chondrocytes;
- ✓ the capacity of HT and of efficient autophagy to prevent H_2O_2-induced cell death and DNA damage in C-28/I2 cell line and human primary chondrocytes;
- ✓ the role of SIRT-1 in HT-mediated chondrocyte protection and autophagy promotion;
- ✓ the role of miR-9 as post-transcriptional regulator of SIRT-1 and modulator of the response to HT and H_2O_2 treatments in C-28/I2 cell line and human OA chondrocytes;
- ✓ the genuine relationship between miR-9 and SIRT-1;

- ✓ the role of miR-155 for successful autophagy induction in T-C28a2 cell line and human adult chondrocytes;
- ✓ target candidates of miR-155 involved in different steps of autophagy in response to changes of miR-155 levels;
- ✓ the involvement of mTOR pathway in miR-155-mediated modulation of autophagy.

2. MATERIALS AND METHODS

2.1 Hydroxytyrosol prevents chondrocyte death under oxidative stress by inducing autophagy through sirtuin 1-dependent and -independent mechanisms

Cell cultures and viability

C-28/I2 chondrocytes (*127*), kindly provided by Dr. Mary Goldring, are a human cell line representative of primary chondrocytes that has been used extensively as a reproducible ‘‘in vitro’’ model to study chondrocyte physiopathology in experiments requiring large numbers of cells. They were grown in DMEM-F12 medium supplemented with 10% fetal bovine serum as previously detailed (*128*). With local Ethics Committee approval, primary cultures of chondrocytes were used and prepared from fragments of articular cartilage obtained from two adult OA patients undergoing knee arthroplasty as described (*128*). The cells were incubated in the absence or presence of 100 µM H2O2 for 2 to 48 h as indicated in the various figures; 100 µM HT (from Cayman Chemical) was added 30 min before H2O2, on the basis of a published previous study (*129*). Autophagy inhibitors 3-methyladenine and cloroquine and the autophagy inducer rapamycin (all from Sigma-Aldrich) were used at 10 mM, 50 µM and 500 nM, respectively, and were added to cell medium 30′ before other treatments. Control cells received the corresponding volume of vehicle. Viable cells were directly counted following the trypan blue exclusion test. Dead cells including the dye were reported as a percentage of the total number of cells. The use of the human cells in this study was in accordance with the Helsinki Declaration of 1975.

Western blotting

In western blotting procedure equal amounts of cell extract were subjected to electrophoresis in 15% gels, blotted onto nitrocellulose membranes as previously described (*130*), and probed with primary antibody at 4°C overnight. The following antibodies were used: anti-LC3A/B (Cell

Signaling Technology), anti-p62 (Santa Cruz Biotechnology), anti-β-actin (Sigma-Aldrich), anti-SIRT-1 (Santa Cruz Biotechnology).

After washes, membranes were incubated with horseradish peroxidase-conjugated anti-rabbit (Cell Signaling Technology) or anti-mouse (Santa Cruz Biotechnology) IgG for 1 h. The chemiluminescent signals were detected using an ECL system (LuminataTM Crescendo, Millipore). β-actin was used as loading control. A representative image of visualized immunoreactive bands and densitometric analysis show the relative intensity of protein expression.

Detection of γH2AX

The extent of oxidative DNA damage and in particular the amount of double strand breaks tagged by the phosphorylation of the histone H2AX were evaluated by flow cytometer on cells previously fixed with 2% PFA and then post-fixed with 90% methanol on ice, as described before (*129*). After a treatment with 0.02 U/ml chondroitinase ABC (Sigma) in Tris/HCl pH 8, 20' at 37°C in a humid chamber and a step of blocking of nonspecific bindings (with 150µl 5% BSA in TBS with the addition of 0.1% Triton), a mouse anti-γH2AX monoclonal antibody (Millipore 05–636, IgG1, at 5 µg/ml) was incubated overnight at 4°C and then revealed by an Alexa Fluor 647 Donkey anti-mouse IgG (Jackson Immunoresearch). Specificity was checked by running an isotypic control for each sample under analysis: cells were probed with normal mouse immunoglobulins of the same isotype (IgG1) and at the same concentration of the anti-γH2AX antibody. Analyses were performed by using a FACS Canto II flow cytometer (BD) on at least 5000 cells per sample. For each sample the level of "median channel of fluorescence intensity (MCFI) increment" of γ-H2AX staining was calculated as the difference between the median channel of fluorescence intensity of the samples stained for γH2AX and that of the same sample probed with the isotypic control.

Immunocytochemical detection of autophagy and mitophagy

To carry out immunocytochemical studies C-28/I2 chondrocytic cells were seeded in chamber slides. Autophagy was assessed by staining the cells with monodansylcadaverine (MDC) (Sigma-

Aldrich), a lysosomotropic agent that accumulates in late autophagic vacuoles as a function of the acidity of their content. MDC was used at 50 µM on viable cells 1 hour at 37°C. Then cells were washed, fixed with 2% PFA 10 min at RT and then few drops of an anti-fading agent (50 mg/ml 1,4-diazabicyclo[2.2.2]octane, SIGMA, in 90% glycerol in Tris-HCl, 0.1 M pH 8.0) were added before mounting the coverslips. Pictures were taken with a Nikon ELIPSE 90i Fluorescence Microscope equipped with a NIS software using the UV-2A filter set. Filter settings were as follows: excitation (EX): 330-380 nm, dichroic mirror (DM) at 400 nm and barrier filter (BA) for emission at 420 nm.

Immunofluorescence on cells grown on glass slides was used to detect the extent of "mitophagy" as assessed by colocalization of LC3 A/B positive autophagic vacuoles and the mitochondrial marker TOM20. At the end of the treatment, C-28/I2 cells were carefully washed, gently fixed with 2% PFA for 10 min and then the slides were stored at 4°C in PBS until processing.

Each condition was prepared in duplicate to allow for comparison of the cells stained with antibodies to LC3 A/B and TOM20 with cells stained with control antibodies. In the immunocytochemical protocol primary and secondary antibodies were diluted in 3% BSA in TBS with the addition of 0.1% Triton. Between each step, two washings with 3%BSA TBS left for 5′ at RT under continuous stirring were performed to remove unbound reagents.

Before immunocytochemistry, further steps of permeabilization were carried out using a 10′ treatment with ice-cold 90% methanol (100µl per well) followed by a treatment with 0.02 U/ml chondroitinase ABC (Sigma) in Tris/HCl pH 8, 20′ at 37°C in a humid chamber. After a step of blocking of nonspecific bindings (with 150µl 5% BSA in TBS with the addition of 0.1% Triton), primary antibodies were delivered at the same time and left overnight at 4°C: a rabbit polyclonal anti-LC3A/B antibody (Cell signaling) and a mouse monoclonal anti-TOM20 antibody (Santa Cruz Biotechnology). Immunodetection was performed by addition to all wells (sample and controls) of a biotinylated goat anti-rabbit polyclonal antiserum (DAKO) that was left for 30′. Then, to reveal

the stained proteins, the cells underwent addition of an Alexa Fluor 555 conjugated streptavidin (Molecular Probes) together with an Alexa Fluor 488 polyclonal donkey anti-mouse IgG (H+L) (Molecular Probes). At the end of a 30′ incubation at RT, cells were washed and then underwent nuclear counterstaing with DAPI (Molecular Probes) left for 30′ at RT. Finally, ProLong® Diamond Antifade Mountant (Molecular Probes) was applied to fluorescently labeled cells before image acquisition at the Nikon ELIPSE 90i Fluorescence Microscope. Distinct images were acquired for the green (TOM20), red (LC3A/B) and blue (nuclei) fluorescence and then merged to evidence sequestering of damaged mitochondria into autophagosomes. TOM20 green fluorescence was acquired with a FITC filter set (Ex=465-495; DM=505; BA=515-555); LC3A/B red fluorescence was acquired with a TRITC filter set (Ex=540/25; DM=565; BA=605/55); DAPI blue nuclear counterstaining was acquired with a UV-2A filter set as described above. Confirmation of mitophagy occurrence, was also carried out exploiting confocal laser scanning microscopy, using a NIKON confocal microscope system A1 equipped with a Nikon Eclipse Ti microscope and an Argon Ion laser for a 488 nm line and a DPSS laser for a 561 nm line. Emission signals were detected by a photomultiplier tube (DU4) preceded by emission filters BP 525/50 nm and BP 595/50 nm for AlexaFluor 488 and AlexaFluor 555 respectively. Laser scanning, image acquisition and processing were performed with Nikon Imaging Software NIS Elements AR-4 (Nikon Inc., USA). Fields of 210 µmx210µm (acquired with a Nikon plan apo 60x1.40 oil objective) were acquired and analyzed.

Immunocytochemical analysis of SIRT-1 protein

The level and subcellular localization of SIRT-1 were investigated by a colorimetric detection system, using the Supersensitive link-label (biotin based) IHC kit (Biogenex) and Fast red substrate (Biogenex), essentially as described by the manufacturer. The immunodetection was carried out on cells treated, fixed and permeabilized with both methanol and chondroitinase ABC as described above. SIRT-1 was detected with a mouse monoclonal anti-SIRT-1 antibody (LS-Bio) and signal

specificity was checked by comparison with isotype controls, i.e. mouse IgG1 monoclonal (MAB002). At the end, to facilitate their automatic counting, the cells were treated with a DAPI nuclear counterstaining. Then, an automatic analysis procedure was employed exploiting the NIS software that combined colorimetric and fluorescent staining to easily count the cells. At least four fields (with 40-160 cells each) were counted for each condition. For each field the percentage of cells with SIRT-1 localized in the nucleus was assessed. This experiment was carried out 4 times. To compare the different culture conditions, the average values of the four fields were taken into account for each experiment.

RNA interference

For transient transfection experiments, C-28/I2 cells were seeded at a density of 20000/cm2 in 6-well plates in antibiotic-free growth medium. When the cells reached 70% confluence, they were transfected with 25nM ON-TARGETplus Human Sirt1 siRNA or ON-TARGETplus non-targeting pool (Dharmacon) by Lipofectamine® RNAiMAX Reagent in Opti-MEM® Medium (Life Technologies) according to manufacturer's instructions. The cells were incubated for 24 hours before evaluating mRNA expression or protein expression.

RNA isolation, cDNA synthesis and Real-Time PCR

Total cellular RNA was extracted with 700 µl TRIZOL (Invitrogen), according to manufacturer's instructions. The RNA pellets were treated with DNAse (DNA-free, Ambion, Austin, TX) and, after buffer exchange, were quantified by using RiboGreen RNA quantitation reagent (Molecular Probes, Eugene OR). The same quantity of total RNA (100ng) was reverse transcribed by using random primers and the reagents provided with the Superscript VILO System for RT-PCR (Invitrogen). The cDNA mixture (2 µl) was used in Real time PCR analysis in a LightCycler Instrument (Roche Molecular Biochemicals) by means of the QuantiTect SYBR Green PCR kit (TaKaRa, Japan) with the following protocol: initial activation of HotStart Taq DNA polymerase at 95°C for 10″, followed by amplification (40 cycles: 95°C for 5″ followed by appropriate annealing temperature

for each target as detailed below kept for 20″). The protocol was concluded by melting curve analysis to check amplicon specificity. The following primers were used: human p62 forward AAG-CCG-GGT-GGG-AAT-GTT-G and reverse GCT-TGG-CCC-TTC-GGA-TTC-T (Sigma-Aldrich); human LC3 forward AGC-ATC-CAA-CCA-AAA-TCC-CG and reverse TGA-GCT-GTA-AGC-GCC-TTC-TA (Sigma-Aldrich); human GAPDH forward TGG-TAT-CGT-GGA-AGG-ACT-CA and reverse GCA-GGG-ATG-ATG-TTC-TGG-A (Invitrogen). Primers were annealed at 59°C, except GAPDH at 56°C. The amount of mRNA was normalized for GAPDH expression in each sample and referred to untreated, control sample.

Statistical analysis

All the experiments shown were performed independently at least three times with comparable results. All the data presented in graphs are expressed as means ± SEM. Means of groups were compared with GraphPad Prism 5 statistical software (GraphPad Software, Inc.) and analyzed for statistical significance (* = $p<0.05$, ** = $p<0.01$, *** = $p<0.001$). Differences were considered statistically significant at $p<0.05$.

2.2 MicroRNA-9 mediates oxidative stress-induced cytotoxicity in chondrocytes by targeting SIRT-1

Cell transfection and experimental design

Primary chondrocytes and C-28/I2 cells were seeded in 6-well plates at a density of 2 X 10^5 cells/well and in 96-well plates at a density of 1,28 X 10^3 cells/well without antibiotics. The next day, Ambion® Anti-miR™ miRNA Inhibitors, negative control #1 (antimiR-NC) (50nM) and antimiR-9 (50nM), and Ambion® Pre-miR™ miRNA Precursors, negative control #1 (premiR-NC) (50nM) and premiR-9 (Life Technologies) (50nM) were transfected into cells by using Lipofectamine RNAiMAX (Invitrogen) for 24 h. Anti-miR miRNA Inhibitors are chemically modified, single stranded nucleic acids designed to specifically bind to and inhibit endogenous miR

molecules. These pre-miRNA precursor molecules are small, chemically modified double stranded RNA molecules designed to mimic endogenous mature miRs.

C-28/I2 cells were co-transfected with either antimiR-NC or antimiR-9 and either ON-TARGETplus Human Sirt1 siRNA or ON-TARGETplus non-targeting pool by Lipofectamine® 3000 Reagent in Opti-MEM® Medium (Life Technologies) according to manufacturer's instructions.

Bioinformatics prediction of miR candidates targeting SIRT-1

TargetScan and miRWalk databases were used to predict miR candidates targeting SIRT-1 by detecting the complementarity between their seed sequences and specific sequences in SIRT-1 mRNA.

RNA isolation, cDNA synthesis and real-time PCR (qPCR)

Samples were collected as described above.

MicroRNA reverse transcription was conducted with TaqMan MicroRNA RT kit (Life Technologies) and qPCR was performed with TaqMan Universal Mastermix (Life Technologies) following kit instructions. Mature miR quantification was performed using TaqMan MicroRNA Assays for miR-9 and U6 snRNA (internal control), according to manufacturer recommended protocols (Applied Biosystems). Ten nanograms of total RNA, 50 nM stem-loop RT primer, RT buffer, 0.25 mM each dNTP, 3.33 units/ml MultiScribe reverse transcriptase (RT), and 0.25 units/ml RNase inhibitor were used in 15-μL RT reactions for 30 min at 16 °C, 30 min at 42 °C, and 5 min at 85 °C, using the TaqMan MicroRNA reverse transcription kit (Applied Biosystems). For real-time PCR, 1.33 μL (1:15 dilution) of cDNA, 0.2 mM TaqMan probe, 1.5 mM forward primer, 0.7 mM reverse primer, and TaqMan Universal PCR Master Mix (Applied Biosystems) were added in 20-μL reactions for 10′ at 95 °C and 40 cycles of 15 sec at 95 °C and 1′ at 60 °C.

Protein isolation and Western Blotting

Western blotting procedure was performed as described above.

Determination of caspase activity

Caspase activity was measured by the cleavage of the fluorogenic peptide substrate Ac-Asp-Glu-Val-Asp-7-amido-4-methylcoumarin (Ac-DEVD-AMC) as previously detailed (*128*). Since the sequence DEVD represents a substrate for caspase-3 and other effector caspases, this activity has been referred to as caspase 3-like activity. Caspase activity was expressed per mg protein, and normalized to untreated controls.

Luciferase reporter assay

To confirm that the regulation of SIRT-1 expression is mediated through targeting of its 3′-UTR by miR-9, we used pEZX-MT06 reporter vector carrying miR binding sequences of 3′UTR of SIRT-1 gene (GeneCopoeia, Rockville, MD) in combination with Luc-Pair™ Duo-Luciferase HS Assay Kit (GeneCopoeia, Rockville, MD). This vector has dual reporters including one for regulatory detection (firefly) and another for internal control and signal normalization (Renilla). C-28/I2 cells were co-transfected with either plasmid carrying wild type 3' UTR of SIRT-1 (3' UTR wt), or 3' UTR without the seed-complementary sequence (identified by TargetScan) (3' UTR mut1), or 3' UTR without the seed-complementary sequence and the 3'pairing sequence (identified by TargetScan) (3' UTR mut2), and either premiR-9 or premiR-NC. The transfection was carried out in antibiotics free medium using Lipofectamine 3000 according to the manufacturer's protocol (Invitrogen). The dual luciferase activity of the transfected cells were measured by using WallacVictor2 1420. The results were expressed as percentage of normalized firefly luciferase activity against Renilla luciferase activity. Three individual transfections were carried out and the results were expressed as percentage reduction of luciferase activity in premiR-9 transfected cells in relation to 100% activity for cells transfected with Pre-miR negative control.

Statistical analysis

To evaluate normal distribution of the data, we performed the Kolmogorov-Smirnov test and homogeneity of variance using Bartlett's test. Statistically significant differences between 2 groups were determined with Student's unpaired t-test. P values less than 0.05 were considered significant.

2.3 MicroRNA-155 suppresses autophagy in chondrocytes by modulating expression of autophagy proteins

Cell culture of human chondrocytes

Normal human cartilage was harvested during autopsy from the femoral condyles and the tibial plateaus from 4 adult donors (age < 50) without history of joint diseases and with macroscopically normal cartilage surfaces. The collection of human tissue was under the approval by the Scripps Human Subjects Committee. Chondrocytes were isolated as described previously (*131*) and cultured in DMEM supplemented with 10% calf serum with antibiotics. First or second-passage cells were used in this study.

Immortalized human primary chondrocytes, T/C-28a2 (*127*), were obtained from Dr. Mary Goldring and maintained in Dulbecco's modified Eagle's medium (DMEM) (Life Technologies, NY, USA) supplemented with 10% Fetal Bovine Serum (FBS) (Life Technologies), with antibiotics at 37°C in the presence of 5% CO_2.

Cell transfection and experimental design

Primary chondrocytes and T/C28a2 cells were seeded in 24-well plates at a density of 5 X 10^4 cells/well and in 96-well plates at a density of 1 X 10^4 cells/well without antibiotics. The next day, LNA™ GapmeR control (LNA nc) and LNA miR-155 (40nM) (Exiqon) and Mission® microRNA mimic control (mimic nc) and mimic miR-155 (10nM) (Sigma Aldrich) were transfected into cells using Lipofectamine RNAiMAX (Invitrogen) for 24 h.

To assess autophagic flux, time course experiments were conducted in cells stimulated with rapamycin (RAPA, 50nM), 2-deoxy-glucose (2-DG, 5mM) or vehicle in the presence or absence of chloroquine (CQ, 25μM). Maximal induction of autophagy was achieved at different time points depending on the cell type and treatment employed; subsequently, these specific time points were selected for miR-155 functional experiments as indicated for each experiment. Briefly, primary human chondrocytes were treated with RAPA for 12 h or maintained for 24 h under basal conditions. T/C28a2 cells were treated with RAPA or 2-DG for 4 and 2 h, respectively. Then, RNA or protein samples were collected for qPCR and western blot analysis, or cells were subjected to Cyto-ID dye detection as described below. Doses of the various agents were selected to be non-toxic based on prior studies (*132-134*). In addition, at completion of each experiment cell morphology was monitored and there was no apparent cell shrinkage, rounding or detachment from the culture plates.

Bioinformatics prediction of miR-155 targets

TargetScan and miRWalk databases were used to predict potential targets of miR-155 directly and indirectly involved in the autophagic pathway.

RNA isolation, cDNA synthesis and real-time PCR (qPCR)

Samples were collected in Qiazol (Qiagen) at room temperature and after the addition of chloroform, centrifuged at 12,000*g* at 4°C for 15′. RNA was extracted by using miRneasy minikit (Qiagen) to separate small RNAs from total RNA. Two different fractions were used to assess miR-155 levels and gene expression of potential miR-155 targets, respectively. MicroRNA reverse transcription was conducted with TaqMan MicroRNA RT kit (Life Technologies) and qPCR was performed with TaqMan Universal Mastermix (Life Technologies) following kit instructions. Specific primers for miR-155 and RNU48 (internal control) were purchased from Life Technologies. RNA reverse transcription and qPCR were performed with TaqMan Reverse Transcription kit (Life Technologies) and LightCycler 480 Probes Master (Roche), respectively.

Pre-designed primers for *GAPDH* (internal control), *FOXO3, RICTOR, ATG14, ATG3, GABARAPL1, MAP1LC33, ULK1* and *ATG5* were obtained from Life Technologies.

Protein isolation and Western Blotting

Cells were lysed in RIPA buffer, sonicated at 4°C and centrifuged at 12,000*g* for 15′. Proteins were separated on 4%-20% SDS-polyacrylamide gels and transferred to nitrocellulose membranes (Amersham), blocked in Odyssey blocking buffer 1X (LI-COR Bioscience) for 60′ at room temperature and incubated overnight with primary antibodies diluted in Odyssey Blocking Buffer 1:1 with phosphate-buffered saline-PBS and 0.1% Tween 20. Antibodies for RICTOR (1:1000), ULK1 (1:1000), FOXO3 (1:1000), ATG14 (1:1000), P-AKT (Ser473) (1:2000), AKT (1:1000), ATG5 (1:1000) ATG3 (1:1000), P-S6 (S235/S236) (1:2000), S6 (1:1000), LC3A/B (1:1000) were purchased from Cell Signaling. Antibody for Gabarapl1 (1:500) was purchased from Fisher Scientific and that for β-actin (1:5000) from Abcam. After three washes with Tris-buffered saline–0.1% Tween (TBST), membranes were incubated with IR Dye labelled secondary antibody (goat anti-Mouse 1:10000 and goat anti-Rabbit 1:5000, LI-COR Biosciences) diluted in Odyssey Blocking Buffer 1:1 with PBS, 0.1% Tween 20 and 0.01% SDS. Subsequently, the membranes were washed 3 times with TBST, kept in water and visualized by Odyssey Scanner (LI-COR Biosciences). Densitometry was performed using LI-COR Odyssey Software Version 4.0 (LI-COR Biosciences).

Cyto-ID dye detection

Cyto-ID assay (Enzo) measures autophagic vacuoles and monitors autophagic flux in live cells using a dye that selectively labels autophagic vacuoles. The dye has been optimized through the identification of titratable functional moieties that allows minimal staining of lysosomes while exhibiting bright fluorescence upon incorporation into pre-autophagosomes, autophagosomes, and autolysosomes (autophagolysosomes) (*135*). Fluorescence was measured at 360 Ex/460 Em (Hoechst 33342 nuclear stain) and 480 Ex/530 Em (Cyto-ID green autophagy detection reagent)

with a plate reader (TECAN Safire II from Tecan Systems). Cyto-ID intensity was first normalized to Hoechst intensity and then to the control sample in order to evaluate the fold changes.

Statistical analysis

The data are reported as mean ± standard deviation (SD) of the indicated number of independent experiments. Some experiments were conducted with primary chondrocytes samples from four different donors, each performed either in duplicate or in triplicate. All datasets were assessed for normal population distribution using the Kolmogorov-Smirnov test, and homogeneity of variance using Bartlett's test. Analysis of variance (ANOVA) was used to compare group means from datasets that met all the assumptions of this test, followed by planned pairwise comparisons using the Bonferroni procedure for these selected pairs of groups. The overall ANOVA tests were performed at the alpha = 0.05 level of significance, and the alpha levels of the subsequent individual comparisons were adjusted so as to preserve the familywise error rate at the 0.05 level. Not-normally distributed populations were compared using the nonparametric Kruskal-Wallis test with Dunn’s method. Statistical analysis was conducted using Prism (GraphPad Software version 5.0). $P < 0.05$ was considered statistically significant.

4 RESULTS

4.1 Hydroxytyrosol prevents chondrocyte death under oxidative stress by inducing autophagy through sirtuin 1-dependent and -independent mechanisms

Hydroxytyrosol leads to autophagy induction in C-28/I2 chondrocytes

In a previous work with primary chondrocyte cultures exposed to oxidative stress, we found that HT protects against DNA damage and cell death (*129*). To investigate the cellular and molecular mechanisms involved in these HT beneficial effects, we have performed a new study with C-28/I2 chondrocytes, which are widely used as representative of primary chondrocytes and allow abundant availability of cell material. First we have evaluated the ability of HT to stimulate autophagy. In order to monitor the autophagic process, two proteins widely used as markers of autophagy have been considered: the mammalian ortholog of yeast Atg8, light chain 3 (LC3), and SQSTM1/P62 (*95*). LC3 can be detected by western blot in non-lipidated and lipidated forms, termed LC3-I and LC3-II, respectively. This protein participates in phagophore assembly and, conjugated with phosphatidylethanolamine, in autophagosome formation. On the other hand, P62 operates as a molecular link between LC3 and ubiquitinated substrates, thus docking them to autophagy degradation. Decreased P62 levels, in combination with increased LC3-II, are commonly associated with autophagy activation. In the current study, C-28/I2 cells were exposed to oxidative stress by the treatment with hydrogen peroxide for 2 h, in presence or absence of HT in the culture medium. HT induced LC3-II expression markedly and independently of the condition of oxidative stress (Fig. 4.1A and B). At the same time the level of P62 protein was reduced by HT treatment (Fig. 4.1A and C). These findings indicate that HT is able to stimulate the autophagic process.

Monodansylcadaverine (MDC) is an autofluorescent compound that stains late autophagic compartments (in particular autolysosomes). In our experiments we observed a reduced MDC

fluorescence in C-28/I2 chondrocytes under oxidative stress conditions, 2 h after treatment with hydrogen peroxide (Fig. 4.1D). An opposite effect was shown in presence of HT. Moreover in this condition we assessed the increase in LC3-II puncta that colocalize with mitochondria, highlighted with an antibody specific for the translocase of outer mitochondrial membrane, a protein with a Mw of 20 kDa (TOM20). Confocal laser scanning microscopy confirmed these findings, via a marked increase of these colocalized signals, evident as a yellow staining (Fig. 4.1E). Thus HT treatment promotes mitophagy along with autophagy in C-28/I2 cells.

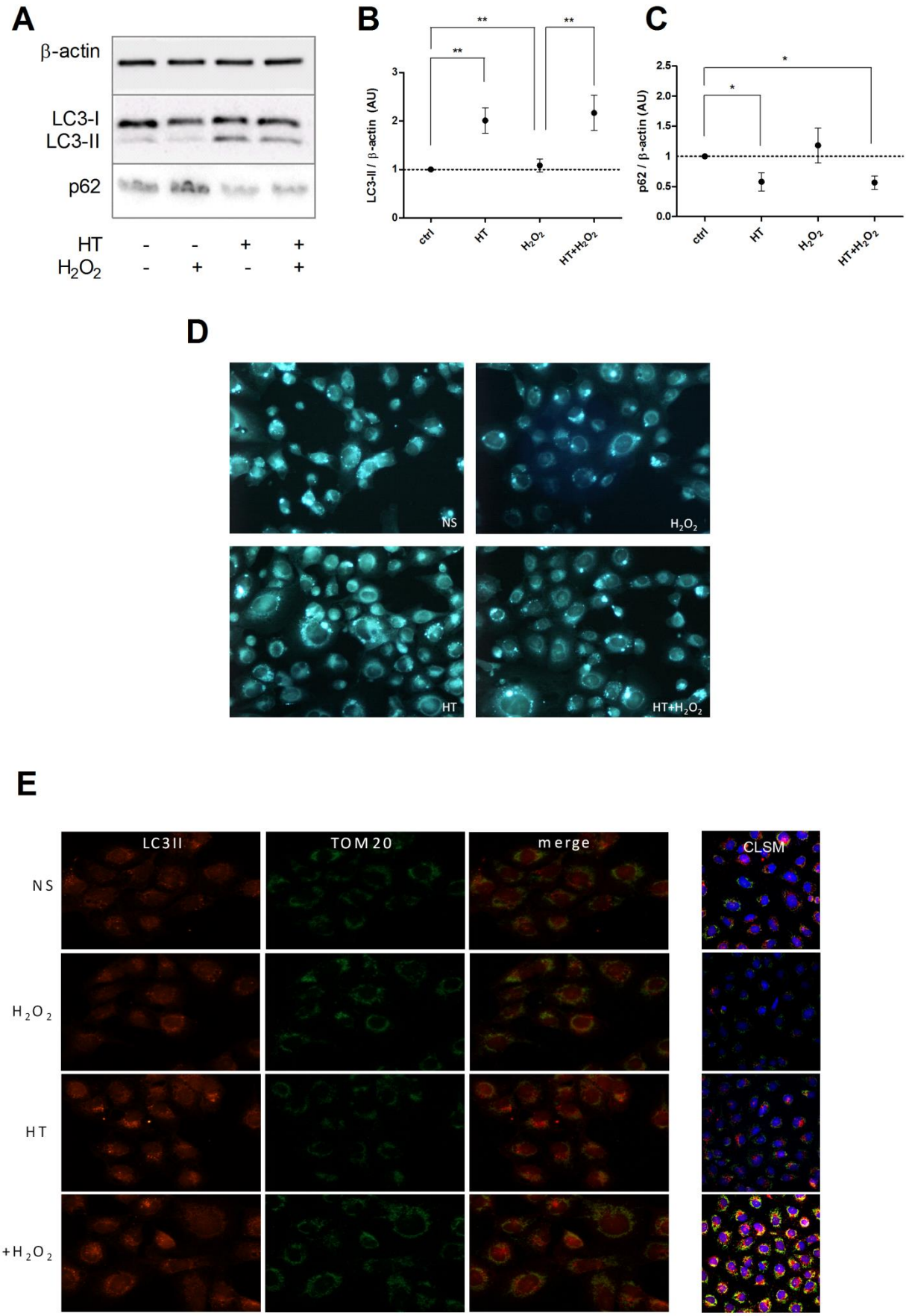
A
β-actin
LC3-I
LC3-II
p62
HT - - + +
H2O2 - + - +
B
LC3-II / β-actin (AU)
ctrl
HT
H2O2
HT+H2O2
C
p62 / β-actin (AU)
ctrl
HT
H2O2
HT+H2O2
D
NS
H2O2
HT
HT+H2O2
E
LC3II
TOM20
merge
CLSM
NS
H2O2
HT
HT+H2O2

Figure 4.1: Hydroxytyrosol stimulates autophagy in C-28/I2 chondrocytes. C-28/I2 cells were pre-incubated in the absence or in the presence of HT for 30 min before addition of H_2O_2. After a further 2h incubation, cells were harvested for LC3, P62 and β-ACTIN detection by western blotting. Representative images (A) and relative quantification for LC3-II/β-ACTIN (B) and P62/β-ACTIN (C) ratios are shown. Values are expressed as means ± SEM, *p<0.05, **p<0.01. Alternatively in immunocytochemical studies, C-28/I2 cells were stained at the end of incubation with monodansylcadaverine (D: 200x, original magnification), with antibodies to LC3 A/B and TOM20 (E). DAPI was used as a nuclear counterstaining. The labeled cells were visualized by fluorescence microscopy (left pictures, showing separate and merged TOM20 and LC3 signals, 400x, original magnification) and confirmation of mitophagy was also carried out with confocal laser scanning microscopy (CLSM, right column, 180x, original magnification:). Representative fields of control, non-stimulated cells (NS) or cells treated with HT and/or H_2O_2 are shown.

Autophagy protects C-28/I2 cells from oxidative stress-induced DNA damage and cell death

Next we evaluated the ability of HT and autophagy to protect C-28/I2 chondrocytes against DNA damage and cell death under conditions of oxidative stress. In order to assess the degree of DNA damage and cell death, a phosphorylated form of histone H2AX referred to as γH2AX was detected as a marker of DNA double strand breaks, while the percentage of dead cells was estimated by trypan blue exclusion test. We found that HT as well as the autophagy inducer rapamycin significantly reduced the DNA damage elicited by hydrogen peroxide after 2 h treatment (Fig. 4.2A). Moreover both compounds were able to decrease the percentage of dead C-28/I2 cells after 24 h (Fig. 4.2B). Conversely the pro-survival effect of HT was abolished in presence of autophagy inhibitors; in particular we used 3-methyladenine and cloroquine, operating at different steps in the autophagic process. These compounds alone did not change cell viability significantly. Thus, these data indicated that HT exerts its cell protective action by autophagy induction.

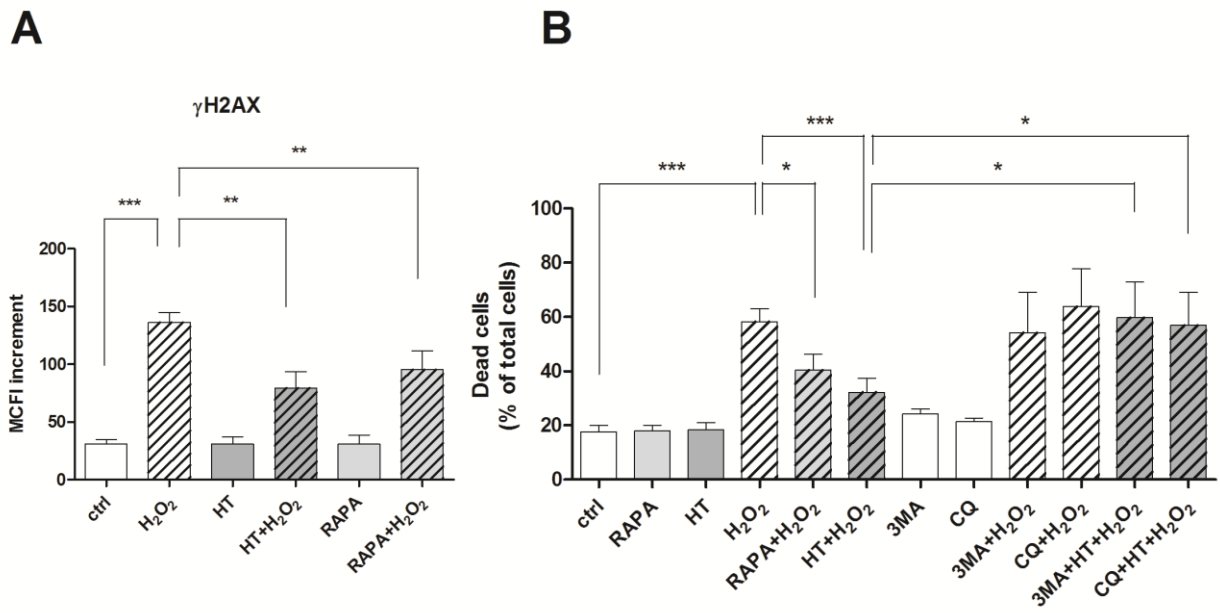

Figure 4.2: Autophagy protects C-28/I2 cells from oxidative stress-induced DNA damage and cell death. C-28/I2 cells were pre-treated with or without hydroxytyrosol (HT), rapamycin (RAPA), 3-methyladenine (3MA) or cloroquine (CQ) for 30 min before addition of H_2O_2. After further 2h incubation, cells were evaluated for the extent of DNA damage by detection of γH2AX and calculation of the increment of the mean channel fluorescence intensity (MCFI) over basal fluorescence (A). Alternatively after 24 h incubation with or without H_2O_2, cells were counted to assess cell viability by trypan blue exclusion test (B). Values are expressed as means ± SEM, *p<0.05, **p<0.01,***p<0.001.

HT modulates autophagy by SIRT-1-dependent and –independent mechanisms

SIRT-1, belonging to the sirtuin family of proteins, is considered a "longevity" and "anti-aging" factor and known to play a regulatory role in a variety of cellular processes, including autophagy (*46*). Moreover, according to recent evidence, it can exert a pivotal role in the protection of cartilage from OA (*52*). Therefore we have investigated the involvement of SIRT-1 in HT action. Immunostaining showed that this protein is localized both in the nucleus and cytosol of control, untreated C-28/I2 chondrocytes (Fig. 3A). Oxidative stress inducted in cells by hydrogen peroxide reduced nuclear signal compared with control, whereas HT, alone or in association with hydrogen peroxide, was able to significantly increase SIRT-1 level and nuclear localization (Fig. 4.3A and B).

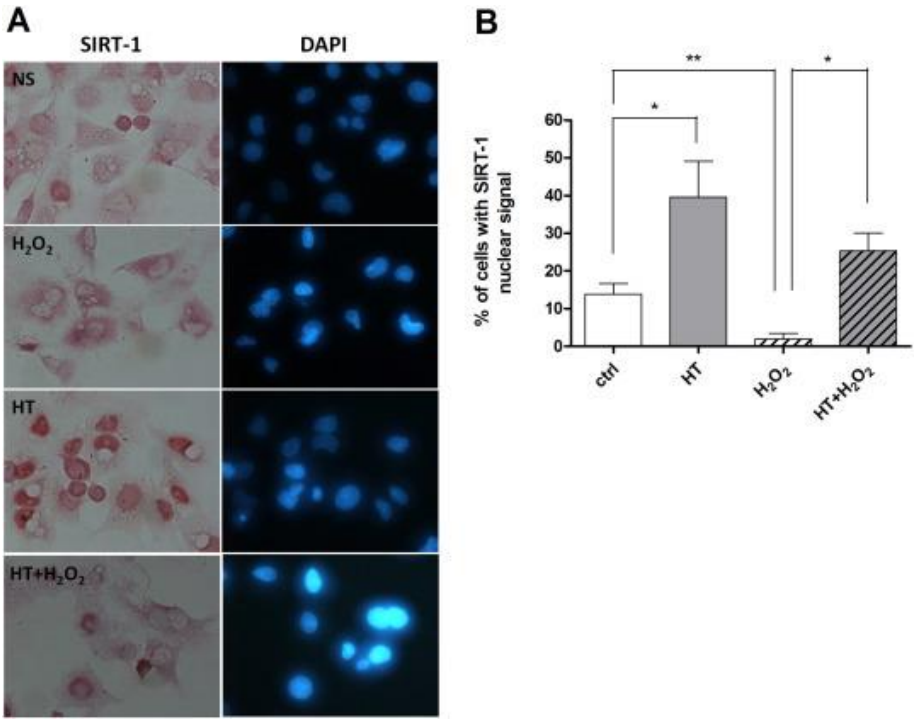

Figure 4.3: Hydroxytyrosol increases SIRT-1 nuclear localization**.** C-28/I2 cells were pre-incubated in the absence or in the presence of hydroxytyrosol (HT) for 30 min before addition of H_2O_2. After further 2h incubation, cells were processed for immunodetection of SIRT-1 and finally treated with a DAPI nuclear counterstaining. The labeled cells were visualized and representative fields of control cells (NS) or cells treated with HT and/or H_2O_2 are shown (**A**: 400x, original magnification). Quantitative analysis of the percentage of cells with SIRT-1 localized in the nucleus was assessed as described in Materials and Methods (**B**). Data are means ± SEM, *p<0.05, **p<0.01.

The role of this modulation was evaluated by silencing the gene and testing the cell survival ability after oxidative stress in presence or absence of HT. The level of SIRT-1 protein in C-28/I2 chondrocytes was reduced by more than 60% after silencing procedure compared with control cells (Fig. 4.4A and B). The knockdown of SIRT-1 did not affect cell survival significantly under basal conditions or after hydrogen peroxide treatment, but it was able to abolish the protective effect of HT after oxidative stress (Fig. 4.4C).

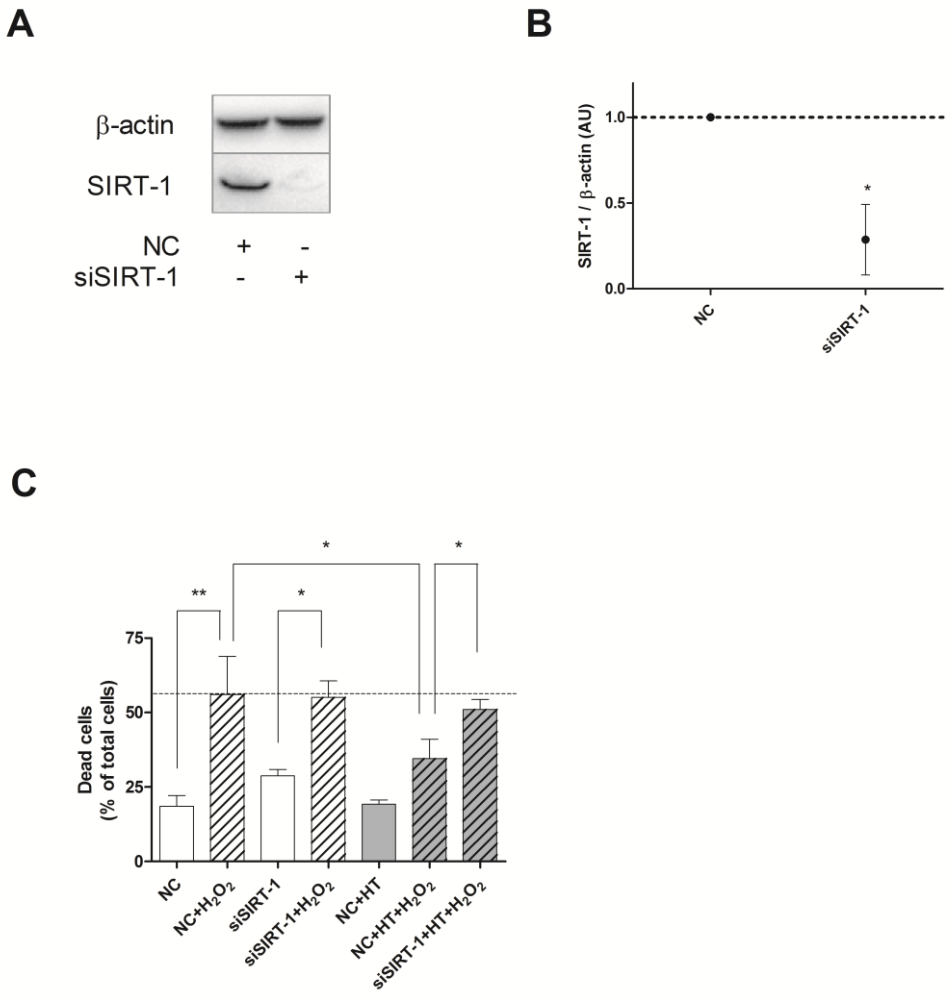

Figure 4.4: SIRT-1 is required for the cytoprotective effect of hydroxytyrosol under oxidative stress. (A, B) C-28/I2 cells were transfected for 48h with SIRT1-siRNA (siSIRT-1) or siRNA negative control (NC). SIRT-1 levels were determined by Western blotting. Representative images (A) and relative quantification for SIRT-1/β-actin ratio (B) are shown. (C) 24h after transfection, C-28/I2 cells were treated with H_2O_2 for 24h. Hydroxytyrosol (HT) was added 30 min before H_2O_2. At the end of incubation, cells were counted to assess cell viability by trypan blue exclusion test. Values are expressed as means ± SEM, *p<0.05, **p<0.01.

Then, to assess the role of SIRT-1 in autophagy stimulation, C-28/I2 cells were treated with cloroquine for 24 h, so as to block autophagy flux and allow accumulation of the autophagic protein LC3-II, thus affording a better observation by western blot analysis. Figure 4.5A and 4.5B show that LC3-II accumulated in C-28/I2 chondrocytes treated with HT, but not in SIRT-1 silenced cells. LC3-II level was significantly higher in HT-treated cells with respect to correspondent SIRT-1 knockdown cells already in the absence of cloroquine, and increased further in the presence of

cloroquine. SIRT-1 silencing alone did not affect LC3-II content. Therefore the ability of HT to induce LC3-II formation depends on SIRT-1 expression.

Subsequently, we tested the effect of HT on p62 and LC3 gene expression in order to investigate an additional, possible mechanism of autophagy modulation employed by SIRT-1. While no notable change in LC3 transcript content was observed (data not shown), HT significantly induced an up-regulation of p62 mRNA (Fig. 4.5C). However the modulation is not dependent on SIRT-1 because the HT ability to induce p62 expression was preserved in SIRT-1 knocked-down C-28/I2 cells. Therefore HT appears to stimulate the autophagic process by affecting both SIRT-1 dependent and independent pathways.

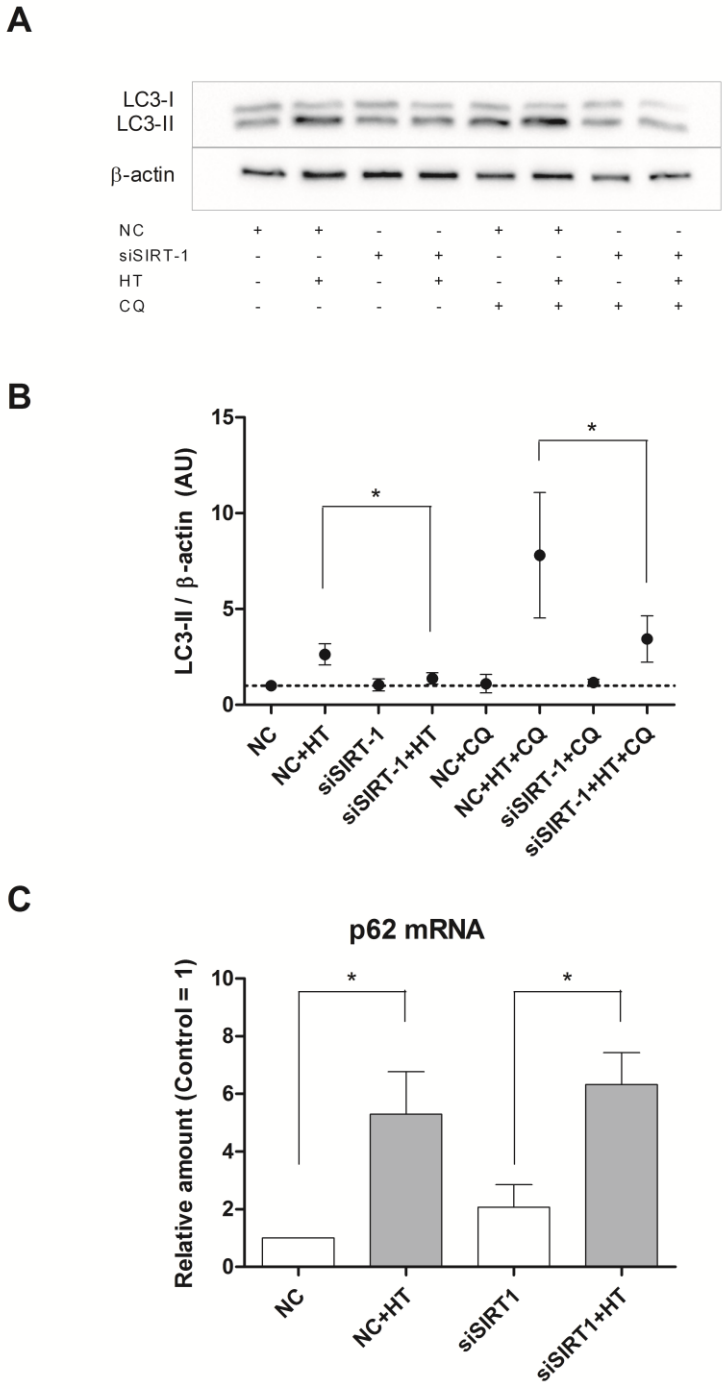

Figure 4.5: Hydroxytyrosol stimulates autophagy by SIRT-1-dependent and –independent mechanisms. (A,B) 24h after transfection with SIRT1-siRNA (siSIRT-1) or siRNA negative control (NC), C-28/I2 cells were treated with hydroxytyrosol (HT) for 24h. Cloroquine (CQ) was added 30 min before HT. At the end of incubation, cells were harvested for LC3 and β-actin detection by western blotting. Representative images (A) and relative quantification for LC3-II/β-actin ratio (B) are shown. (C) 24h after transfection with SIRT1-siRNA (siSIRT-1) or siRNA negative control (NC), C-28/I2 cells were treated with hydroxytyrosol (HT) for 24h. Then cells were harvested and analyzed by qRT-PCR for the amount of p62 mRNA. Values are expressed as means ± SEM, *$p<0.05$.

HT-induced autophagy protects human primary OA chondrocytes

In order to validate the findings on the role of autophagy in the HT protective effects in C-28/I2 cell line, some experiments were performed with human primary chondrocytes isolated from OA patients. Essentially similar results were found in primary chondrocytes treated with HT and exposed to oxidative stress, as documented in Fig. 4.6. In fact accumulation of LC3-II protein together with reduction of p62 protein was visualized by Western Blot following a brief HT treatment (Fig. 4.6A). Although differences were not statistically significant due to large variability (Fig. 4.6B,C), the ability of HT to stimulate the autophagic process was confirmed by immunofluorescence images showing increase in LC3-II puncta colocalizing with mitochondria (Fig. 4.6D), regardless of H_2O_2 exposure, which, alone, has an inhibiting effect on autophagy.

Next it was evaluated the ability of HT and autophagy to protect primary chondrocytes against DNA damage and cell death following oxidative stress. As well as described before with C-28/I2 cells, HT and the autophagy inducer rapamycin were able to reduce the DNA damage elicited by H_2O_2 (Fig. 4.6E) and the percentage of dead cells significantly (Fig. 4.6F). Again the pro-survival effect of HT was eliminated by pre-treatment with autophagy inhibitors. Thus, these data indicated that HT exerts its cell protective action in C-28/I2 line and human OA chondrocytes by the same modalities.

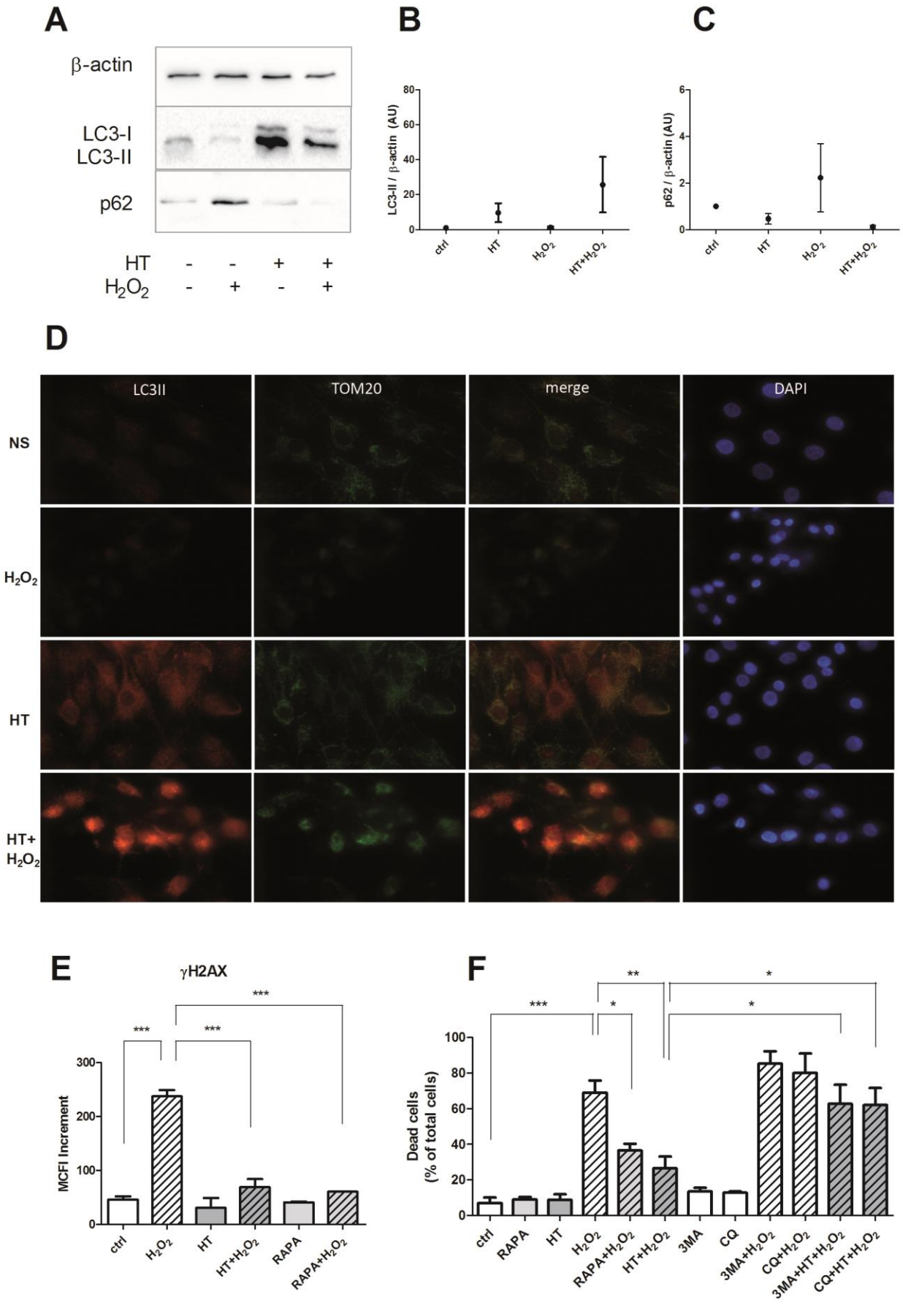
A
β-actin
LC3-I
LC3-II
p62
HT - - + +
H2O2 - + - +
B
LC3-II / β-actin (AU)
ctrl
HT
H2O2
HT+H2O2
C
p62 / β-actin (AU)
D
LC3II
TOM20
merge
DAPI
NS
H2O2
HT
HT+ H2O2
E
γH2AX
MCFI Increment
F
Dead cells (% of total cells)
RAPA
3MA
CQ
3MA+H2O2
CQ+H2O2
3MA+HT+H2O2
CQ+HT+H2O2

Figure 4.6: Hydroxytyrosol-induced autophagy protects human primary OA chondrocytes from oxidative stress. Human primary chondrocytes were pre-incubated in the absence or in the presence of hydroxytyrosol (HT) and/or other compounds as indicated, for 30 min before addition of H_2O_2. After further 2h incubation, cells were harvested for LC3, p62 and β-actin detection by western blotting. Representative images (A) and relative quantification for LC3-II/β-actin (B) and p62/β-actin (C) ratios are shown. Cells were also stained at the end of incubation with antibodies to LC3 A/B and TOM20 (D). The labeled cells were visualized by fluorescence microscopy, showing separate and merged LC3 and TOM20 signals (400x, original magnification). Representative fields of control, non-stimulated cells (NS) or cells treated with HT and/or H_2O_2 are shown. DAPI was used as a nuclear counterstaining. Alternatively cells were evaluated for the extent of DNA damage by detection of γH2AX (E). Finally, after 24 h incubation with or without H_2O_2, cells were counted to assess cell viability by trypan blue exclusion test (F). Values are expressed as means ± SEM, *p<0.05, **p<0.01,***p<0.001

4.2 MicroRNA-9 mediates oxidative stress-induced cytotoxicity in chondrocytes by targeting SIRT-1

Opposite variations of miR-9 and Sirt-1 levels in response to H2O2 and HT treatments in human primary chondrocytes

In the previous chapter it has been described that HT is able to reduce H_2O_2-induced cell death and this effect was associated to crucial nucleus-cytoplasm translocation. Next, we hypothesized a possible modulation of SIRT-1 expression by HT and H_2O_2. In a previous study by our group (*129*), SIRT-1 mRNA levels, measured by qPCR, showed no significant change in human primary chondrocytes and C-28/I2 cells when treated with HT or/and H_2O_2. In the present work immunoblotting assay was performed to evaluate protein levels of SIRT-1. Interestingly H_2O_2 treatment reduced the expression of SIRT-1 protein, whereas HT alone or after pre-treatment with H_2O_2 was able to increase it (Fig. 4.7 A, B). This result was particularly intriguing and opened a new project branch spurring us to investigate the molecular mechanism underlying the post-transcriptional changes of SIRT-1 protein levels by HT and H_2O_2. By exploiting miR-target prediction tools of different databases available online (TargetScan, miRanda, miRWalk), some miRs, including miR-22, miR-34 and miR-9, were selected because of the presence of seed-

complementary sequences in SIRT-1 3′UTR. After 4h of treatment we evaluated miR levels by using specific primers (TaqMan microRNA assays) able to detect mature miR sequences discriminating them from their precursors (pri-miR, pre-miR). Significant variations were appreciated in miR-9 levels: H_2O_2 led to a substantial increase of miR-9, whereas HT reduced this effect (Fig.4.7 C). The site of matching identified by TargetScan browser was shown in the panel D of fig.4.7. The opposite variations of miR-9 and SIRT-1 indicate that the latter is a possible target of miR-9 as predicted by the site of matching.

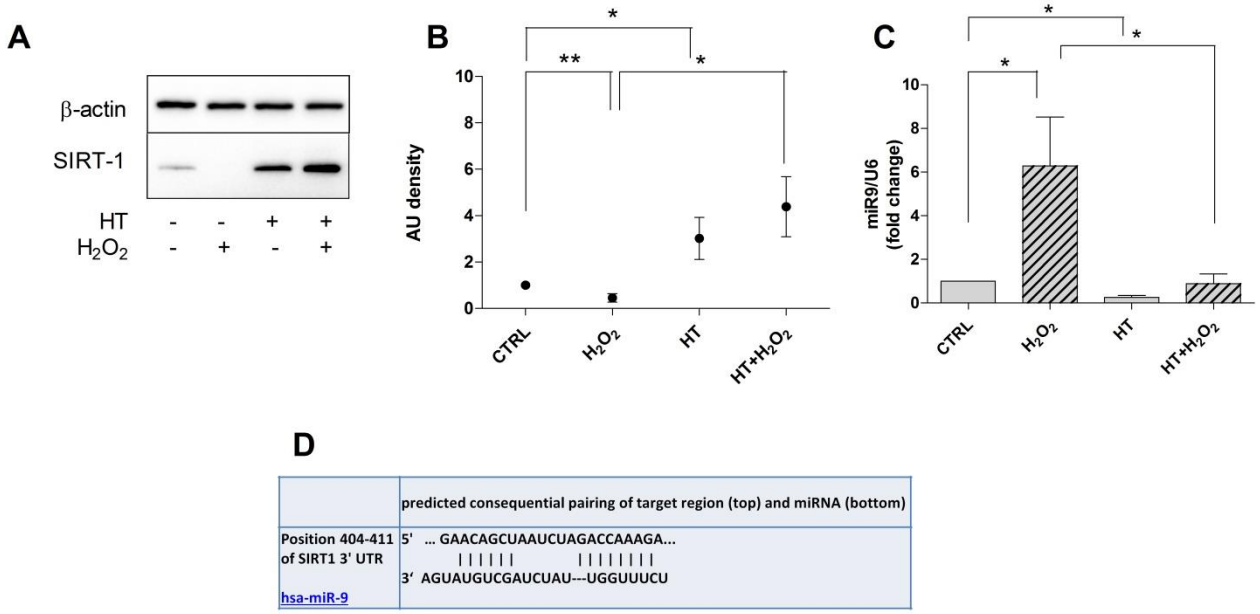

Figure 4.7: Opposite variations of miR-9 and Sirt-1 levels in response to H_2O_2 and HT treatments in human primary chondrocytes. Human primary chondrocytes were pre-incubated in the absence or in the presence of hydroxytyrosol (HT) and/or other compounds as indicated, for 30 min before addition of H_2O_2. After 24h of incubation cells were harvested for SIRT-1 detection by western blotting. Representative images (A) and relative quantification for SIRT-1/ β-actin (B) ratio are shown. After 4h of incubation samples were collected for miR-9 quantification by qPCR analysis (C). Sites of matching between SIRT-1 3'UTR and miR-9 sequences (provided by TargetScan database) are shown (D). Values are expressed as means ± SEM, *p<0.05, **p<0.01

Opposite variations of miR-9 and Sirt-1 levels in response to H2O2 and HT treatments in C-28/I2 cells

In order to use C-28/I2 cell line for further investigations, SIRT-1 protein and miR-9 variations were evaluated in response to treatments with HT and/or H_2O_2. As shown in fig. 4.8A and 4.8B HT was able to rescue SIRT-1 protein levels that decreased after H_2O_2 treatment. In accordance with human primary cell results, miR-9 levels vary after treatments in an opposite manner to SIRT-1 levels in C-28/I2 (Fig. 4.8C).

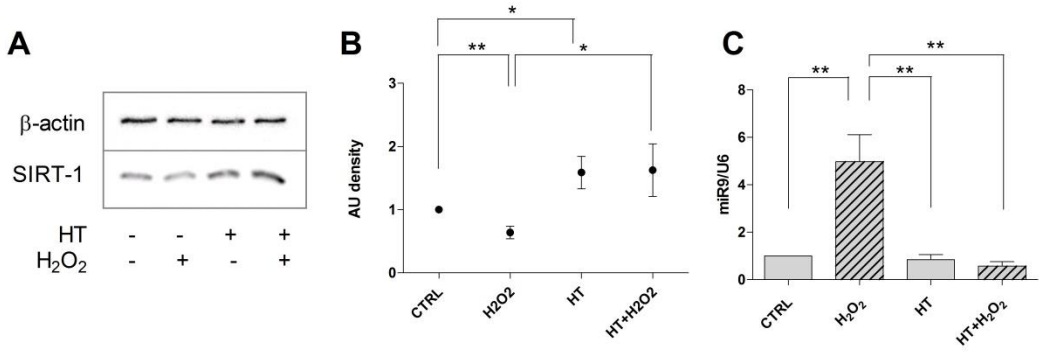

Figure 4.8: Opposite variations of miR-9 and Sirt-1 levels in response to H_2O_2 and HT treatments in C-28/I2 cell line. C-28/I2 cells were pre-incubated in the absence or in the presence of hydroxytyrosol (HT) and/or other compounds as indicated, for 30 min before addition of H_2O_2. After 24h of incubation cells were harvested for SIRT-1 detection by western blotting. Representative images (A) and relative quantification for SIRT-1/ β-actin (B) ratio is shown. After 4h of incubation samples were collected for miR-9 quantification by means of qPCR (C). Values are expressed as means ± SEM, *p<0.05, **p<0.01

Impact of miR-9 silencing and overexpression on H2O2 -induced toxicity and HT-mediated protection in C-28/I2 cell line and human primary chondrocytes

Next, we evaluated the role of miR-9 in cell death elicited by H_2O_2 as well as in the protection afforded by HT in human primary chondrocytes and C-28/I2 cells. First, we tested the silencing efficiency of Ambion® Anti-miR™ miRNA Inhibitors by using qPCR (Fig.4.9A and 4.10A). We

found out that miR-9 silencing rescued protein levels of Sirt-1 reduced by H_2O_2 treatment and led to a complete loss of the H_2O_2-induced cell death (Fig. 4.9B, C, D and 4.10B, C, D). Accordingly, H_2O_2 treatment in antimiR-9 transfected cells led to a reduced caspase 3-like activity compared to H_2O_2 treatment in CTRL transfected cells (Fig. 4.9E). Then, in order to estimate the importance of SIRT-1 in the protection obtained by silencing miR-9, primary chondrocytes and C-28/I2 cells were silenced for both miR-9 and SIRT-1 and treated with H_2O_2. Fig. 4.9F and 4.10E show that SIRT-1 knockdown reduced the protection afforded by antimiR-9 transfection versus H_2O_2-induced cell death. Indeed, we found a significant difference between and SIRT-1 plus miR-9 -silenced cells and miR-9 only-silenced cells when treated with H_2O_2.

However the prevention of cell death inhibition was not complete, as antimiR-9 transfection concomitantly with SIRT-1 knockdown was still able to partially reduce H_2O_2-induced cell death. Therefore it is conceivable that miR-9 may influence more targets, in addition to SIRT-1, implicated in the control of apoptotic cell death mediated by oxidative stress.

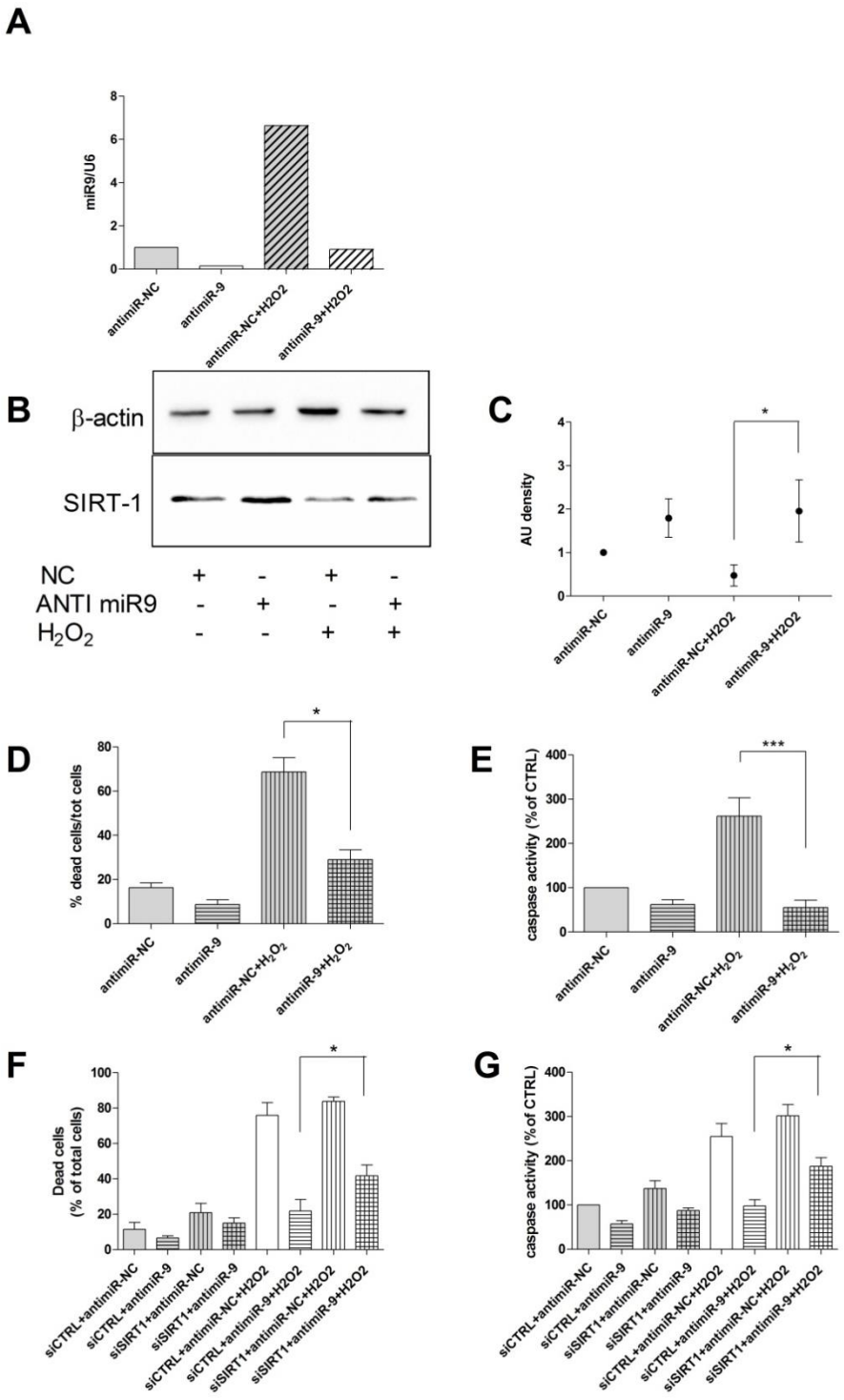

Figure 4.9: Impact of the miR-9 silencing on the toxicity of H_2O_2 in human primary chondrocytes. Primary cells were transfected for 24h with antimiR-9 or antimiR-NC (50nM). After 4h incubation cells were harvested and miR-9 levels were determined by qPCR (A). After 24 h incubation with or without H_2O_2, cells were collected for SIRT-1 detection by western blotting. Representative images (B) and relative quantification of SIRT-1/ β-actin ratio (C) are shown. Alternatively, cells were

counted to assess cell viability by trypan blue exclusion test (D) or harvested and analyzed for caspase activity (E). In addition, cells were transfected for 24h with antimiR-9 or antimiR-NC (50nM) and siCTRL or siSIRT1 (25nM). After 24h incubation with or without H_2O_2, cells were counted to assess cell viability by trypan blue exclusion test (F) or harvested and analyzed for caspase activity (G). Values are expressed as means ± SEM, *p<0.05, ***p<0.001

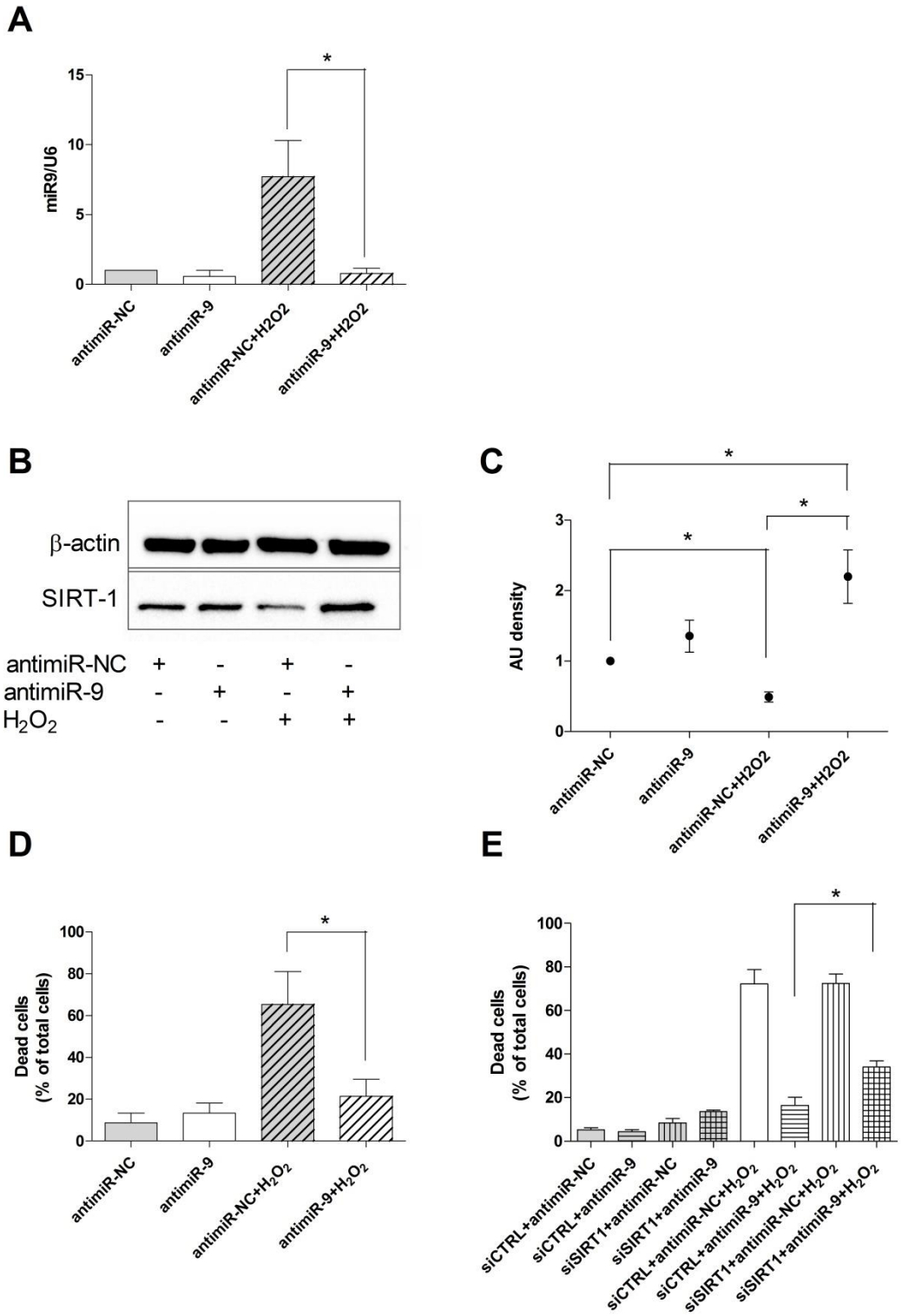

Figure 4.10: Impact of miR-9 silencing on the toxicity of H_2O_2 in C-28/I2 cell line. C-28/I2 cells were transfected for 24h with antimiR-9 or antimiR-NC (50nM). After 4h incubation cells were harvested and miR-9 levels were determined by qPCR (A). After 24 h incubation with or without H_2O_2, cells were collected for SIRT-1 detection by western blotting. Representative images (B) and relative quantification for SIRT-1/ β-actin ratio (C) are shown. Alternatively, cells were counted to assess cell viability by trypan blue exclusion test (D). C-28/I2 cells were transfected for 24h with antimiR-9 or antimiR-NC (50nM) and siCTRL or siSIRT1 (25nM). After 24h incubation with or without H_2O_2, cells were counted to assess cell viability by trypan blue exclusion test (E). Values are expressed as means ± SEM, *$p<0.05$

Then, we verified the efficacy of Ambion® Pre-miR™ miRNA Precursors transfection by performing qPCR: as shown in Fig. 4.11A and in Fig. 4.12A, these oligonucleotides are able to raise dramatically mature miR-9 levels. We observed that pre-miR-9 transfection decreased protein expression of SIRT-1 in control and HT-treated cells (Fig. 4.11B, C – 4.12B, C). Moreover, increased levels of miR-9 induced cell death compared to correspondent control cells and the loss of HT protection in cells exposed to H_2O_2-mediated oxidative stress (Fig. 4.11D and 4.12D). Consistently with the chances of cell death rate, Fig. 4.11E shows that premiR-9 transfection enhanced caspase 3-like activity as well and led to a partial loss of caspase inhibition provoked by HT pre-treatment.

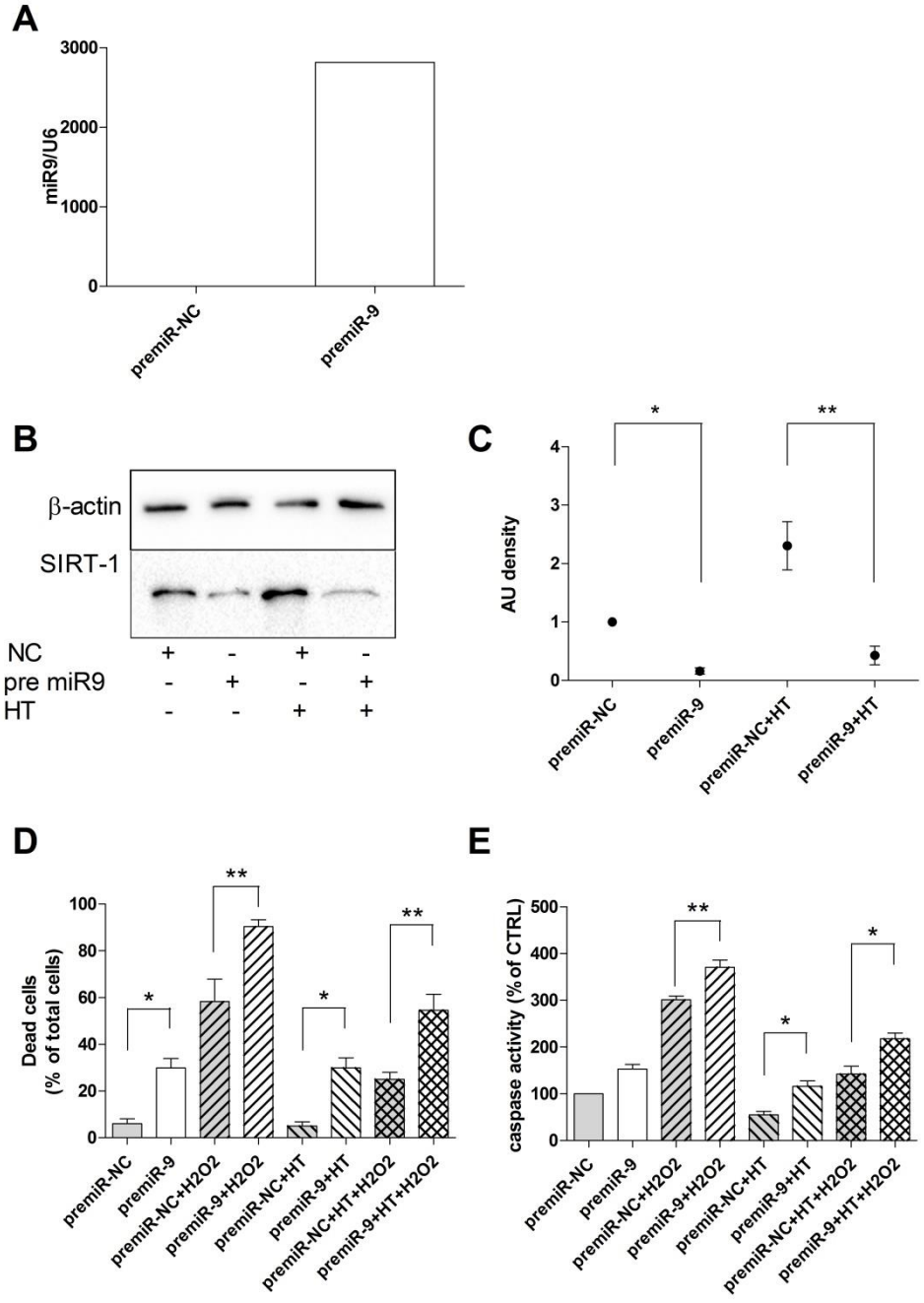

Figure 4.11: Impact of premiR-9 transfection on the HT-mediated protection in human primary chondrocytes. Cells were transfected for 24h with premiR-9 or premiR-NC (50nM). After 4h incubation cells were harvested and miR-9 levels were determined by qPCR (A). After 24 h incubation with or without HT, cells were collected for SIRT-1 detection by western blotting. Representative images (B) and relative quantification for SIRT-1/ β-actin ratio (C) are shown. Alternatively after 24h incubation with H_2O_2 or HT, cells were counted to assess cell viability by trypan blue exclusion test (D) or harvested and analyzed for caspase activity (E). Values are expressed as means ± SEM, *p<0.05, **p<0.01

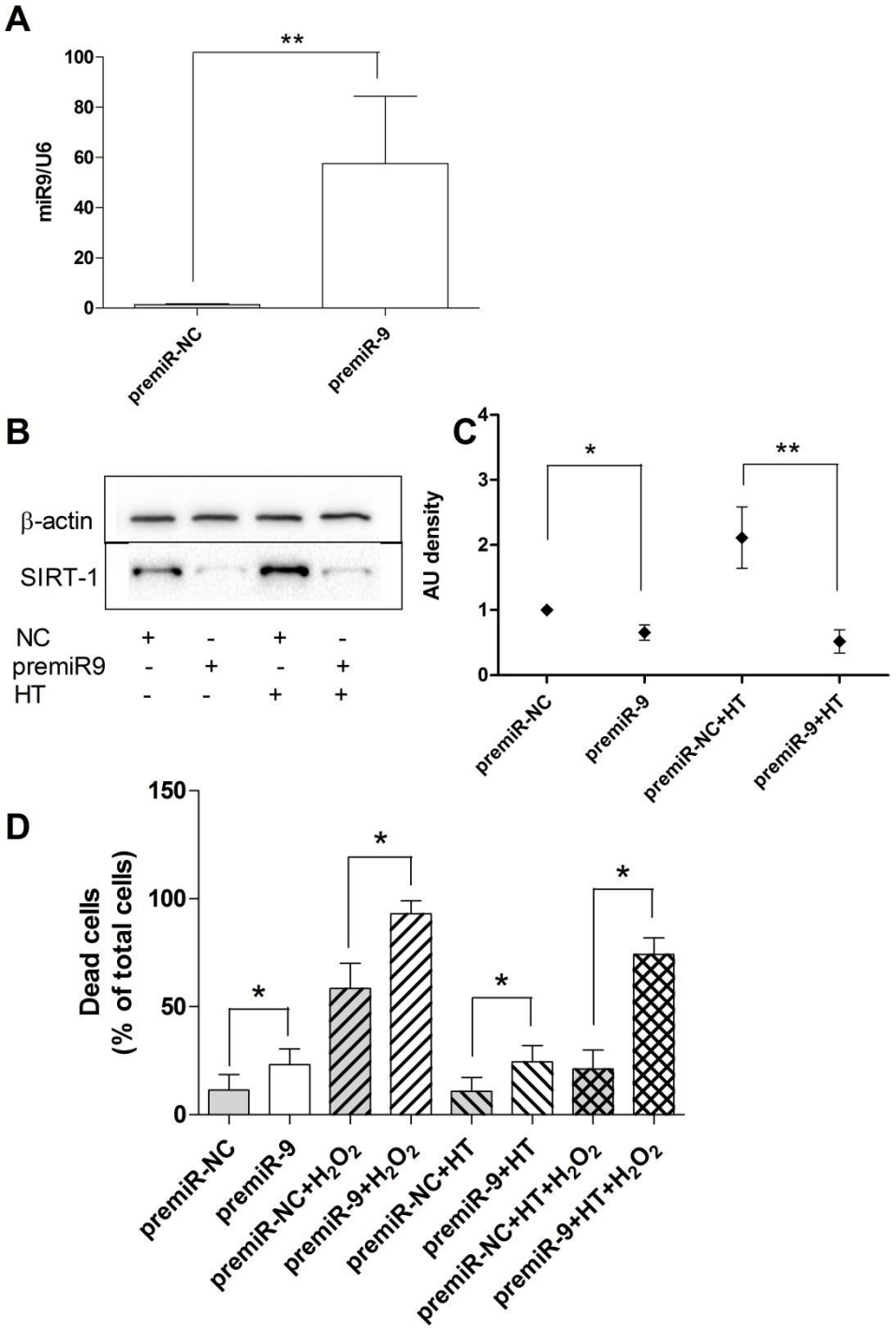

Figure 4.12: Impact of premiR-9 transfection on the HT-mediated protection in C-28/I2 cell line. C-28/I2 cells were transfected for 24h with premiR-9 or premiR-NC (50nM). After 4h incubation cells were harvested and miR-9 levels were determined by qPCR (A). After 24 h incubation with or without HT, cells were collected for SIRT-1 detection by western blotting. Representative images (B) and relative quantification for SIRT-1/ β-actin ratio (C) are shown. Alternatively after 24h incubation with H_2O_2 or HT, cells were counted to assess cell viability by trypan blue exclusion test (D). Values are expressed as means ± SEM, *p<0.05, **p<0.01

SIRT-1 is a direct target of miR-9 in C-28/I2 cells

At this point, we were sure that changes in miR-9 levels correspond to opposite expression of SIRT-1 protein but the critical question was “is SIRT-1 a direct or indirect target of miR-9?”. One of the most popular approaches to demonstrate this actual linking is luciferase-based gene reporter assay. This assay involves placing a genetic regulatory element upstream or 3'UTR downstream of a luciferase gene and then transferring the resulting reporter construct into the cells through transfection, transformation or injection. Expression of the luciferase reporter gene is then measured to quantify the activity of the regulatory element (cis-acting) or proteins (trans-acting) in the biological pathway affected by the target element. As illustrated in the drawing below, luminescence intensity will be less or more strong with or without miR interaction, respectively.

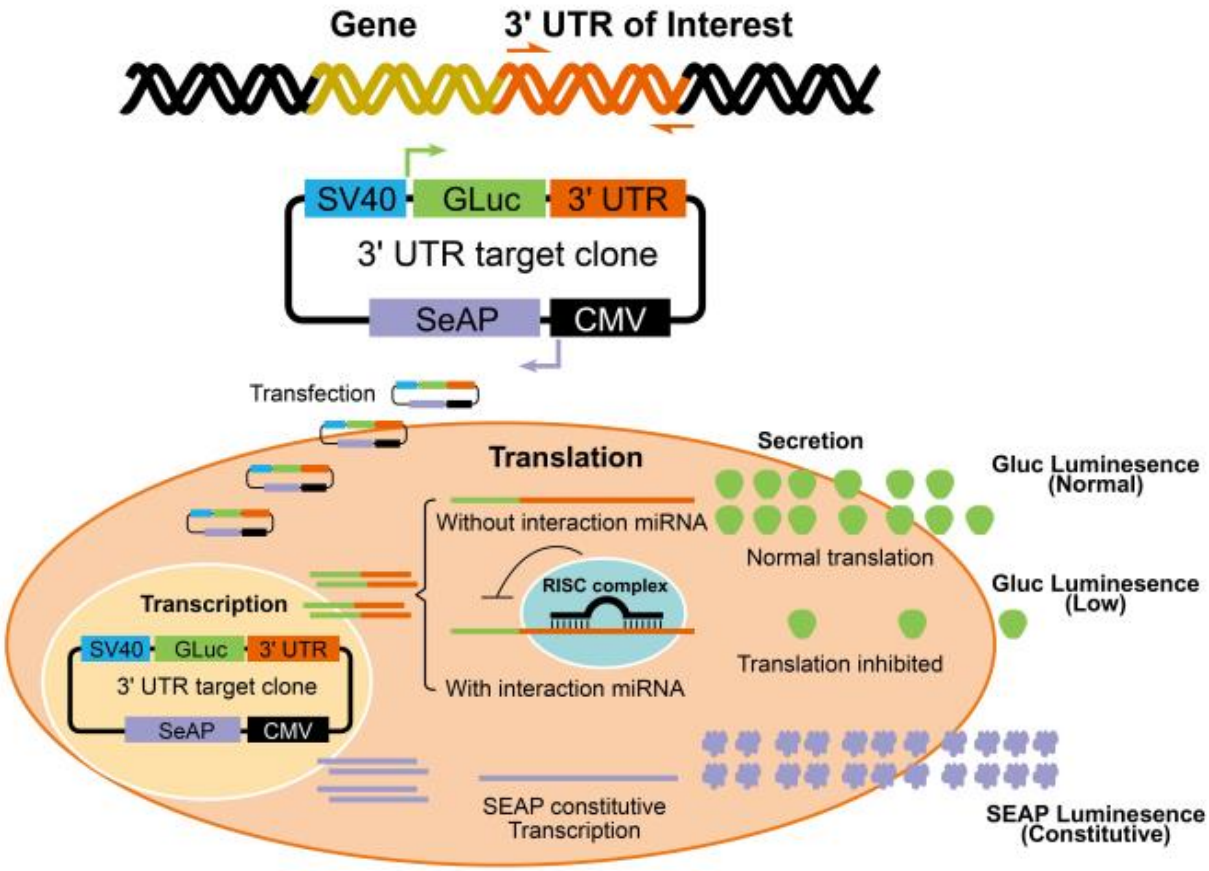

We transfected three different gene sequences (Fig. 4.13A) inserted in the plasmid provided by Genecopoeia: 3'UTR mut1 is 3'UTR SIRT-1 without miR-9 seed sequence identified by

TargetScan bioinformatic tool; 3'UTR mut2 lacks seed sequence and the miR-9 3'pairing sequence; 3'UTR wt is the full 3'UTR sequence of SIRT-1.

After 24h incubation the enzymatic activity of reporter protein was evaluated and only cells transfected with the full 3'UTR showed a decreased signal (around 50%) of bioluminescence (Fig. 4.13B). Moreover, a 10% difference between 3'UTR mut1and 3'UTR mut2 let us speculate that the sequence upstream of seed-complementary sequence (blue highlighted in Fig. 4.13A) may increase the silencing efficiency of the seed sequence. Overall this data confirm that SIRT-1 is a genuine target of miR-9.

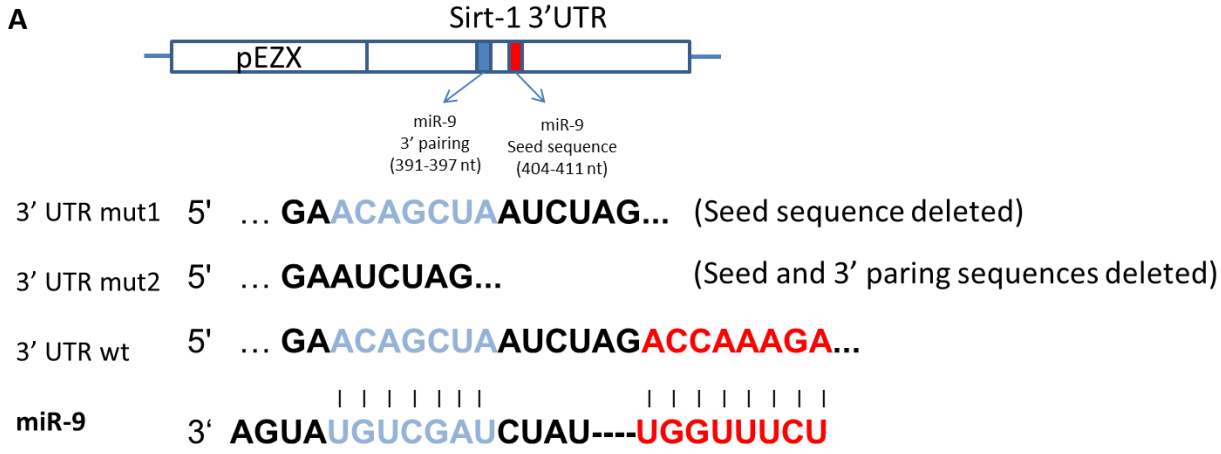

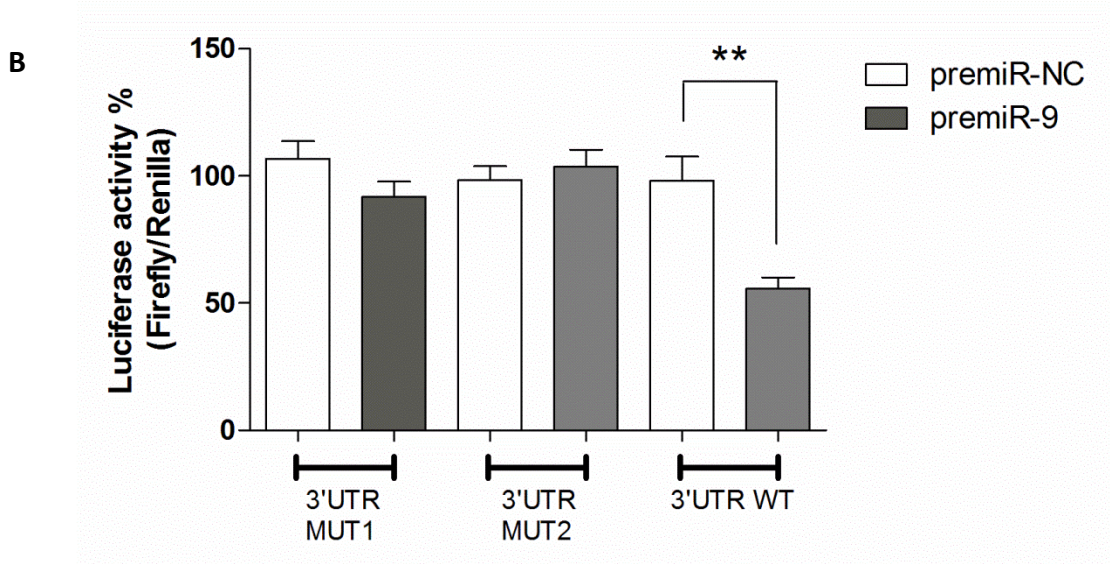

Figure 4.13: SIRT-1 is a direct target of miR-9 in C-28/I2 cells. Three different sequences were designed and provided within pEZX-MT06 reporter vector (Genecopoeia); a first sequence deleted of seed sequences (3'UTR mut1); a second one deleted of miR-9 3' pairing sequence as well as of seed sequence (3'UTR mut2); a last one with the full 3'UTR sequence (3'UTR wt) (A). Cells were co-transfected with either plasmid carrying 3'UTR mut1, 3'UTR mut2 or 3'UTR wt, with premiR-9 or premiR-NC. The dual luciferase activity of the transfected cells was detected and the luciferase activity was normalized on renilla activity (B). Values are expressed as means ± SEM, **p<0.01

4.3 MicroRNA-155 suppresses autophagy in chondrocytes by modulating expression of autophagy proteins

MiR-155 modulates autophagy in T/C28a2 cells

In a Next Generation Sequencing study, miR-155 was found to be one of the most highly upregulated miRs in human OA knee cartilage compared to normal cartilage. Searching miR target databases revealed that miR-155 seed-complementary sequences are present in several autophagy-related genes and identified GABARAPL1, ATG3, ATG5 and FOXO3 as putative targets. In light of this, and previous findings of dysfunctional autophagy in OA (*136*), we analyzed the potential role of miR-155 in chondrocyte autophagy.

We transfected T/C28a2 human immortalized cell line with LNA nc and LNA miR-155, mimic nc and mimic miR-155 in order to downregulate and raise endogenous miR-155 levels, respectively, as validated by qPCR (Figure 4.14A). Autophagy is a highly dynamic process that involves the formation, maturation and degradation of autophagosomes (*95*). Autophagic flux can be monitored by measuring the conversion of LC3-I to LC3-II (*137*). We analyzed autophagy flux after treatment with the autophagy inducers RAPA or 2-DG. Both compounds are widely employed for autophagy stimulation in vitro and in vivo studies due to their ability to block the mTOR pathway or reduce intracellular ATP thus activating AMPK, respectively (*95*). Moreover, T/C28a2 cells were simultaneously treated with or without CQ, to block autophagy flux and allow accumulation of the autophagic protein LC3-II, given its fast protein turnover, thus affording a better observation by

western blot analysis (*95*). As shown in Figure 4.14B and 4.14C, the autophagy flux, as evaluated by the LC3-II/LC3-I ratio, was enhanced by CQ alone, indicating basal autophagy activation under the culture conditions used. This was significantly increased in samples transfected with LNA miR-155 compared to those with LNA nc, and was significantly decreased in cells transfected with mimic miR-155, compared to mimic nc.

Consistent with these results on LC3 conversion, the downregulation of miR-155 by LNA miR-155 increased and mimic miR-155 transfection decreased the number of autophagic vacuoles as assessed in live cells by Cyto-ID dye incorporation, specifically targeting autophagosomes (Figures 4.14D and 4.14E).

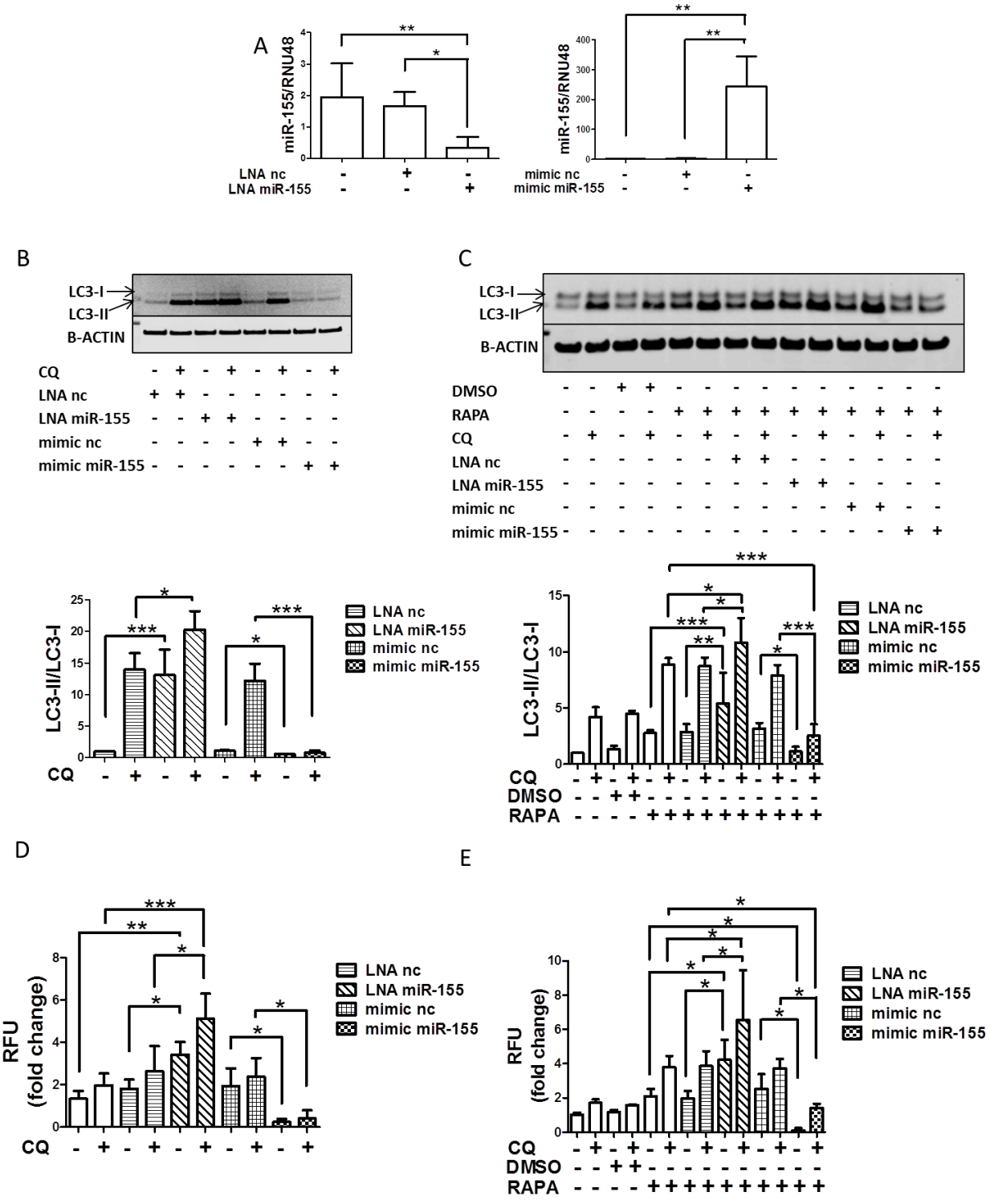

Figure 4.14: MiR-155 modulates autophagy in T/C28a2 cells. (A) T/C28a2 cells were transfected for 24h with LNA miR-155 and LNA negative control (LNA-nc) (40nM), mimic miR-155 and mimic negative control (mimic nc) (10nM). MiR-155 levels were determined by qPCR (n=4). (B) 24h after transfection cells were treated with DMSO or 50nM rapamycin (RAPA) and/or 25μM chloroquine (CQ) for 4h or (C) 5mM 2-deoxy-glucose (2-DG) and/or 25μM CQ for 2h and then harvested for LC3 and β-actin detection by western blotting. Representative images and relative

quantification for LC3-II/LC3-I ratios are shown (n=5), (D) 24h after transfection cells were incubated for 18h with DMSO or 50nM RAPA and/or 25µM CQ or (E) 5mM 2-DG and/or 25µM CQ and stained with Cyto-ID (1:1000) and Hoechst 33342 (1:2000) (n=3). Values are expressed as mean ± SD of 4 independent experiments in A, 5 independent experiments in B and C, 3 independent experiments in D and E, *P<0.05, **P<0.01,***P<0.001.

MiR-155 modulates autophagy in human primary chondrocytes

In order to confirm these observations, we evaluated the autophagic activity in primary chondrocytes transfected with LNA nc and LNA miR-155, mimic nc and mimic miR-155 to modulate cellular miR-155 levels (Figure 4.15A). A significant increase in basal autophagic flux was seen when cells were transfected with LNA miR-155 compared to the LNA nc while mimic miR-155 transfection resulted in a significant attenuation of LC3-I conversion (Figure 4.15B).

We also tested the effects of miR-155 modulation in RAPA-induced autophagy in chondrocytes after LNA and mimic transfection. Under this condition, autophagy flux was significantly increased by miR-155 downregulation and significantly reduced by mimic miR-155 transfection (Figure 4.15C). These results were confirmed by quantification of Cyto-ID dye intensity (Figures 4.15D and 4.15E).

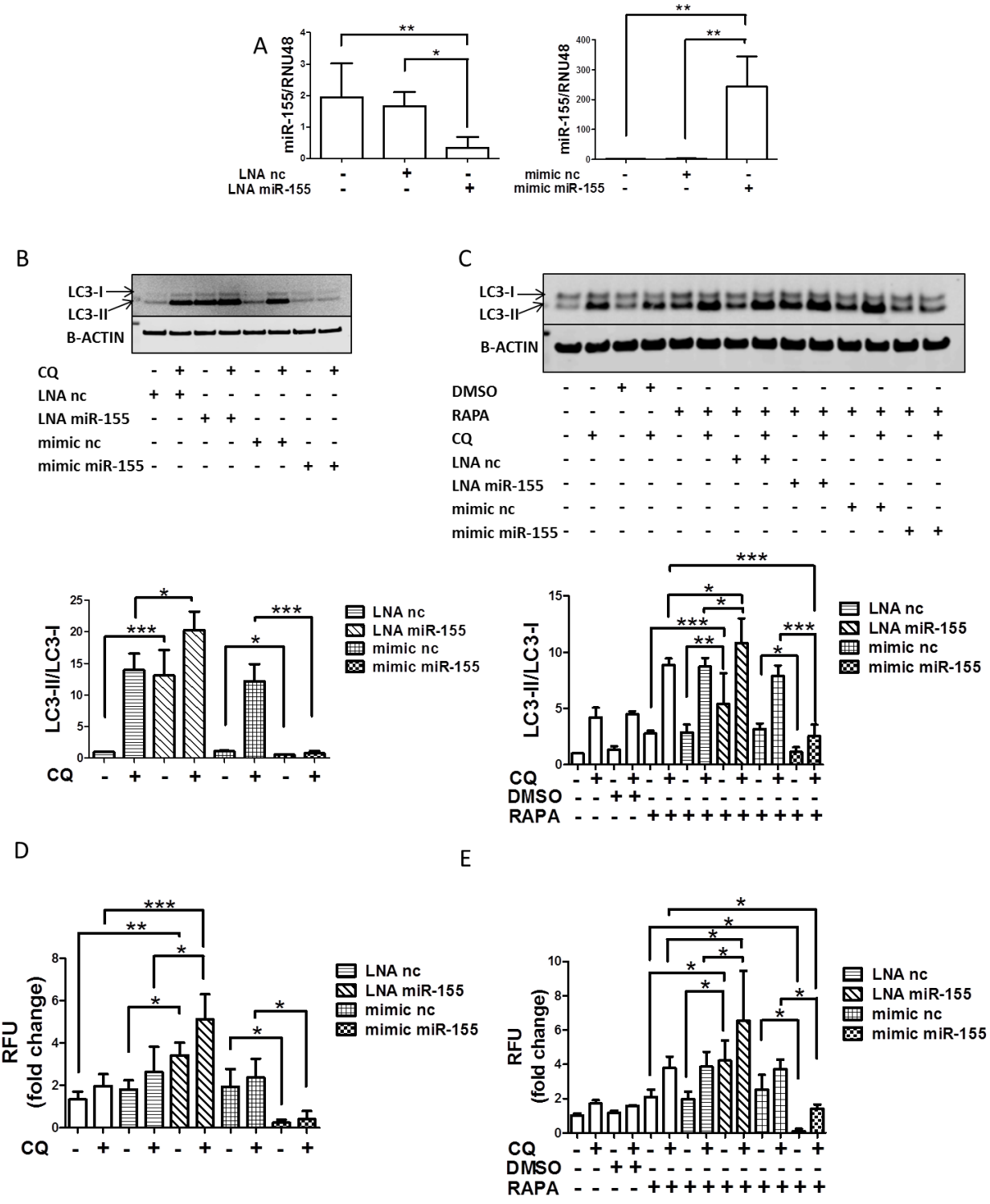

Figure 4.15: MiR-155 modulates autophagy in human primary chondrocytes. (A) Cells were transfected for 24h with LNA miR-155 and LNA nc, mimic miR-155 and mimic nc. MiR-155 levels were determined by qPCR (n=5). (B) 24h after transfection cells were treated with or without 25μM CQ for 12h or (C) DMSO or 50nM RAPA and/or 25μM CQ for 12h and then harvested for LC3 and β-actin detection by western blotting. Representative images and relative quantification for LC3-II/LC3-I ratios are shown (n=5), (D) 24h after transfection cells were incubated for 18h with

or without 25µM CQ or (E) DMSO or 50nM RAPA and/or 25µM CQ and stained with Cyto-ID (1:1000) and Hoechst 33342 (1:2000) and intracellular fluorescence was measured (n=3). Values are expressed as mean ± SD, *P<0.05, **P<0.01,***P<0.001.

MiR-155 regulates autophagy by suppressing MAP1LC3, GABARAPL1, ATG3, ATG5, ATG14, ULK1 and FOXO3

To characterize the mechanism underlying autophagy suppression by miR-155, we tested the bioinformatics-based prediction that miR-155 targets autophagy genes. We performed qPCR analysis on RNA from T/C28a2 cells and from human primary chondrocytes transfected with LNA nc, LNA miR-155, mimic nc and mimic miR-155.

As shown in Figure 3A, LNA miR-155 but not LNA nc, led to a significant increase in the mRNA levels of GABARAPL1, ATG3, ATG5 and FOXO3. Conversely, mimic miR-155 but not mimic nc significantly reduced mRNA levels of GABARAPL1, ATG3, ATG5 and FOXO3 (Figures 4.16A and 4.16B). Furthermore, we analyzed autophagy-related genes that are not predicted targets of miR-155 and discovered that mRNA levels of ULK1, ATG14 and MAP1LC3 were modulated by miR-155 LNA and mimic (Figures 4.16A and 4.16B). Similar results were obtained in human primary chondrocytes (Figure 4.17).

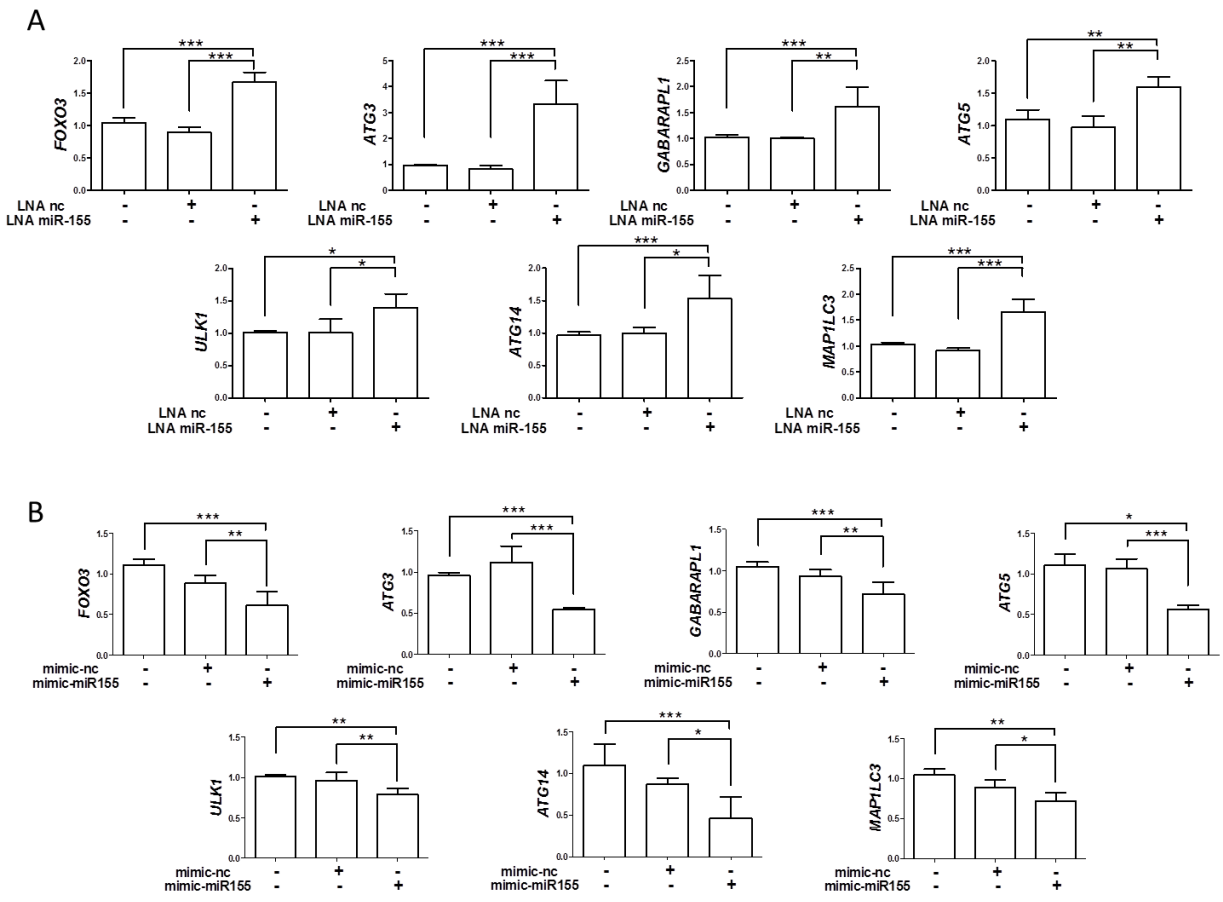

Figure 4.16: MiR-155 regulates autophagy by suppressing gene expression of *MAP1LC3*, *GABARAPL1*, *ATG3*, *ATG5*, *ULK1*, *ATG14*, and *FOXO3*. Cells were transfected for 24h with LNA miR-155 and LNA nc, mimic miR-155 and mimic nc. (A) qRT-PCR analysis of mRNA expression levels of direct and indirect targets of miR-155 in T/C28a2 cells following transfection with LNA or (B) mimic. Values are expressed as mean ± SD, *P<0.05, **P<0.01, ***P<0.001.

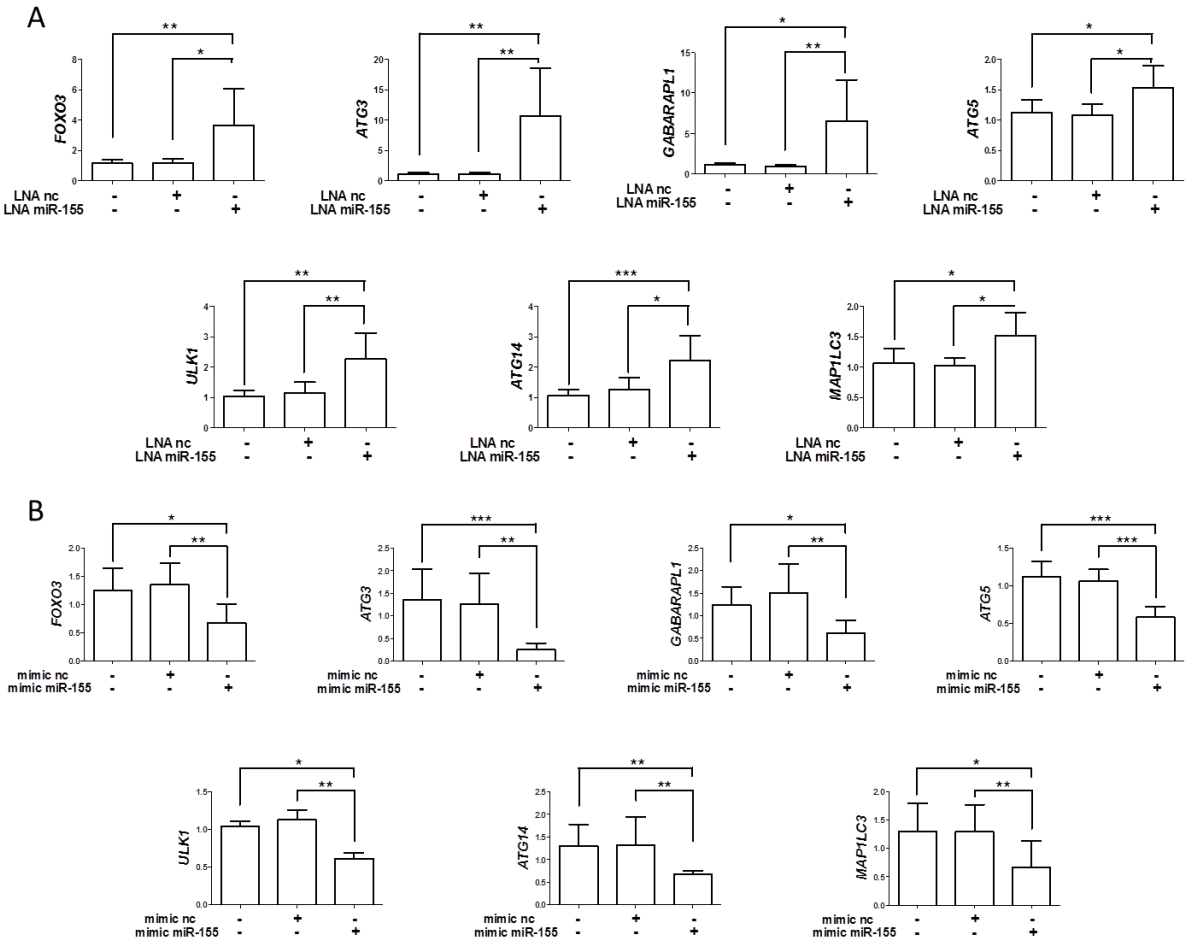

Figure 4.17: MiR-155 regulates autophagy by suppressing autophagy-related gene expression in human primary chondrocytes. Cells were transfected for 24h with LNA miR-155 and LNA nc, mimic miR-155 and mimic nc. (A) qRT-PCR analysis of mRNA expression levels of direct and indirect targets of miR-155 in primary chondrocytes following transfection with LNA or (B) mimic. Values are expressed as mean ± SD, *P<0.05, **P<0.01, ***P<0.001.

To confirm that the changes in mRNA levels of miR-155 targets corresponded to changes in protein expression, we performed western blotting on T/C28a2 cells transfected with LNA miR-155 or mimic miR-155. As shown in Figure 4.18, knockdown of endogenous miR-155 increased levels of GABARAPL1, ATG3, ATG5, FOXO3, ULK1, ATG14 and LC3 proteins and mimic miR-155 transfection strongly decreased these proteins.

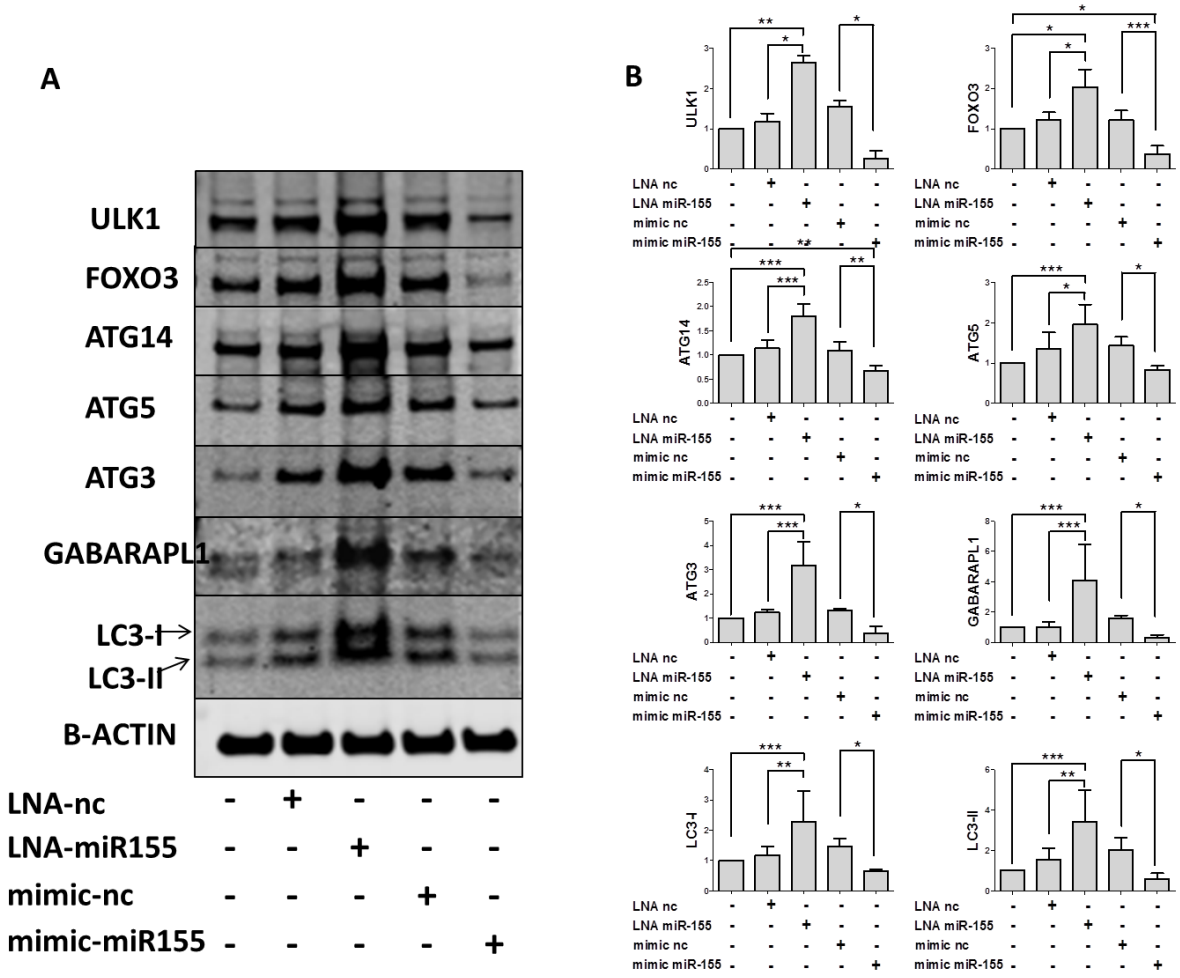

Figure 4.18: MiR-155 regulates autophagy by reducing protein levels of MAP1LC3, GABARAPL1, ATG3, ATG5, ULK1, ATG14, and FOXO3. T/C28a2 cells were transfected for 24h with LNA miR-155 and LNA nc, mimic miR-155 and mimic nc. Western blotting analysis of MAP1LC3, GABARAPL1, ATG3, ATG5, ULK1, ATG14, FOXO3 and β-ACTIN proteins. Representative images and relative quantifications are shown (n=4). Values are expressed as mean ± SD, *P<0.05, **P<0.01, ***P<0.001.

MiR-155 regulates mTOR activity

As mTOR is a critical negative regulator of autophagy (*138-140*), we examined whether it was involved in miR-155 effects. mTOR pathway activity was detected by analyzing the phosphorylation levels of ribosomal protein s6 (P-s6, S235/S236) and AKT (P-AKT, S473) in response to LNA miR-155 and mimic miR-155 transfection in T/C28a2 cells. Contrary to our expectations, P-S6 and P-AKT, in ratio to their total levels, were significantly increased following knockdown of miR-155 and significantly attenuated after mimic miR-155 transfection (Figure

4.19A). We next evaluated the expression of RICTOR, an essential mTOR complex-2 (mTORC2) component that can activate mTOR complex-1 (mTORC1) through phosphorylation of AKT (S473) (*82*, *83*), which was identified as a miR-155 target in the bioinformatics analysis. As shown in Figures 4.19B and 4.19C, both RICTOR protein and mRNA levels were increased and decreased by LNA miR-155 and mimic miR-155 transfection, respectively.

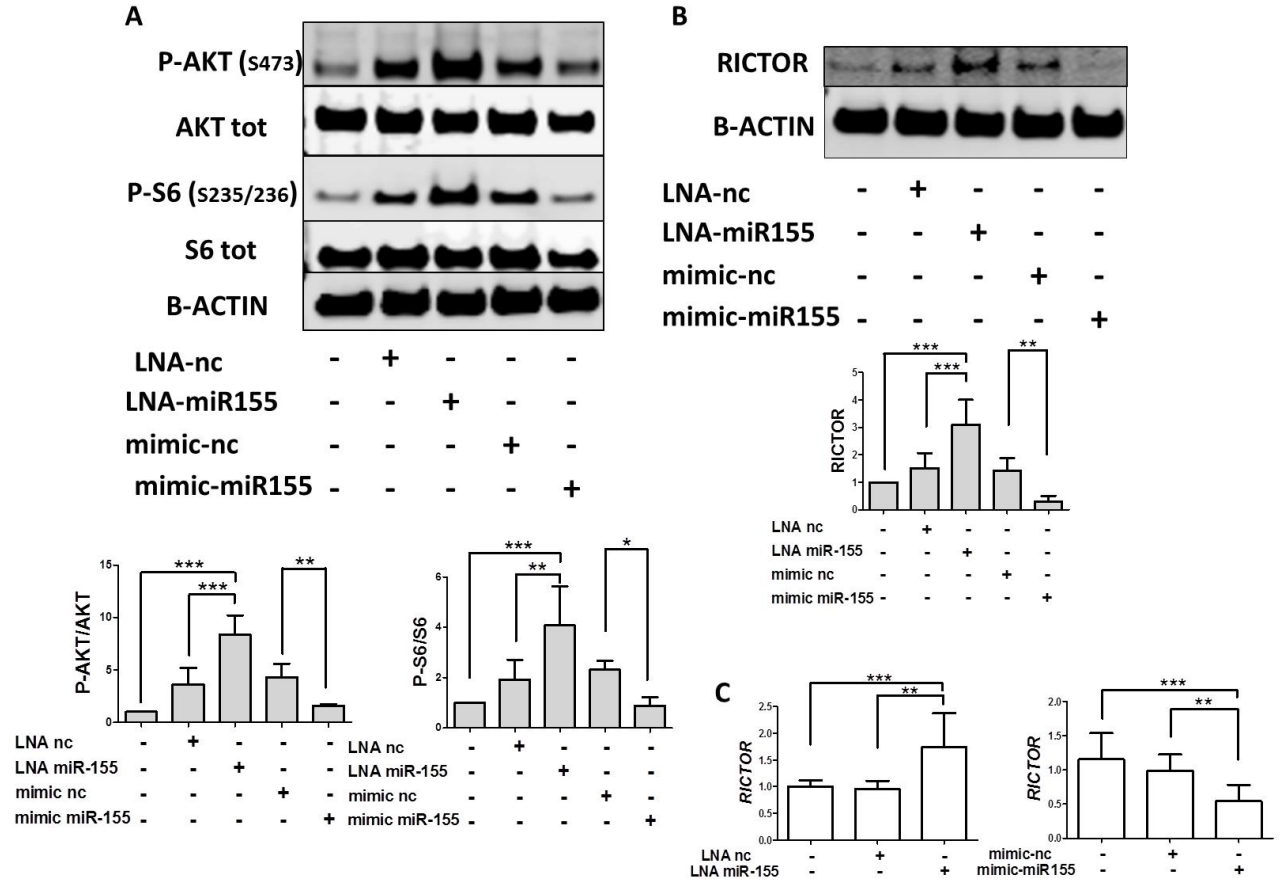

Figure 4.19: Effect of miR-155 on mTOR activity. T/C28a2 cells were transfected for 24h with LNA miR-155 and LNA nc, mimic miR-155 and mimic nc. (A) Western blotting analysis of P-AKT (Ser473), AKT total, P-S6 (Ser235/Ser236), S6 total and β-ACTIN levels by using specific antibodies. (B) Western blotting analysis of RICTOR and β-ACTIN. Representative images and relative quantifications are shown (n=4). (C) qRT-PCR analysis of mRNA expression levels of *RICTOR* are shown (n=4). Values are expressed as mean ± SD, *P<0.05, **P<0.01, ***P<0.001.

5. DISCUSSION AND CONCLUSIONS

Osteoarthritis (OA) is a multifactorial degenerative disease of the cartilage and the most common form of arthritis, whose millions of people worldwide suffer, affecting 60% of men and 70% of women above 65 (*12*). Indeed aging is considered the main risk factor of OA, followed by obesity (*37*).

So far, palliative therapy for arthritic diseases is the only approach to treat patient symptoms and is mainly based on NSAIDs (*53*) that lack efficacy to counteract and slow OA progression and result in several side effects. The only resident cell population of cartilage is represented by chondrocytes. Therefore, a better understanding of molecular mechanisms underlying cellular changes of OA chondrocyte is required in order to identify alternative therapies.

A promising mechanism as potential target can be found in autophagy pathway, maintaining homeostatic balance through removal, degradation and recycling of damaged organelles or proteins. In fact defective autophagy has recently emerged as a feature of articular cartilage in OA-affected joints in both human and in animal models. Studies in mouse models showed that in normal cartilage there is a constitutive or basal level of autophagy that is of higher magnitude as compared to liver in the same animal (*141*). With aging and OA development, the number of autophagosomes and the size of the autophagosomes decrease in cartilage. Conceptually, defective autophagy could be due to abnormal expression of autophagy proteins or abnormal signalling and regulation of autophagy activation. Several studies provided evidence for aging and OA-associated reduction in autophagy proteins, including ATG5, ULK1, BECLIN1 and LC3 (*98, 141*). There is also evidence for abnormal autophagy signalling, most importantly, hyperactivation of mTOR, possibly due to reduced activation of AMPK (*138, 142*).

In this thesis we propose HT, a nutraceutical compound, as modulator of OA changes and protective agent against oxidative stress by promoting autophagy successfully. Moreover, we have

investigated the involvement of microRNA network and identified two miRs that could be implicated in the complex pattern of deregulated gene expression in OA chondrocytes.

Autophagy and hydroxytyrosol

Nutraceuticals have shown to exhibit a role not merely as anti-oxidant or ROS scavengers, but also as efficient modulators of gene expression of key factors underlying the OA onset. On this purpose, we and others have showed the ability of sulforaphane, a natural isothiocyanate derived from edible cruciferous vegetables, to protect chondrocytes in vitro (*62, 63*), and, quite recently, a sulforaphane-rich diet was found effective in a murine OA model (*63*).

In a recently published paper (*129*), we have reported how HT prevented or reduced ROS accumulation, DNA damage, expression of proinflammatory, ECM degrading- and other OA-related genes, as well as cell death of human chondrocytes treated with stressors involved in OA pathogenesis, i.e. H_2O_2 and GROα. In the present study we have investigated some cellular and molecular events mechanistically involved in the protective action of HT in human chondrocytes treated with H_2O_2. The main findings of the present work are the following: 1) HT induces autophagy activation; 2) autophagy stimulation by HT mediates its protective action against cell death under oxidative stress; 3) autophagy stimulation by HT occurs through SIRT-1-dependent and -independent mechanisms.

It has been reported in a variety of non-tumoral cells and biological systems that HT can exert anti-oxidant, anti-inflammatory, anti-apoptotic and other protective effects, which may prevent or slow progression of degenerative diseases (*64, 143*). However the mechanism of action of HT is largely undefined and can be only partly ascribed to its free-radical scavenging activity and direct anti-oxidant power. It has been shown in some experimental settings that HT can enhance the cellular anti-oxidant and detoxifying defence systems through the modulation of signaling pathways impacting on key transcription factors, such as Nrf2 or FOXO3 (*70, 144*). However the role of autophagy in these events was not investigated. To our knowledge this is the first study showing

that HT can activate the autophagy process, thus protecting from cell death. This ability of this compound to induce autophagy may not be limited to chondrocytes and would be interesting the study of HT potential protective effects in other cell types and experimental models.

SIRT-1 is a protein deacetylase that plays a role in chondrocyte survival and cartilage homeostasis (*145*). The overexpression of SIRT-1 (*146*) or its activation by resveratrol (*147*) protects chondrocytes and inhibits OA-like gene expression changes in vitro, whereas selective knockout of SIRT-1 in chondrocytes accelerates OA development in mice (*59*). However the involvement of autophagy in the chondroprotective effects of SIRT-1 has not been reported. Actually it is known that SIRT-1 may regulate autophagy in different ways (*148*). In fact SIRT-1 can modulate the expression of genes involved in autophagy by deacetylating key transcription factors or directly the activity of autophagic proteins by deacetylation. We have previously found that HT may enhance SIRT-1 expression in human chondrocytes (*129*). Other research groups also reported an increased expression of SIRT-1 mRNA or protein in the heart of SAMP8 mice fed with a diet rich in olive oil phenolics (*149*), in the heart of HT-treated Sprague-Dawley rats (*150*), and in the brain of HT-treated db/db mice (*151*), but the functional role of SIRT-1 in the HT action was not investigated. In the present paper we show by mechanistic experiments that HT induces autophagy and protects from oxidative stress-induced cell death in a SIRT-1 dependent manner. In fact LC3-II formation, a critical event in autophagy, increased in C-28/I2 chondrocytes treated with HT, but not in SIRT-1 silenced cells. Instead LC3 gene expression was not affected by HT. Huang et al. (*152*) have demonstrated that LC3 deacetylation by SIRT-1 in the nucleus is required for LC3 export to cytosol where it is able to bind Atg7 and other autophagy factors and undergoes phosphatidylethanolamine conjugation to preautophagic membranes (and can be detected by western blot as LC3-II). The nuclear localization of SIRT-1 has proved to be critical also for its pro-survival and anti-apoptotic action (*153, 154*). In H_2O_2-treated C-28/I2 cells nuclear localization of SIRT-1 decreases, confirming previous findings of reduced SIRT-1 levels in a variety of cell types under oxidative

stress (*155*), whereas in HT-treated C-28/I2 cells SIRT-1 becomes concentrated in the nucleus. Interestingly an increase of nuclear localization in the hearts of HT-treated rats has also been reported (*150*). We may therefore hypothesize that following HT treatment SIRT-1 accumulates in the nucleus where catalyzes the deacetylation of LC3, which in its turn translocates to the cytosol to drive the autophagic process. Indeed SIRT-1 silencing per se did not affect LC3-II accumulation, sustaining the view that HT-induced nuclear translocation is necessary for SIRT-1 effect on LC3-II formation. Moreover, HT supports autophagy even by increasing transcription of p62, required for autophagic degradation of polyubiquitin-containing bodies (*136*). Thus, the enhanced expression of SQSTM1/p62 gene may sustain the increased p62 protein turnover. Accordingly, it has been reported that SQSTM1/p62 can be transcriptionally up-regulated in some situations of augmented autophagic flux. Notably HT induced an increase of p62 mRNA also in siSIRT-1 cells, indicating an additional, SIRT-1 independent mechanism for autophagy activation. In this regard it should be considered that p62/SQSTM1 is a target gene for the stress and anti-oxidant responsive transcription factor Nrf2, which in its turn can be stimulated by HT as already mentioned (*144*). Overall, by promoting key steps, HT appears able to increase the autophagic flux in chondrocytes.

In our cell model autophagy activation mediated protection from cell death as demonstrated by experiments carried out with either inhibitors or activators of autophagy, including HT and SIRT-1. Our findings, documented by immunocytochemistry, support previous reports indicating that mitophagy is effective in protecting chondrocytes from apoptosis induced through the mitochondrial pathway (*103, 156*). It is also worthy to underline that reducing the extent of oxidative DNA damage in chondrocytes, HT appears promising as a therapeutic tool to limit chondrocyte senescence, a major problem in OA as well as in aging cartilage (*157*).

It should be noted however that in some contexts prolonged or sustained autophagy may not have a protective outcome. For instance, even if autophagy is required to maintain muscle mass (*158*), excessive autophagy is believed to aggravate muscle wasting in animal models. Interestingly HT

supplementation to rats inhibited the negative effects of exhaustive exercise on muscle together with the deregulated increase in autophagy (*159*). Therefore HT may have a homeostatic effect, activating autophagy to the extent required to limit cell damage after an acute insult, but also preventing excessive autophagy.

HT appears to resemble resveratrol, a polyphenol found in red wine and grapes, under some aspects, such as the multiple cellular targets and the ability to induce autophagy in a SIRT-1 dependent manner but also through other pathways (*148, 155*). Interestingly resveratrol can directly induce autophagy via activation of AMPK (*148*), and HT is also known to stimulate AMPK in some experimental models (*71, 151*). Actually AMPK and SIRT-1 may regulate their activities reciprocally, albeit indirectly, and contribute to autophagy induction. Thus AMPK might be involved in the stimulation of autophagic process by HT in chondrocytes. Finally resveratrol, as mentioned above for HT, has been reported to attenuate excessive autophagy (*46, 155*).

MiR-9 and hydroxytyrosol

MiRs have been implicated in fundamental cellular processes such as lipid metabolism, cell differentiation and proliferation, stem cell maintenance and organ development. The run of identifying miR role in cellular function and in the scenario of a specific pathology is going hand in hand with new miR targets being revealed.

Loss of Dicer studies indicate that the miR pathway is fundamental in the skeletal development. For instance, Dicer knockout in limb mesenchyme led to the growth of a smaller limb and skeletal growth defects (*160*). Furthermore, premature death occurred in Dicer-deficient chondrocytes derived from Dicer-null mice. Since Dicer composes the microRNA processor, this finding indirectly unveiled the fundamental role of miRs in chondrogenesis and bone development (*116*). Although the importance of microRNAs in cartilage development and in the pathology of osteoarthritis has been established, numerous researchers keep investigating the roles of specific

microRNAs in specific molecular aspects of development and outcome of osteoarthritis in order to open new perspectives for diagnosis and therapy.

So far, miR-140 is the best characterized miR implicated in OA playing a role in chondrogenesis and cartilage development (*119*).

MiR-140 was reported to target different factors involved in OA, including HDAC4, a known corepressor of RUNX-2 (*118*), CXCL12 and Smad3 (*161, 162*). Then, SOX9, the major transcription factor implicated in the differentiation of chondrocyte phenotype and prevention of cellular hypertrophy, has been shown to regulate miR-140 levels (*163*).

Studies on miR deregulation in OA are performed by comparing the expression of these molecules between OA tissue specimens and their normal articular counterparts (*117*). Functional studies shed light upon the specific role of a deregulated miR in OA through assessment of the modulation of endogenous miR levels and subsequent evaluation of pathological phenotypes in several *in vitro* cellular models.

In order to further characterize the molecular mechanisms underlying the protective effect of HT against H_2O_2-induced cell death, we tried to identify a common factor targeted by both HT and H_2O_2 and able to address chondrocyte fate. Indeed, immunofluorescence assay showed that HT induced nuclear localization and increased intensity of SIRT-1 signal (Fig 4.3). Furthermore immunoblotting assay showed that H_2O_2 treatment reduced protein levels of SIRT-1, while HT alone or after pre-treatment with H_2O_2 increased SIRT-1 expression (Fig. 4.7 A, B). Our data of discordant mRNA and protein levels of SIRT-1 suggested a post-transcriptional regulation modulated by H_2O_2 and HT. These results were particularly intriguing and opened a new project branch spurring us to investigate the actual mechanism underlying HT and H_2O_2 effects on SIRT-1 protein independently of mRNA changes. As a matter of fact miRs comprise the most popular class of short non-coding RNAs that is able to regulate gene expression post-transcriptionally. By

exploiting miR-target prediction tools of many databases available online (TargetScan, miRanda, miRWalk), some miR, including miR-22, miR-34, miR-9, were selected based on the presence of seed-complementary sequences in SIRT-1 3'UTR. Significant variations were appreciated in miR-9 levels by means of qPCR: H_2O_2 led to substantial increase of miR-9, while HT reduced this effect (Fig.4.7 C). The seed sequence (5'-UCUUUGGU-3') identified by TargetScan browser is highly conserved among species and let us hypothesize that SIRT-1 may be a genuine target of miR-9 in our experimental model. Indeed, luciferase reporter assay confirmed that miR-9 targets SIRT-1 in C/28-I2 cell line (Fig. 4.11B) and maybe more. Two mutant vectors with deletions in seed sequence and 3' pairing sequence (Fig. 4.11A) showed 10% difference of luciferase activity in response to premiR-9 transfection. It is conceivable that the upstream sequence of pairing confers a more efficient matching.

Accordingly, Saunders et al. reported that 5 different miRs suppressed SIRT-1 protein expression and miR-9 was among these regulators (*164*). Other authors found this relationship between miR-9 and SIRT-1 (*165, 166*); however our study is the first to demonstrate that SIRT-1 is a real target of miR-9 in human primary chondrocytes and in C-28/I2 cell line. As we had previously showed that HT protected chondrocytes from H_2O_2-induced cell death via SIRT-1 -dependent and-independent mechanisms, we speculated that miR-9 was the missing piece of puzzle through which HT was able to express its protective potential against oxidative stress in our experimental model. In order to confirm this hypothesis we explored how modulation of miR-9 levels could influence the effects of both HT and H_2O_2 treatments by transfecting antimiR-9 and premiR-9 in human primary chondrocytes and in C-28/I2 cell line. First, in both cell systems we observed that antimiR-9 rescued SIRT-1 protein levels under H_2O_2 treatment and, conversely premiR-9 suppressed SIRT-1 levels in control cells and after HT treatment. Next, our data showed that miR-9 mediates cell death induced by H_2O_2 and the protective effect of HT, as observed in human primary chondrocytes

and C/28-I2 cell line transfected with antimiR-9 and premiR-9 by trypan blue exclusion and caspase activity assays (Fig 4.9 and 4.10).

Another interesting question is whether downregulation of SIRT-1 could compromise the protective action by antimiR-9 transfection in cells exposed to oxidative stress. Loss of SIRT-1 in antimiR-9-transfected chondrocytes also resulted in HT-induced protection of H_2O_2-treated chondrocytes, even though less marked (Fig. 4.9F, G and 4.10E). Thus it may be concluded that SIRT-1 is only partially required for the protection exerted by HT and, actually, miR-9 is the real hub of cellular response to HT and H_2O_2 treatments.

Altered expression of miR-9 in OA vs normal cartilage has been reported (*117, 121*). Jones et al. found up-regulated levels of miR-9 and miR-98 and down-regulated levels of miR-146 in OA samples and ascribed to these miRs a protective role during late-stage OA. In particular, MMP-13 was shown to be a direct target of miR-9 (*121*). Recently Haqqi and collaborators showed that in human OA chondrocytes monocyte chemo-attractant protein1-induced protein 1 (MCPIP-1) down-regulation corresponds to an increased expression of miR-9, which is initially expressed at low levels (*167*). In accordance with our findings, miR-9 results to be overexpressed in other cellular models, including MELA cybrid cells under NF-κB stimulation (*168*) and HLF-1 under H_2O_2 and TGF-β1 stimulation (*169*) confirming that miR-9 responds to perturbations in the redox state. Overall these data suggest that miR-9 may act as the main player of H_2O_2-induced changes in human chondrocytes and is likely involved in oxidative stress-related and possibly other molecular aspects of the pathology of OA.

Autophagy and miR-155

Our study carried out at The Scripps Research Institute, La Jolla, CA, USA, was based on the discovery in Prof. Lotz's laboratory that miR-155 was one of the most upregulated miR in human OA cartilage and aimed at determining the role of miR-155 in chondrocyte autophagy. MiR-155 appeared as a potential regulator of autophagy based on the presence of miR-155 seed-

complementary sequences in the autophagy-related genes (ATG3, GABARAPL1, ATG5, ATG2B, LAMP2, FOXO3).

Our data show that miR-155 suppresses autophagy flux in T/C28a2 cells and primary human chondrocytes as measured by LC3 conversion and by utilizing a Cyto-ID cationic amphiphilic tracer dye that specifically recognizes autophagosomes (*135*). Accordingly, the number of autophagosomes was significantly increased when miR-155 was blocked by LNA and it was reduced when cells were treated with miR-155 mimic. These autophagy modulating effects of miR-155 LNA and mimic were observed under basal culture conditions and under cell treatment with rapamycin in human chondrocytes and after treatment with rapamycin and 2-DG in T/C28a2 cells.

We explored mechanisms by which miR-155 suppressed autophagy and discovered that multiple factors involved in the autophagic cascade are miR-155 targets. By transfecting LNA and mimic specific for miR-155 in T/C28a2 and in human primary chondrocytes, we observed a negative correlation between miR-155 and its target mRNAs, including ATG3, GABARAPL1, ATG5, FOXO3 and other autophagy-related factors not predicted by miR target databases, including ULK1, MAP1LC3 and ATG14 (Fig. 4.16 and 4.17). These data suggest that miR-155 is able to modulate the autophagy activity by regulating post-transcriptionally several components involved in different stages of autophagy, from the induction to elongation steps. Furthermore, consistent with changes in mRNA levels, miR-155 modulated protein levels of these factors. It is conceivable that miR-155 influences the expression of MAP1LC3, ATG14 and ULK1 by suppression of the transcriptional factor FOXO3 (*170, 171*).

Moreover, by investigating potential involvement of mTOR as a critical negative regulator of autophagy (*138-140*) in miR-155-mediated autophagy suppression, we discovered that miR-155 inhibits mTOR activity rather than activating it, as demonstrated by detection of phosphorylation levels of ribosomal protein s6, as a downstream substrate of mTORC1, and of AKT, as an upstream regulator of mTORC1. This unexpected result can be explained by miR-155 effects on gene and

protein expression of RICTOR, a critical component of mTORC2 (*82*), which induces mTORC1 activation via AKT phosphorylation (*83*). We found that LNA and mimic miR-155 transfection increased and reduced protein and mRNA levels of RICTOR, respectively. This data indicates that the regulation of downstream autophagy-related factors by miR-155 is sufficient to affect the level of autophagy, independently of mTOR activity.

Taken together, these data identify miR-155 as a potent regulator of autophagy under physiological conditions. MiR-155 is able to modulate this process via multiple mechanisms as proposed in the model shown below.

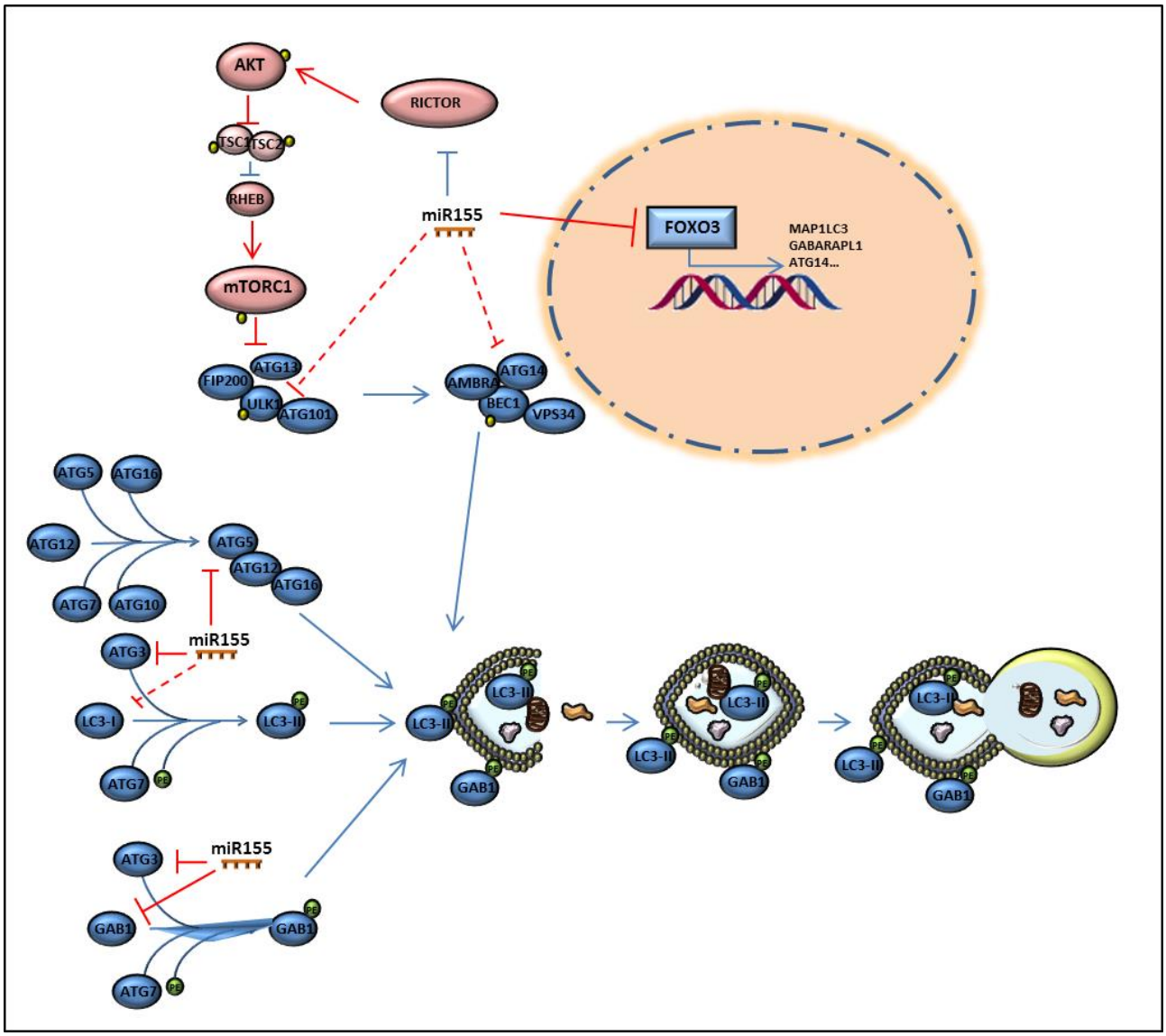

In pathological conditions when miR-155 levels are upregulated, as in OA cartilage, the autophagy flux is compromised. We propose that a critical factor might be an exact threshold level of miR-155 that controls the autophagic response to cellular metabolic requests.

In accordance with our findings, Holla et al. described an inhibitory role of miR155 on interferon-γ-induced autophagy in macrophages (*172*). However, another study found that miR-155 enhanced hypoxia-induced autophagy in human cancer cell lines by inhibiting the mTOR pathway (*173*). Although we also found a reduction of mTOR activity in response to mimic miR-155 transfection, this was not sufficient to reverse the strong inhibitory effect of miR-155 on autophagy flux. Thus it is likely that the final effect of miR-155 on autophagy is stimulus and cell-specific and may be dependent on other factors implicated in the post-transcriptional and post-translational regulation of autophagy-related genes.

MiR-155 has been implicated in other aspects linked to OA pathophysiology, in particular in regulating inflammatory responses (*174-176*). For example, CD14+ monocytes and macrophages overexpressing miR-155 exhibited increased production of proinflammatory cytokines while these were reduced in miR-155-deficient mice (*177*). In line with these data, Li et al. showed previously that miR-155 upregulated TNF-α and IL-1β in peripheral blood macrophages (*178*).

Our study reveals that miR-155 can profoundly impact the autophagic cascade. We showed an inverse correlation between the miR-155 levels and autophagic flux in human chondrocytes. Furthermore, we demonstrated that increased levels of miR-155 inhibit GABARAPL1, ATG3, ATG5, ATG14, FOXO3, MAP1LC3, and ULK1 expression, and drastically suppress autophagy independently of its regulation on RICTOR expression and on mTOR signalling. In light of this study we can hypothesize that miR-155 is responsible, at least in part, to autophagy failure associated with the pathophysiology of OA.

Although further investigations on the role of miR-155 in dysfunction of autophagy and in other processes involved in the development of OA are required, the present study proposes an attractive opportunity to develop a future strategy based on miR-155 blockage for OA treatment.

Concluding remarks

As widely described in this thesis, articular chondrocyte capacity to maintain normal cartilage matrix structure and successful autophagy declines in elders critically contributing to progression in cartilage degradation. Thus, pharmacological activation of autophagy and well-known molecular factors considered important for adaptive responses to environmental stresses, including SIRT-1 or Nrf-2, may be an appropriate therapeutic approach for OA. These studies showed how HT may represent a valid agent of prevention against oxidative stress in OA by protecting against DNA damage and cell death, and by stimulating autophagy. Furthermore, we demonstrated that HT exerts its beneficial effect by suppressing miR-9 levels increased by H_2O_2 treatment and that this mechanism is only partially SIRT-1-dependent. The second miR involved in OA pathology, miR-155, is implicated in the failure of autophagy in human adult chondrocytes. The involvement of miRs across human diseases has been widely reported and motivated the development of miRs-based therapies. MiRs are promising targets as a single miR is able to regulate multiple genes in dysregulated pathways in a disease. Thus, the identification of a single miR, involved simultaneously in several disease-related pathways, discloses a potent therapeutic target. Indeed the unveiling of bioactive compounds able to influence miR network may open a new topic of research with huge potential and not yet well explored.

6. BIBLOGRAPHY

1. J. Martel-Pelletier, C. Boileau, J. P. Pelletier, P. J. Roughley, Cartilage in normal and osteoarthritis conditions. *Best Pract Res Clin Rheumatol* **22**, 351-384 (2008).
2. A. J. Sophia Fox, A. Bedi, S. A. Rodeo, The basic science of articular cartilage: structure, composition, and function. *Sports Health* **1**, 461-468 (2009).
3. D. Heinegård, T. Saxne, The role of the cartilage matrix in osteoarthritis. *Nat Rev Rheumatol* **7**, 50-56 (2011).
4. C. M. Lapière, A. Lenaers, L. D. Kohn, Procollagen peptidase: an enzyme excising the coordination peptides of procollagen. *Proc Natl Acad Sci U S A* **68**, 3054-3058 (1971).
5. A. Colige *et al.*, Domains and maturation processes that regulate the activity of ADAMTS-2, a metalloproteinase cleaving the aminopropeptide of fibrillar procollagens types I-III and V. *J Biol Chem* **280**, 34397-34408 (2005).
6. C. Wermter *et al.*, The protease domain of procollagen C-proteinase (BMP1) lacks substrate selectivity, which is conferred by non-proteolytic domains. *Biol Chem* **388**, 513-521 (2007).
7. E. Schipani *et al.*, Hypoxia in cartilage: HIF-1alpha is essential for chondrocyte growth arrest and survival. *Genes Dev* **15**, 2865-2876 (2001).
8. S. R. Goldring, M. B. Goldring, Clinical aspects, pathology and pathophysiology of osteoarthritis. *J Musculoskelet Neuronal Interact* **6**, 376-378 (2006).
9. M. B. Goldring, Update on the biology of the chondrocyte and new approaches to treating cartilage diseases. *Best Pract Res Clin Rheumatol* **20**, 1003-1025 (2006).
10. A. M. DeLise, L. Fischer, R. S. Tuan, Cellular interactions and signaling in cartilage development. *Osteoarthritis Cartilage* **8**, 309-334 (2000).
11. M. B. Goldring, Articular cartilage degradation in osteoarthritis. *HSS J* **8**, 7-9 (2012).
12. P. Sarzi-Puttini *et al.*, Osteoarthritis: an overview of the disease and its treatment strategies. *Semin Arthritis Rheum* **35**, 1-10 (2005).

13. D. T. Felson, Clinical practice. Osteoarthritis of the knee. *N Engl J Med* **354**, 841-848 (2006).

14. M. E. Miller, W. J. Rejeski, S. P. Messier, R. F. Loeser, Modifiers of change in physical functioning in older adults with knee pain: the Observational Arthritis Study in Seniors (OASIS). *Arthritis Rheum* **45**, 331-339 (2001).

15. D. T. Felson *et al.*, Osteoarthritis: new insights. Part 1: the disease and its risk factors. *Ann Intern Med* **133**, 635-646 (2000).

16. H. A. Wieland, M. Michaelis, B. J. Kirschbaum, K. A. Rudolphi, Osteoarthritis - an untreatable disease? *Nat Rev Drug Discov* **4**, 331-344 (2005).

17. D. Patra, L. J. Sandell, Recent advances in biomarkers in osteoarthritis. *Curr Opin Rheumatol* **23**, 465-470 (2011).

18. R. F. Loeser, Age-related changes in the musculoskeletal system and the development of osteoarthritis. *Clin Geriatr Med* **26**, 371-386 (2010).

19. L. C. Tetlow, D. J. Adlam, D. E. Woolley, Matrix metalloproteinase and proinflammatory cytokine production by chondrocytes of human osteoarthritic cartilage: associations with degenerative changes. *Arthritis Rheum* **44**, 585-594 (2001).

20. W. Wu *et al.*, Sites of collagenase cleavage and denaturation of type II collagen in aging and osteoarthritic articular cartilage and their relationship to the distribution of matrix metalloproteinase 1 and matrix metalloproteinase 13. *Arthritis Rheum* **46**, 2087-2094 (2002).

21. L. A. Neuhold *et al.*, Postnatal expression in hyaline cartilage of constitutively active human collagenase-3 (MMP-13) induces osteoarthritis in mice. *J Clin Invest* **107**, 35-44 (2001).

22. M. B. Goldring *et al.*, Roles of inflammatory and anabolic cytokines in cartilage metabolism: signals and multiple effectors converge upon MMP-13 regulation in osteoarthritis. *Eur Cell Mater* **21**, 202-220 (2011).

23. R. F. Loeser, S. R. Goldring, C. R. Scanzello, M. B. Goldring, Osteoarthritis: a disease of the joint as an organ. *Arthritis Rheum* **64**, 1697-1707 (2012).

24. A. M. Reginato, C. Sanz-Rodriguez, A. Diaz, R. M. Dharmavaram, S. A. Jimenez, Transcriptional modulation of cartilage-specific collagen gene expression by interferon gamma and tumour necrosis factor alpha in cultured human chondrocytes. *Biochem J* **294 (Pt 3)**, 761-769 (1993).

25. C. Baugé *et al.*, Interleukin-1beta impairment of transforming growth factor beta1 signaling by down-regulation of transforming growth factor beta receptor type II and up-regulation of Smad7 in human articular chondrocytes. *Arthritis Rheum* **56**, 3020-3032 (2007).

26. A. Moustakas, S. Souchelnytskyi, C. H. Heldin, Smad regulation in TGF-beta signal transduction. *J Cell Sci* **114**, 4359-4369 (2001).

27. M. B. Goldring, F. Berenbaum, The regulation of chondrocyte function by proinflammatory mediators: prostaglandins and nitric oxide. *Clin Orthop Relat Res*, S37-46 (2004).

28. K. Okazaki, J. Li, H. Yu, N. Fukui, L. J. Sandell, CCAAT/enhancer-binding proteins beta and delta mediate the repression of gene transcription of cartilage-derived retinoic acid-sensitive protein induced by interleukin-1 beta. *J Biol Chem* **277**, 31526-31533 (2002).

29. M. G. Chambers, T. Kuffner, S. K. Cowan, K. S. Cheah, R. M. Mason, Expression of collagen and aggrecan genes in normal and osteoarthritic murine knee joints. *Osteoarthritis Cartilage* **10**, 51-61 (2002).

30. J. R. Matyas, D. Huang, M. Chung, M. E. Adams, Regional quantification of cartilage type II collagen and aggrecan messenger RNA in joints with early experimental osteoarthritis. *Arthritis Rheum* **46**, 1536-1543 (2002).

31. A. A. Young *et al.*, Regional assessment of articular cartilage gene expression and small proteoglycan metabolism in an animal model of osteoarthritis. *Arthritis Res Ther* **7**, R852-861 (2005).

32. N. Fukui *et al.*, Zonal gene expression of chondrocytes in osteoarthritic cartilage. *Arthritis Rheum* **58**, 3843-3853 (2008).

33. R. F. Loeser, Aging cartilage and osteoarthritis--what's the link? *Sci Aging Knowledge Environ* **2004**, pe31 (2004).

34. H. Iwanaga *et al.*, Enhanced expression of insulin-like growth factor-binding proteins in human osteoarthritic cartilage detected by immunohistochemistry and in situ hybridization. *Osteoarthritis Cartilage* **13**, 439-448 (2005).

35. N. Moulharat *et al.*, Effects of transforming growth factor-beta on aggrecanase production and proteoglycan degradation by human chondrocytes in vitro. *Osteoarthritis Cartilage* **12**, 296-305 (2004).

36. S. Chubinskaya, K. E. Kuettner, Regulation of osteogenic proteins by chondrocytes. *Int J Biochem Cell Biol* **35**, 1323-1340 (2003).

37. M. Blagojevic, C. Jinks, A. Jeffery, K. P. Jordan, Risk factors for onset of osteoarthritis of the knee in older adults: a systematic review and meta-analysis. *Osteoarthritis Cartilage* **18**, 24-33 (2010).

38. A. Freund, A. V. Orjalo, P. Y. Desprez, J. Campisi, Inflammatory networks during cellular senescence: causes and consequences. *Trends Mol Med* **16**, 238-246 (2010).

39. M. C. Haigis, B. A. Yankner, The aging stress response. *Mol Cell* **40**, 333-344 (2010).

40. M. De la Fuente, J. Miquel, An update of the oxidation-inflammation theory of aging: the involvement of the immune system in oxi-inflamm-aging. *Curr Pharm Des* **15**, 3003-3026 (2009).

41. Y. Henrotin, B. Kurz, T. Aigner, Oxygen and reactive oxygen species in cartilage degradation: friends or foes? *Osteoarthritis Cartilage* **13**, 643-654 (2005).

42. D. M. Olszewska-Słonina *et al.*, Oxidative equilibrium in the prophylaxis of degenerative joint changes: an analysis of pre- and postoperative activity of antioxidant enzymes in patients with hip and knee osteoarthritis. *Med Sci Monit* **16**, CR238-245 (2010).

43. J. L. Scott *et al.*, Superoxide dismutase downregulation in osteoarthritis progression and end-stage disease. *Ann Rheum Dis* **69**, 1502-1510 (2010).

44. Y. E. Henrotin, P. Bruckner, J. P. Pujol, The role of reactive oxygen species in homeostasis and degradation of cartilage. *Osteoarthritis Cartilage* **11**, 747-755 (2003).

45. N. Verzijl, R. A. Bank, J. M. TeKoppele, J. DeGroot, AGEing and osteoarthritis: a different perspective. *Curr Opin Rheumatol* **15**, 616-622 (2003).

46. S. Cetrullo, S. D'Adamo, B. Tantini, R. M. Borzi, F. Flamigni, mTOR, AMPK, and Sirt1: Key Players in Metabolic Stress Management. *Crit Rev Eukaryot Gene Expr* **25**, 59-75 (2015).

47. S. Hekimi, J. Lapointe, Y. Wen, Taking a "good" look at free radicals in the aging process. *Trends Cell Biol* **21**, 569-576 (2011).

48. F. Yeung *et al.*, Modulation of NF-kappaB-dependent transcription and cell survival by the SIRT1 deacetylase. *EMBO J* **23**, 2369-2380 (2004).

49. A. Salminen, K. Kaarniranta, A. Kauppinen, Crosstalk between Oxidative Stress and SIRT1: Impact on the Aging Process. *Int J Mol Sci* **14**, 3834-3859 (2013).

50. V. Gagarina *et al.*, SirT1 enhances survival of human osteoarthritic chondrocytes by repressing protein tyrosine phosphatase 1B and activating the insulin-like growth factor receptor pathway. *Arthritis Rheum* **62**, 1383-1392 (2010).

51. K. Takayama *et al.*, SIRT1 regulation of apoptosis of human chondrocytes. *Arthritis Rheum* **60**, 2731-2740 (2009).

52. O. Gabay *et al.*, Sirtuin 1 enzymatic activity is required for cartilage homeostasis in vivo in a mouse model. *Arthritis Rheum* **65**, 159-166 (2013).

53. J. Clouet *et al.*, From osteoarthritis treatments to future regenerative therapies for cartilage. *Drug Discov Today* **14**, 913-925 (2009).

54. L. Das, E. Bhaumik, U. Raychaudhuri, R. Chakraborty, Role of nutraceuticals in human health. *J Food Sci Technol* **49**, 173-183 (2012).

55. Y. Henrotin, C. Lambert, D. Couchourel, C. Ripoll, E. Chiotelli, Nutraceuticals: do they represent a new era in the management of osteoarthritis? - a narrative review from the lessons taken with five products. *Osteoarthritis Cartilage* **19**, 1-21 (2011).

56. W. P. Chen, P. F. Hu, J. P. Bao, L. D. Wu, Morin exerts antiosteoarthritic properties: an in vitro and in vivo study. *Exp Biol Med (Maywood)* **237**, 380-386 (2012).

57. T. Phitak *et al.*, Chondroprotective and anti-inflammatory effects of sesamin. *Phytochemistry* **80**, 77-88 (2012).

58. A. Villalvilla, R. Gómez, R. Largo, G. Herrero-Beaumont, Lipid transport and metabolism in healthy and osteoarthritic cartilage. *Int J Mol Sci* **14**, 20793-20808 (2013).

59. T. Matsuzaki *et al.*, Disruption of Sirt1 in chondrocytes causes accelerated progression of osteoarthritis under mechanical stress and during ageing in mice. *Ann Rheum Dis* **73**, 1397-1404 (2014).

60. B. P. Hubbard *et al.*, Evidence for a common mechanism of SIRT1 regulation by allosteric activators. *Science* **339**, 1216-1219 (2013).

61. E. Mével *et al.*, Nutraceuticals in joint health: animal models as instrumental tools. *Drug Discov Today* **19**, 1649-1658 (2014).

62. A. Facchini *et al.*, Sulforaphane protects human chondrocytes against cell death induced by various stimuli. *J Cell Physiol* **226**, 1771-1779 (2011).

63. R. K. Davidson *et al.*, Sulforaphane represses matrix-degrading proteases and protects cartilage from destruction in vitro and in vivo. *Arthritis Rheum* **65**, 3130-3140 (2013).

64. S. Granados-Principal, J. L. Quiles, C. L. Ramirez-Tortosa, P. Sanchez-Rovira, M. C. Ramirez-Tortosa, Hydroxytyrosol: from laboratory investigations to future clinical trials. *Nutr Rev* **68**, 191-206 (2010).

65. R. W. Owen *et al.*, Identification of lignans as major components in the phenolic fraction of olive oil. *Clin Chem* **46**, 976-988 (2000).

66. M. N. Vissers, P. L. Zock, A. J. Roodenburg, R. Leenen, M. B. Katan, Olive oil phenols are absorbed in humans. *J Nutr* **132**, 409-417 (2002).

67. K. L. Tuck, M. P. Freeman, P. J. Hayball, G. L. Stretch, I. Stupans, The in vivo fate of hydroxytyrosol and tyrosol, antioxidant phenolic constituents of olive oil, after intravenous and oral dosing of labeled compounds to rats. *J Nutr* **131**, 1993-1996 (2001).

68. C. L. Xu, M. K. Sim, Reduction of dihydroxyphenylacetic acid by a novel enzyme in the rat brain. *Biochem Pharmacol* **50**, 1333-1337 (1995).

69. D. J. Edwards, M. Rizk, Conversion of 3, 4-dihydroxyphenylalanine and deuterated 3, 4-dihydroxyphenylalanine to alcoholic metabolites of catecholamines in rat brain. *J Neurochem* **36**, 1641-1647 (1981).

70. H. Zrelli *et al.*, Hydroxytyrosol induces proliferation and cytoprotection against oxidative injury in vascular endothelial cells: role of Nrf2 activation and HO-1 induction. *J Agric Food Chem* **59**, 4473-4482 (2011).

71. H. Zrelli, M. Matsuoka, S. Kitazaki, M. Zarrouk, H. Miyazaki, Hydroxytyrosol reduces intracellular reactive oxygen species levels in vascular endothelial cells by upregulating catalase expression through the AMPK-FOXO3a pathway. *Eur J Pharmacol* **660**, 275-282 (2011).

72. X. Zhang, J. Cao, L. Zhong, Hydroxytyrosol inhibits pro-inflammatory cytokines, iNOS, and COX-2 expression in human monocytic cells. *Naunyn Schmiedebergs Arch Pharmacol* **379**, 581-586 (2009).

73. X. Zhang, J. Cao, L. Jiang, C. Geng, L. Zhong, Protective effect of hydroxytyrosol against acrylamide-induced cytotoxicity and DNA damage in HepG2 cells. *Mutat Res* **664**, 64-68 (2009).

74. X. Zhang, J. Cao, L. Jiang, L. Zhong, Suppressive effects of hydroxytyrosol on oxidative stress and nuclear Factor-kappaB activation in THP-1 cells. *Biol Pharm Bull* **32**, 578-582 (2009).

75. C. DE DUVE, The lysosome. *Sci Am* **208**, 64-72 (1963).

76. S. L. CLARK, Cellular differentiation in the kidneys of newborn mice studies with the electron microscope. *J Biophys Biochem Cytol* **3**, 349-362 (1957).

77. R. L. Deter, C. De Duve, Influence of glucagon, an inducer of cellular autophagy, on some physical properties of rat liver lysosomes. *J Cell Biol* **33**, 437-449 (1967).

78. D. Glick, S. Barth, K. F. Macleod, Autophagy: cellular and molecular mechanisms. *J Pathol* **221**, 3-12 (2010).

79. N. Mizushima, Autophagy: process and function. *Genes Dev* **21**, 2861-2873 (2007).

80. D. M. Sabatini, mTOR and cancer: insights into a complex relationship. *Nat Rev Cancer* **6**, 729-734 (2006).

81. D. A. Guertin, D. M. Sabatini, Defining the role of mTOR in cancer. *Cancer Cell* **12**, 9-22 (2007).

82. D. D. Sarbassov *et al.*, Rictor, a novel binding partner of mTOR, defines a rapamycin-insensitive and raptor-independent pathway that regulates the cytoskeleton. *Curr Biol* **14**, 1296-1302 (2004).

83. D. D. Sarbassov, D. A. Guertin, S. M. Ali, D. M. Sabatini, Phosphorylation and regulation of Akt/PKB by the rictor-mTOR complex. *Science* **307**, 1098-1101 (2005).

84. S. Alers, A. S. Löffler, S. Wesselborg, B. Stork, Role of AMPK-mTOR-Ulk1/2 in the regulation of autophagy: cross talk, shortcuts, and feedbacks. *Mol Cell Biol* **32**, 2-11 (2012).

85. S. Díaz-Troya, M. E. Pérez-Pérez, F. J. Florencio, J. L. Crespo, The role of TOR in autophagy regulation from yeast to plants and mammals. *Autophagy* **4**, 851-865 (2008).

86. K. Ogura *et al.*, Caenorhabditis elegans unc-51 gene required for axonal elongation encodes a novel serine/threonine kinase. *Genes Dev* **8**, 2389-2400 (1994).

87. R. C. Scott, O. Schuldiner, T. P. Neufeld, Role and regulation of starvation-induced autophagy in the Drosophila fat body. *Dev Cell* **7**, 167-178 (2004).

88. S. Alers *et al.*, Atg13 and FIP200 act independently of Ulk1 and Ulk2 in autophagy induction. *Autophagy* **7**, 1423-1433 (2011).

89. C. Liang *et al.*, Autophagic and tumour suppressor activity of a novel Beclin1-binding protein UVRAG. *Nat Cell Biol* **8**, 688-699 (2006).

90. R. C. Russell *et al.*, ULK1 induces autophagy by phosphorylating Beclin-1 and activating VPS34 lipid kinase. *Nat Cell Biol* **15**, 741-750 (2013).

91. S. Wesselborg, B. Stork, Autophagy signal transduction by ATG proteins: from hierarchies to networks. *Cell Mol Life Sci* **72**, 4721-4757 (2015).

92. H. Weidberg *et al.*, LC3 and GATE-16/GABARAP subfamilies are both essential yet act differently in autophagosome biogenesis. *EMBO J* **29**, 1792-1802 (2010).

93. S. Shaid, C. H. Brandts, H. Serve, I. Dikic, Ubiquitination and selective autophagy. *Cell Death Differ* **20**, 21-30 (2013).

94. B. Levine, D. J. Klionsky, Development by self-digestion: molecular mechanisms and biological functions of autophagy. *Dev Cell* **6**, 463-477 (2004).

95. D. J. Klionsky *et al.*, Guidelines for the use and interpretation of assays for monitoring autophagy (3rd edition). *Autophagy* **12**, 1-222 (2016).

96. D. C. Rubinsztein, P. Codogno, B. Levine, Autophagy modulation as a potential therapeutic target for diverse diseases. *Nat Rev Drug Discov* **11**, 709-730 (2012).

97. H. I. Roach, T. Aigner, J. B. Kouri, Chondroptosis: a variant of apoptotic cell death in chondrocytes? *Apoptosis* **9**, 265-277 (2004).

98. B. Caramés, N. Taniguchi, S. Otsuki, F. J. Blanco, M. Lotz, Autophagy is a protective mechanism in normal cartilage, and its aging-related loss is linked with cell death and osteoarthritis. *Arthritis and rheumatism* **62**, 791-801 (2010).

99. Y. Zhang *et al.*, Cartilage-specific deletion of mTOR upregulates autophagy and protects mice from osteoarthritis. *Ann. Rheum. Dis.*, (2014).

100. B. Caramés *et al.*, Glucosamine activates autophagy in vitro and in vivo. *Arthritis and rheumatism* **65**, 1843-1852 (2013).

101. T. Matsuzaki *et al.*, Intra-articular administration of gelatin hydrogels incorporating rapamycin-micelles reduces the development of experimental osteoarthritis in a murine model. *Biomaterials* **35**, 9904-9911 (2014).

102. R. M. Borzì *et al.*, Polyamine delivery as a tool to modulate stem cell differentiation in skeletal tissue engineering. *Amino Acids* **46**, 717-728 (2014).

103. H. Sasaki *et al.*, Autophagy modulates osteoarthritis-related gene expression in human chondrocytes. *Arthritis and rheumatism* **64**, 1920-1928 (2012).

104. K. Takayama *et al.*, Local intra-articular injection of rapamycin delays articular cartilage degeneration in a murine model of osteoarthritis. *Arthritis Res Ther* **16**, 482 (2014).

105. R. C. Lee, R. L. Feinbaum, V. Ambros, The C. elegans heterochronic gene lin-4 encodes small RNAs with antisense complementarity to lin-14. *Cell* **75**, 843-854 (1993).

106. B. Wightman, I. Ha, G. Ruvkun, Posttranscriptional regulation of the heterochronic gene lin-14 by lin-4 mediates temporal pattern formation in C. elegans. *Cell* **75**, 855-862 (1993).

107. B. J. Reinhart *et al.*, The 21-nucleotide let-7 RNA regulates developmental timing in Caenorhabditis elegans. *Nature* **403**, 901-906 (2000).

108. A. Rodriguez, S. Griffiths-Jones, J. L. Ashurst, A. Bradley, Identification of mammalian microRNA host genes and transcription units. *Genome Res* **14**, 1902-1910 (2004).

109. A. F. Olena, J. G. Patton, Genomic organization of microRNAs. *J Cell Physiol* **222**, 540-545 (2010).

110. D. P. Bartel, MicroRNAs: genomics, biogenesis, mechanism, and function. *Cell* **116**, 281-297 (2004).

111. D. P. Bartel, MicroRNAs: target recognition and regulatory functions. *Cell* **136**, 215-233 (2009).

112. C. Napoli, C. Lemieux, R. Jorgensen, Introduction of a Chimeric Chalcone Synthase Gene into Petunia Results in Reversible Co-Suppression of Homologous Genes in trans. *Plant Cell* **2**, 279-289 (1990).

113. A. Fire *et al.*, Potent and specific genetic interference by double-stranded RNA in Caenorhabditis elegans. *Nature* **391**, 806-811 (1998).

114. L. He, G. J. Hannon, MicroRNAs: small RNAs with a big role in gene regulation. *Nat Rev Genet* **5**, 522-531 (2004).

115. J. R. Lytle, T. A. Yario, J. A. Steitz, Target mRNAs are repressed as efficiently by microRNA-binding sites in the 5' UTR as in the 3' UTR. *Proc Natl Acad Sci U S A* **104**, 9667-9672 (2007).

116. T. Kobayashi *et al.*, Dicer-dependent pathways regulate chondrocyte proliferation and differentiation. *Proc Natl Acad Sci U S A* **105**, 1949-1954 (2008).

117. D. Iliopoulos, K. N. Malizos, P. Oikonomou, A. Tsezou, Integrative microRNA and proteomic approaches identify novel osteoarthritis genes and their collaborative metabolic and inflammatory networks. *PLoS One* **3**, e3740 (2008).

118. L. Tuddenham *et al.*, The cartilage specific microRNA-140 targets histone deacetylase 4 in mouse cells. *FEBS Lett* **580**, 4214-4217 (2006).

119. S. Miyaki *et al.*, MicroRNA-140 is expressed in differentiated human articular chondrocytes and modulates interleukin-1 responses. *Arthritis Rheum* **60**, 2723-2730 (2009).

120. M. J. Barter, C. Bui, D. A. Young, Epigenetic mechanisms in cartilage and osteoarthritis: DNA methylation, histone modifications and microRNAs. *Osteoarthritis Cartilage* **20**, 339-349 (2012).

121. S. W. Jones *et al.*, The identification of differentially expressed microRNA in osteoarthritic tissue that modulate the production of TNF-alpha and MMP13. *Osteoarthritis Cartilage* **17**, 464-472 (2009).

122. N. Akhtar *et al.*, MicroRNA-27b regulates the expression of matrix metalloproteinase 13 in human osteoarthritis chondrocytes. *Arthritis Rheum* **62**, 1361-1371 (2010).

123. Y. Huang, A. Y. Chuang, E. A. Ratovitski, Phospho-ΔNp63α/miR-885-3p axis in tumor cell life and cell death upon cisplatin exposure. *Cell Cycle* **10**, 3938-3947 (2011).

124. Y. Yang, C. Liang, MicroRNAs: an emerging player in autophagy. *ScienceOpen Res* **2015**, (2015).

125. Y. Chang *et al.*, miR-375 inhibits autophagy and reduces viability of hepatocellular carcinoma cells under hypoxic conditions. *Gastroenterology* **143**, 177-187.e178 (2012).

126. H. Zhu *et al.*, Regulation of autophagy by a beclin 1-targeted microRNA, miR-30a, in cancer cells. *Autophagy* **5**, 816-823 (2009).

127. M. B. Goldring *et al.*, Interleukin-1 beta-modulated gene expression in immortalized human chondrocytes. *J Clin Invest* **94**, 2307-2316 (1994).

128. I. Stanic *et al.*, Polyamine depletion inhibits apoptosis following blocking of survival pathways in human chondrocytes stimulated by tumor necrosis factor-alpha. *J Cell Physiol* **206**, 138-146 (2006).

129. A. Facchini *et al.*, Hydroxytyrosol prevents increase of osteoarthritis markers in human chondrocytes treated with hydrogen peroxide or growth-related oncogene α. *PLoS One* **9**, e109724 (2014).

130. B. Tantini *et al.*, Involvement of polyamines in apoptosis of cardiac myoblasts in a model of simulated ischemia. *J Mol Cell Cardiol* **40**, 775-782 (2006).

131. F. J. Blanco, R. L. Ochs, H. Schwarz, M. Lotz, Chondrocyte apoptosis induced by nitric oxide. *Am. J. Pathol.* **146**, 75-85 (1995).

132. A. R. Shikhman, D. C. Brinson, J. Valbracht, M. K. Lotz, Cytokine regulation of facilitated glucose transport in human articular chondrocytes. *J. Immunol.* **167**, 7001-7008 (2001).

133. B. Carames *et al.*, Glucosamine activates autophagy in vitro and in vivo. *Arthritis and rheumatism* **65**, 1843-1852 (2013).

134. Y. Akasaki *et al.*, FoxO transcription factors support oxidative stress resistance in human chondrocytes. *Arthritis Rheumatol.* **66**, 3349-3358 (2014).

135. C. L. Oeste, E. Seco, W. F. Patton, P. Boya, D. Pérez-Sala, Interactions between autophagic and endo-lysosomal markers in endothelial cells. *Histochem. Cell Biol.* **139**, 659-670 (2013).

136. M. K. Lotz, B. Caramés, Autophagy and cartilage homeostasis mechanisms in joint health, aging and OA. *Nat Rev Rheumatol* **7**, 579-587 (2011).

137. N. Mizushima, T. Yoshimori, B. Levine, Methods in mammalian autophagy research. *Cell* **140**, 313-326 (2010).

138. J. Kim, M. Kundu, B. Viollet, K. L. Guan, AMPK and mTOR regulate autophagy through direct phosphorylation of Ulk1. *Nat Cell Biol* **13**, 132-141 (2011).

139. C. H. Jung, S. H. Ro, J. Cao, N. M. Otto, D. H. Kim, mTOR regulation of autophagy. *FEBS Lett* **584**, 1287-1295 (2010).

140. T. Noda, Y. Ohsumi, Tor, a phosphatidylinositol kinase homologue, controls autophagy in yeast. *J Biol Chem* **273**, 3963-3966 (1998).

141. B. Caramés, M. Olmer, W. B. Kiosses, M. Lotz, The relationship of autophagy defects and cartilage damage during joint aging in a mouse model. *Arthritis Rheumatol*, (2015).

142. J. Kim, K. L. Guan, Regulation of the autophagy initiating kinase ULK1 by nutrients: roles of mTORC1 and AMPK. *Cell Cycle* **10**, 1337-1338 (2011).

143. T. Hu, X. W. He, J. G. Jiang, X. L. Xu, Hydroxytyrosol and its potential therapeutic effects. *J Agric Food Chem* **62**, 1449-1455 (2014).

144. M. A. Martín *et al.*, Hydroxytyrosol induces antioxidant/detoxificant enzymes and Nrf2 translocation via extracellular regulated kinases and phosphatidylinositol-3-kinase/protein kinase B pathways in HepG2 cells. *Mol Nutr Food Res* **54**, 956-966 (2010).

145. O. Gabay, C. Sanchez, Epigenetics, sirtuins and osteoarthritis. *Joint Bone Spine* **79**, 570-573 (2012).

146. T. Matsushita *et al.*, The overexpression of SIRT1 inhibited osteoarthritic gene expression changes induced by interleukin-1β in human chondrocytes. *J Orthop Res* **31**, 531-537 (2013).

147. M. Lei *et al.*, Resveratrol inhibits interleukin 1β-mediated inducible nitric oxide synthase expression in articular chondrocytes by activating SIRT1 and thereby suppressing nuclear factor-κB activity. *Eur J Pharmacol* **674**, 73-79 (2012).

148. F. Ng, B. L. Tang, Sirtuins' modulation of autophagy. *J Cell Physiol* **228**, 2262-2270 (2013).

149. B. Bayram *et al.*, A diet rich in olive oil phenolics reduces oxidative stress in the heart of SAMP8 mice by induction of Nrf2-dependent gene expression. *Rejuvenation Res* **15**, 71-81 (2012).

150. S. Mukherjee, I. Lekli, N. Gurusamy, A. A. Bertelli, D. K. Das, Expression of the longevity proteins by both red and white wines and their cardioprotective components, resveratrol, tyrosol, and hydroxytyrosol. *Free Radic Biol Med* **46**, 573-578 (2009).

151. A. Zheng *et al.*, Hydroxytyrosol improves mitochondrial function and reduces oxidative stress in the brain of db/db mice: role of AMP-activated protein kinase activation. *Br J Nutr* **113**, 1667-1676 (2015).

152. R. Huang *et al.*, Deacetylation of nuclear LC3 drives autophagy initiation under starvation. *Mol Cell* **57**, 456-466 (2015).

153. Q. Jin *et al.*, Cytoplasm-localized SIRT1 enhances apoptosis. *J Cell Physiol* **213**, 88-97 (2007).

154. M. Tanno *et al.*, Induction of manganese superoxide dismutase by nuclear translocation and activation of SIRT1 promotes cell survival in chronic heart failure. *J Biol Chem* **285**, 8375-8382 (2010).

155. S. Chung *et al.*, Regulation of SIRT1 in cellular functions: role of polyphenols. *Arch Biochem Biophys* **501**, 79-90 (2010).

156. P. López de Figueroa, M. K. Lotz, F. J. Blanco, B. Caramés, Autophagy activation and protection from mitochondrial dysfunction in human chondrocytes. *Arthritis Rheumatol* **67**, 966-976 (2015).

157. L. Wu *et al.*, Mitochondrial pathology in osteoarthritic chondrocytes. *Curr Drug Targets* **15**, 710-719 (2014).

158. E. Masiero *et al.*, Autophagy is required to maintain muscle mass. *Cell Metab* **10**, 507-515 (2009).

159. Z. Feng *et al.*, Mitochondrial dynamic remodeling in strenuous exercise-induced muscle and mitochondrial dysfunction: regulatory effects of hydroxytyrosol. *Free Radic Biol Med* **50**, 1437-1446 (2011).

160. B. D. Harfe, M. T. McManus, J. H. Mansfield, E. Hornstein, C. J. Tabin, The RNaseIII enzyme Dicer is required for morphogenesis but not patterning of the vertebrate limb. *Proc Natl Acad Sci U S A* **102**, 10898-10903 (2005).

161. F. E. Nicolas *et al.*, Experimental identification of microRNA-140 targets by silencing and overexpressing miR-140. *RNA* **14**, 2513-2520 (2008).

162. H. Pais *et al.*, Analyzing mRNA expression identifies Smad3 as a microRNA-140 target regulated only at protein level. *RNA* **16**, 489-494 (2010).

163. J. Yang *et al.*, MiR-140 is co-expressed with Wwp2-C transcript and activated by Sox9 to target Sp1 in maintaining the chondrocyte proliferation. *FEBS Lett* **585**, 2992-2997 (2011).

164. L. R. Saunders *et al.*, miRNAs regulate SIRT1 expression during mouse embryonic stem cell differentiation and in adult mouse tissues. *Aging (Albany NY)* **2**, 415-431 (2010).

165. D. Ramachandran *et al.*, Sirt1 and mir-9 expression is regulated during glucose-stimulated insulin secretion in pancreatic β-islets. *FEBS J* **278**, 1167-1174 (2011).

166. N. Schonrock, D. T. Humphreys, T. Preiss, J. Götz, Target gene repression mediated by miRNAs miR-181c and miR-9 both of which are down-regulated by amyloid-β. *J Mol Neurosci* **46**, 324-335 (2012).

167. M. S. Makki, A. Haseeb, T. M. Haqqi, MicroRNA-9 promotion of interleukin-6 expression by inhibiting monocyte chemoattractant protein-induced protein 1 expression in interleukin-1β-stimulated human chondrocytes. *Arthritis Rheumatol* **67**, 2117-2128 (2015).

168. S. Meseguer, A. Martínez-Zamora, E. García-Arumí, A. L. Andreu, M. E. Armengod, The ROS-sensitive microRNA-9/9* controls the expression of mitochondrial tRNA-modifying enzymes and is involved in the molecular mechanism of MELAS syndrome. *Hum Mol Genet* **24**, 167-184 (2015).

169. M. Fierro-Fernández *et al.*, miR-9-5p suppresses pro-fibrogenic transformation of fibroblasts and prevents organ fibrosis by targeting NOX4 and TGFBR2. *EMBO Rep* **16**, 1358-1377 (2015).

170. J. Füllgrabe, D. J. Klionsky, B. Joseph, The return of the nucleus: transcriptional and epigenetic control of autophagy. *Nat Rev Mol Cell Biol* **15**, 65-74 (2014).

171. X. Xiong, R. Tao, R. A. DePinho, X. C. Dong, The autophagy-related gene 14 (Atg14) is regulated by forkhead box O transcription factors and circadian rhythms and plays a critical role in hepatic autophagy and lipid metabolism. *J Biol Chem* **287**, 39107-39114 (2012).

172. S. Holla, M. Kurowska-Stolarska, J. Bayry, K. N. Balaji, Selective inhibition of IFNG-induced autophagy by Mir155- and Mir31-responsive WNT5A and SHH signaling. *Autophagy* **10**, 311-330 (2014).

173. G. Wan *et al.*, Hypoxia-induced MIR155 is a potent autophagy inducer by targeting multiple players in the MTOR pathway. *Autophagy* **10**, 70-79 (2014).

174. E. Tili *et al.*, Modulation of miR-155 and miR-125b levels following lipopolysaccharide/TNF-alpha stimulation and their possible roles in regulating the response to endotoxin shock. *J Immunol* **179**, 5082-5089 (2007).

175. E. NETTELBLADT, L. SUNDBLAD, Protein patterns in synovial fluid and serum in rheumatoid arthritis and osteoarthritis. *Arthritis Rheum* **2**, 144-151 (1959).

176. F. Du *et al.*, MicroRNA-155 deficiency results in decreased macrophage inflammation and attenuated atherogenesis in apolipoprotein E-deficient mice. *Arterioscler Thromb Vasc Biol* **34**, 759-767 (2014).

177. M. Kurowska-Stolarska *et al.*, MicroRNA-155 as a proinflammatory regulator in clinical and experimental arthritis. *Proc Natl Acad Sci U S A* **108**, 11193-11198 (2011).

178. X. Li, F. Tian, F. Wang, Rheumatoid arthritis-associated microRNA-155 targets SOCS1 and upregulates TNF-α and IL-1β in PBMCs. *Int J Mol Sci* **14**, 23910-23921 (2013).

7. PUBLICATIONS

• S Cetrullo [#], **S D'Adamo** [#], S Guidotti, R M Borzì and F Flamigni. Hydroxytyrosol prevents chondrocyte death under oxidative stress by inducing autophagy through sirtuin 1-dependent and -independent mechanisms. Biochemical and biophysical acta. 2016 Mar 3;1860(6):1181-1191

• **S D'Adamo**, O Alvarez-Garcia, Y Muramatsu, F Flamigni, M K Lotz. MicroRNA-155 suppresses autophagy in chondrocytes by modulating expression of autophagy proteins. Osteoarthritis and Cartilage. 2016 Jan 19. pii: S1063-4584(16)00024-8

• S Cetrullo, **S D'Adamo**, B Tantini, R M Borzì, F Flamigni. mTOR, AMPK, and Sirt1: Key Players in Metabolic Stress Management. Critical Reviews in Eukaryotic Gene Expression. 2015;25(1):59-75

• A Facchini, S Cetrullo, **S D'Adamo**, S Guidotti, M Minguzzi, A Facchini, R M Borzì, F Flamigni. Hydroxytyrosol prevents increase of osteoarthritis markers in human chondrocytes treated with hydrogen peroxide or growth-related oncogene α. PlosONE. 2014;9(10):e109724

• R M Borzì,S Guidotti, M Minguzzi, A Facchini, D Platano, G Trisolino, G Filardo, S Cetrullo, **S D'Adamo**, C Stefanelli, A Facchini, F Flamigni. Polyamine delivery as a tool to modulate stem cell differentiation in skeletal tissue engineering. Amino Acids. 2014 Mar;46(3):717-28

• C Giovannini , M Baglioni, L Gramantieri, M Baron Toaldo, C Ventrucci, **S D'Adamo**, M Cipone, P Chieco, L Bolondi. Notch3 inhibition enhances sorafenib cytotoxic efficacy by promoting GSK3b phosphorylation and p21 down-regulation in hepatocellular carcinoma. Oncotarget. 2013 October; 4(10): 1618–1631

# These authors contributed equally to this work.